

NOTE TO USERS

This reproduction is the best copy available

UMI

**FOREST REGENERATION ASSESSMENT
USING AIRBORNE DIGITAL CAMERA IMAGERY**

by

KIMBERLY ANNE HADDOW, B.A.

A thesis submitted to
the Faculty of Graduate Studies and Research
in partial fulfilment of
the requirements for the degree of
Master of Arts
Department of Geography

Carleton University
Ottawa, Ontario

May, 1998

© copyright

1998, Kimberly Anne Haddow



National Library
of Canada

Acquisitions and
Bibliographic Services

395 Wellington Street
Ottawa ON K1A 0N4
Canada

Bibliothèque nationale
du Canada

Acquisitions et
services bibliographiques

395, rue Wellington
Ottawa ON K1A 0N4
Canada

Your file Votre référence

Our file Notre référence

The author has granted a non-exclusive licence allowing the National Library of Canada to reproduce, loan, distribute or sell copies of this thesis in microform, paper or electronic formats.

The author retains ownership of the copyright in this thesis. Neither the thesis nor substantial extracts from it may be printed or otherwise reproduced without the author's permission.

L'auteur a accordé une licence non exclusive permettant à la Bibliothèque nationale du Canada de reproduire, prêter, distribuer ou vendre des copies de cette thèse sous la forme de microfiche/film, de reproduction sur papier ou sur format électronique.

L'auteur conserve la propriété du droit d'auteur qui protège cette thèse. Ni la thèse ni des extraits substantiels de celle-ci ne doivent être imprimés ou autrement reproduits sans son autorisation.

0-612-36824-6

Canada

ABSTRACT

The purpose of this research was to investigate the potential of low cost, high resolution airborne digital camera imagery for use in forest vegetation management. Airborne imagery with 2.5 cm pixel size was acquired near Sault Ste. Marie, Ontario, over two forest regeneration sites to: i) evaluate capabilities for discrimination of conifer crop species from vegetative competition at various densities using classification of spectral and textural image information, and ii) develop models relating vegetation structure parameters to image spectral and textural information. Results indicate very strong potential for classification and counting of conifer seedlings when competition is low or not visible to the sensor. Systematic decreases in class separability and conifer count accuracy were observed with increases in density of competition vegetation. In biophysical modelling, relations between image and vegetation structure variables were weak yet statistically significant and improvement is needed for operational use.

ACKNOWLEDGEMENTS

This work was undertaken as a result of involvement with the Canadian Forest Service (CFS), without which it would have not been possible. The contribution of assistance and data have been invaluable. I wish to thank Dr. Doug Pitt for all of his assistance and support. In addition, I would like to thank Wayne Bell and others at the Ontario Forest Research Institute (OFRI) for the use of their data and as well as their assistance.

Thanks is extended to my advisor Dr. Doug King. Your support and encouragement over the course of this work have given me an interesting, and most certainly rewarding experience to take into the 'real world'. I would also like to thank Mike Fox, in addition to your valuable comments, you made me remember how much fun statistics can be. I would also like to express my appreciation to everyone else in the Department of Geography, especially Hazel Anderson. Your encouragement and advise about the inner workings of it all have been most valuable. As well, thanks to Danny Patterson your help and support have always been valuable, but thanks for keeping me smiling.

Thanks must go out to all those who went through this before me. Their words of advice and encouragement, and most importantly, the nods of understanding during the difficult times made me remember I'm not alone. To my good friends and family, words are not enough to tell you what you all have done for me. Thanks for being who you are, you helped me be me. Coal, couldn't have done this without you, and I promise no more!

Table of Contents

Acceptance Sheet	ii
Abstract.....	iii
Acknowledgments	iv
Table of Contents	v
List of Tables.....	vii
List of Figures	ix
List of Equations	xi
List of Appendices.....	xii
CHAPTER 1: Introduction.....	1
1.1 Introduction	1
1.2 Context of this Research.....	2
1.3 Research Objectives	6
1.4 Organization of Thesis.....	7
CHAPTER 2: Potential for Remote Sensing in Forest Vegetation Management...9	9
2.1 Forest Vegetation Management.....	9
2.2 Forest Regeneration Assessment.....	10
2.3 Potential for Remote Sensing in Forest Regeneration Assessment	14
2.4 Other Forest Remote Sensing Research Relevant to Regeneration Assessment.....	21
2.5 Summary.....	25
CHAPTER 3: Principles of Remote Sensing.....	27
3.1 Remote Sensing.....	27
3.1.1 Remote Sensing Theory	28
3.1.2 Remote Sensing of Vegetation	30
3.1 Image Classification	31
3.2.1 Image Classifiers.....	35
3.4 Texture Analysis.....	39
3.5 Vegetation Indices.....	41
CHAPTER 4: Study Areas, Image Acquisition, and Field Data.....	44
4.1 Location and Description of Study Areas.....	44
4.2 Data Acquisition.....	49
CHAPTER 5: Methodology	55
5.1 Introduction	55
5.2 Data Preparation	55

5.3 Phase 1.....	56
5.3.1 Separability Analysis.....	56
5.3.2 Production of Mosaic Image for Further Analysis.....	57
5.3.3 Evaluation of Automated Classification Methods.....	58
5.3.4 Texture Analysis.....	61
5.3.5 Accuracy Assessment.....	62
5.3.6 Evaluation of Classification using Searchmont Image Data.....	64
5.1 Phase 2.....	65
5.4.1 Vegetation Indices.....	65
5.4.2 Statistical Database Compilation.....	66
5.4.3 Statistical Analysis.....	67
CHAPTER 6: Results and Discussion.....	69
6.1 Introduction.....	69
6.2 Separability Analysis.....	69
6.3 Evaluation of Automated Classification Methods.....	76
6.3.1 Image Statistics.....	76
6.3.2 Image Classification of Conifers from Spectral Data Alone.....	79
6.3.3 Image Classification of Conifers from Textural and Spectral Information.....	82
6.3.4 Accuracy Assessment of Conifer Seedling Counts.....	85
6.3.5 Assessment of Classification on Searchmont Data.....	96
6.4 Biophysical Modelling Statistical Analysis.....	99
6.4.1 Correlation Analysis.....	99
6.4.2 Regression Analysis.....	105
6.5 Summary of Results.....	116
6.5.1 Phase 1.....	116
6.5.2 Phase 2.....	117
CHAPTER 7: Conclusions.....	119
7.1 Introduction.....	119
7.2 Potential of Airborne Digital Camera Imagery In Vegetation Classification and Biophysical Modelling.....	119
7.3 Discussion.....	121
7.3.1 Benefits of this Research.....	121
7.3.2 Limitations and Recommendations.....	122
7.1 Concluding Remarks.....	124
References.....	126
Appendices.....	131

List of Tables

Table 6.1	Crop and Competition Reference Separabilities which were 'Good'	74
Table 6.2	Crop and Competition Reference Separabilities which were 'Poor'	74
Table 6.3	Partial Density Dependent Separabilities for Large-Leaved Aster and Blue-Joint Grass.....	73
Table 6.4	Errors of Omission and Commission in Counting Conifer Trees for Arboretum Plots: when no competition present	98
Table 6.5	User's and Producer's Accuracies for each Plot when no Competition Present at the Arboretum Site based on Errors of Omission and Commission.....	98
Table 6.6	Errors of Omission and Commission in Counting Conifer Trees for Searchmont Plots	98
Table 6.7	Correlation Coefficients and P-Values for Mean of Image and Field Variables.....	101
Table 6.8	Correlation Coefficients and P-Values for Variance of Image and Field Variables	102
Table 6.9	Stepwise Regression Results for Mean of Image Variables and LAI.....	106
Table 6.10	Stepwise Regression Results for Mean of Image Variables and Percent Cover	107
Table 6.11	Stepwise Regression Results for Variance of Image Variables and LAI.....	114
Table 6.12	Stepwise Regression Results for Variance of Image Variables and Percent Cover	115

Table A-1	Training Sample Statistics for Arboretum Site from Spectral Data	132
Table A-2	Transformed Divergence Separabilities for the Arboretum Site Training Samples using Spectral Data	133
Table A-3	K-means Unsupervised Clustering Statistics for Arboretum Site with Spectral Data	134
Table B-1	Training Sample Statistics for Arboretum Site from Standard Deviation and Variance Texture Data	136
Table B-2	Transformed Divergence Separabilities for the Arboretum Site Training Samples using Spectral and Standard Deviation Texture Data	137
Table B-3	Transformed Divergence Separabilities for the Arboretum Site Training Samples using Spectral and Variance Texture Data	138
Table B-4	Training Sample Statistics for Searchmont Site from Spectral and Standard Deviation Texture Data.....	139
Table B-5	Transformed Divergence Separabilities for the Searchmont Site Training Samples Using Spectral and Standard Deviation Texture Data	140
Table E-1	Means of Image and Field Variables for use in Correlation and Regression Analysis.....	161
Table E-2	Variance of Image and Field Variables for use in Correlation and Regression Analysis.....	163
Table E-3	Skewness and Kurtosis Values for the Means of Image and Field Variables	165
Table E-4	Skewness and Kurtosis Values for the Variance of Image and Field Variables	166

List of Figures

Figure 3.1	Electromagnetic Spectrum.....	29
Figure 3.2	Vegetation Reflectance Characteristics	32
Figure 4.1	Location of Research Study Areas	45
Figure 4.2	Plot, Density, and Conifer Layout based on Competition Species of the Clay Site at the Arboretum	47
Figure 4.3	Plot Layout for Searchmont Site.....	48
Figure 4.4	Mosaic of Digital Camera CIR Imagery for Arboretum Site	53
Figure 4.5	Mosaic of Digital Camera CIR Imagery for Searchmont Site.....	54
Figure 6.1	Transformed Divergence of Trembling Aspen Competition and Two Conifer Species at Various Competition Densities.....	74
Figure 6.2	Transformed Divergence of Upland Willow Competition and Two Conifer Species at Various Competition Densities.....	75
Figure 6.3	Conifer Counting Error (%) for Neural Network Classifier with Spectral and Standard Deviation Texture Data as a function of Competition Species and Density, and the # of Pixels Defining a Seedling.....	89
Figure 6.4	Conifer Counting Error (%) for Context Classifier with Spectral and Variance Texture Data as a function of Competition Species and Density, and the # of Pixels Defining a Seedling	90
Figure 6.5	Conifer Counting Error (%) for Unsupervised Clustering with Spectral Data as a function of Competition Species and Density, and the # of Pixels Defining a Seedling.....	91
Figure 6.6	Conifer Counting Error (%) for Unsupervised Clustering with Spectral and Standard Deviation Texture Data as a function of Competition Species and Density, and the # of Pixels Defining a Seedling.....	92

Figure 6.7	Conifer Counting Error (%) for Unsupervised Clustering with Spectral and Variance Texture Data as a function of Competition Species and Density, and the # of Pixels Defining a Seedling.....	93
Figure 6.8	Conifer Counting Error (%) for a Classifier which Performed Poorly - Neural Network with Spectral Data as a function of Competition Species and Density, and the # of Pixels Defining a Seedling.....	94
Figure C-1	Example of Plot Classification used in determination of User's and Producer's Accuracies.....	143
Figure C-2	Example Spectral Cluster Map of Arboretum Site using Unsupervised Clustering on Spectral Information only	144
Figure C-3	Example Thematic Map of Arboretum Site Using a Maximum Likelihood Classification on Spectral Information only.....	144
Figure C-4	Example Thematic Map of Arboretum Site Using a Neural Network Classification on Spectral Information only.....	145
Figure C-5	Example Thematic Map of Arboretum Site Using a Context Classification on Spectral Information only	145
Figure C-6	Neural Network Classification with Spectral and Standard Deviation Texture Data on the Searchmont Site.....	146

List of Equations

Equation 5.1	Ratio Vegetation Index.....	66
Equation 5.2	Normalized Difference Vegetation Index	66
Equation 5.3	Soil Adjusted Vegetation Index	66

List of Appendices

Appendix A	Statistics and Transformed Divergence Separability Results of Training Samples using Spectral Data for the Arboretum Site	131
Appendix B	Statistics and Transformed Divergence Separability Results of Training Samples using Spectral and Co-occurrence Texture Data for the Arboretum and Searchmont Sites.....	135
Appendix C	Examples of Thematic Maps obtained from Unsupervised Clustering, Maximum Likelihood, Neural Network, and Context Classification	141
Appendix D	Conifer Counting Error Graphs for all Classifications expressed in Percent as a Function of Competition Species and Density, and the Number of Pixels Defining a Seedling Core	147
Appendix E	Statistical Database used in modelling LAI and Percent Cover from Image Derived Information.....	160

Chapter One

Introduction

1.1 Introduction

Forests in Canada play important roles not only for the country as a whole, but for communities and individual Canadians as well. Covering over 45 percent of the Canadian landscape, they directly and indirectly support the economic and social well being of many Canadians. In addition, forests play an important ecological role in the environment. They moderate climate, prevent soil erosion, improve water and air quality, and provide habitats for countless plants and animals.

The importance of Canadian forests demands their proper management to sustain and enhance the roles they play. Ninety-four per cent of Canadian forests are publicly owned, of which 71% are managed by provincial governments, while 23% are managed by federal and territorial governments (Natural Resources Canada, 1996). Approximately 50 million hectares are currently being protected from harvesting activities by government legislation or policy. The legislation and policies governing the 119 million hectares in Canada that are currently being managed for timber production are primarily under provincial jurisdiction (Natural Resources Canada, 1996). All timber related practices, such as harvesting, regeneration, and silviculture activities, in each province or territory, are governed by those provinces' forestry statutes.

Forestry statutes, such as Ontario's Crown Forest Sustainability Act (1994) provide the framework for the use, allocation, and management of all publicly owned

forested lands (Ross, 1995). The Crown Forest Sustainability Act provides for the sustainability of Crown forests in Ontario and outlines objectives for the management of the forest to meet present and future social, economic, and environmental needs (Statutes of Ontario, Chapter 25, 1994). Crown forests are situated on land owned by Her Majesty in Right of Ontario and are under the management of the Ontario government.

To comply with provincial regulations and ensure continued access to crown forests, forest companies utilize standard forest management practices. These practices include not only highly publicized harvest activities, but numerous silvicultural operations that ensure successful forest regeneration. Field investigations enable forest managers to identify and correct, in a timely manner, areas within forest management units¹ that could potentially lead to problems, therefore ensuring successful regeneration.

1.2 Context of this Research

The use of remote sensing in forestry applications has been well researched within the remote sensing and forestry communities (Pitt *et al.*, 1997; Hall *et al.*, 1996; Wulder *et al.*, 1996; Smith *et al.*, 1989). Numerous sensors (optical and radar) and platforms (airborne and satellite) have proven useful in aiding forest managers with various decision-making processes (e.g. herbicide application, supplemental planting)

¹ An aggregate of forest stands that are managed under the same rotation and silvicultural system.

during regeneration and harvest operations. Currently, as in the past, forest companies have primarily used remote sensing in forest mapping and mature forest inventory.

Advancements in technology have led to the development of various new sensors and platforms. One sensor which has potential for use in forest vegetation management is an airborne digital camera. Digital camera systems offer a number of advantages over conventional aerial photography. They are generally lower in cost than 70mm and large format photographic cameras. Furthermore, they eliminate the need for film development and subsequent scanning, which is required when subjecting conventional photography to computer analysis. Digital cameras also offer the capability for in-flight viewing of images, computer control of exposure levels, and a linear response to radiance (King, 1995). Many of these features can be found with other optical sensors (e.g. MEIS, CASI), although costs associated with digital cameras image are significantly less. Furthermore, airborne digital camera systems currently offer higher spatial resolution than other airborne and satellite digital sensors as well as complete flexibility to vary the desired resolution by varying the flight altitude, or lens focal length. Digital cameras, being frame sensors are more similar to the frame format of photography than are line scanners, thus providing more potential for integration into forest management activities which utilize photography.

The belief underlying this research is to develop a methodology that is readily transferable to a user community, in this case the forest managers. Therefore, this research was designed to simulate operational conditions, where the parameters, sensor,

image analysis and classification techniques would have a greater chance of implementation within the forestry sector. Furthermore, the data acquired using the digital camera were left in an uncorrected state. In an operational setting, image degradations from bi-directional reflectance, noise, or radiance decrease with view angle due to optical effects are usually not corrected due to the complicated nature and high costs of the processes involved. Therefore, if computer analysis on uncorrected data using commonly available methods is successful, the transfer, with respect to both functionality and comprehension, to an operational setting would presumably be easier and less complicated.

To transfer the technology and methods presented in this work, several other factors must also be considered. The use of digital frame cameras as opposed to other high resolution sensors, such as the Compact Airborne Spectrographic Imager (CASI), do not require advanced user training, extensive preliminary data processing, or high capacity operating systems. Secondly, imagery obtained from digital frame cameras can be analysed using standard, commercially available software. Although some of the methods used in this research are experimental, they were conducted using a simple set of user inputs with commercially available PC-based software. Lastly, the choice of spatial resolution is also important. For forest regeneration assessment there is a need to 'see' individual conifer seedlings. Other types of sensors typically produce lower resolution images where individual trees are not imaged and analysis must be conducted on a canopy basis.

A workshop held by the Canadian Forest Service in Sault Ste. Marie, Ontario, in December 1995 examined the use of remote sensing for forest vegetation management. The workshop concluded that given current data and cost requirements, the best remote sensing system for implementation in forest vegetation management should include aerial photography. It was noted that aerial photography has been routinely used since the 1950s and has seen substantial improvements in resolution, forward motion compensation, motion stabilization, computer designed lenses, integration of GPS, and exposure control systems (Pitt *et al.*, 1997). Furthermore, aerial films have also been improved to achieve increased film speed, spectral sensitivity, resolution, and colour rendition. Research into the use of aerial photography has demonstrated that a photo scale of approximately 1:1000 may be used to acquire data for crop and non-crop vegetation such as height, density and cover (Pitt *et al.*, 1997). The use of aerial photography has successfully been demonstrated in regeneration surveys (Hall and Aldred, 1992; Hall, 1984). However, the workshop recommended that the immediate focus of research be on the use of digital cameras as replacements for aerial photography to assist in the acquisition of data used in the forest vegetation management decision making process (Pitt *et al.*, 1997).

Digital frame cameras provide a method for obtaining digital images directly. The workshop stated that not only do digital cameras have a similar technical sophistication and format to conventional aerial photography, but they offer the same advantages of digital line scanners at lower cost, permit customization by the user, and

are easy to install in light aircraft (Pitt *et al.*, 1997). Their major limitation is lower ground coverage at a given resolution than photography due to the smaller size(s) of the imaging ships. However, digital camera systems are developing rapidly with continuous improvements in spatial resolutions and greater ground coverage as formats of imaging chips increase in size.

This research addresses this recommendation through the investigation of digital camera data for provision of specific FVM information. The procedures used during this investigation are different from those typically used by forest managers in that methods are image-based and are automated as opposed to the manual photo interpretation.

1.3 Research Objectives

The research conducted for this thesis focuses specifically on using information derived from airborne digital camera imagery as a decision making tool for the planning of silvicultural activities during the regeneration of coniferous forest sites prior to these sites being assessed for free-to-grow status. The evaluation was conducted with the following two objectives: i) assess the capability of airborne digital camera imagery for conifer detection and identification using statistical analysis and automated classification procedures, and ii) assess the capability for statistical modelling of biophysical parameters (leaf area index and percent cover) of regenerating vegetation using spectral and textural information extracted from digital camera imagery.

The first objective involves identification of the objects of interest, in this case the conifer seedlings, within digital images and production of thematic maps of the regeneration plots from the imagery to support the decision-making process. The second objective relates to the evaluation of plant growth and competition levels, which are important in dealing with regeneration of conifer trees. This information can be used in establishing a schedule of where and when to employ certain silviculture activities such as weed control and spacing. This research includes two components which have not been previously investigated in FVM; digital cameras and the use of automated classification.

1.4 Organization of Thesis

To facilitate an evaluation of digital camera imagery as a tool for decision making in forest vegetation management, some knowledge of forest vegetation management and silviculture practices needs to be outlined; this is addressed in Chapter 2. Furthermore, the spectral response of the targets, in this case vegetation, also needs to be summarized. This background is provided in Chapter 3, in addition to a description of the necessary technical and contextual background of the work undertaken. This basic background theory is presented through a progression of past and current remote sensing research. Chapter 4 describes the study area and data used during this research. Chapter 5 provides a detailed discussion of the methods developed to evaluate the use of airborne digital imagery in regeneration assessment. The results of the research are presented and

discussed in Chapter 6. Chapter 7 provides a review of the research, discusses the significance and limitations of the methods and results, and summarizes the conclusions reached. It will also provide recommendations for techniques or methods that could be undertaken in future research.

Chapter Two

Potential for Remote Sensing in Forest Vegetation Management

2.1 Forest Vegetation Management

The management of Canada's forests has typically focused on the growth and production of marketable trees and not on forest ecology. In the past, the goal of management was to ensure a sustainable yield of timber for industry (Canadian Council of Forest Ministers, 1992). Of late, there is a new standard developing that views forest vegetation management (FVM) as a component of silviculture which involves manipulating the rate and course of early plant succession to achieve a desired composition, structure and form for the forest stand within a desired time period (Pitt *et al.*, 1997). FVM involves integrating the knowledge of plant ecology with a wide variety of complementary ecosystem-based methods that are socially and economically acceptable (Wagner, 1994). No longer is the timber component the only concern; forest managers must include non-timber components of a forest ecosystem such as wildlife, recreation and watersheds, into their decision-making processes. Intensive forest management comprises two main activities. The first is that of regeneration through site preparation and planting or through natural regeneration. The second is to tend established stands of timber in order to maintain or improve their growth. This process is subdivided into tending either young regeneration or well-established sites. This research will focus on the tending of young regeneration sites.

FVM decisions have to be justified on a site-specific basis. Justification using quantitative techniques to objectively assess the value of various treatment options on a site-specific basis is difficult because of the lack of quantitative data (Wagner, 1993). This has led to a need within forest management for the use of decision support systems which are based on objective, quantitative assessments. A decision support system (DSS) is a computer-based information system that includes a database, procedures, and an interface between the decision-maker and the procedures which are used to serve as a decision making tool. These systems require large amounts of data, typically more than what can be provided by current field surveys. Remote sensing offers an important source of input data in addition to the field survey data, provided that the remote sensing data can be verified as sound. Decision support systems have been developed to provide a method of organizing technical components to allow for effective decision-making and planning (Thompson and Weetman, 1995). There are two features that are recommended for a forest management DSS: i) include a GIS as its core, and ii) cover all important planning periods from regeneration to harvest (Thompson and Weetman, 1995).

2.2 Forest Regeneration Assessment

To understand how remote sensing can be used in FVM during the regeneration phase, it is necessary to review the objectives of regeneration assessment. Specific field techniques will not be discussed.

A forest regeneration assessment is conducted in order to determine the status of a regenerating site. Regeneration sites must be monitored and data collected to evaluate plant succession and to prescribe necessary silviculture practices to ensure successful regeneration of the site (Pitt *et al.*, 1997). Field methods are currently the predominant means of acquiring information during regeneration assessments.

The *Regeneration Survey Manual for Ontario* (Chaudhry, 1981) contains the procedures, guidelines, and standards used for assessing regeneration in Ontario. There are numerous activities involved in a forest regeneration assessment; however, only those relevant to this research will be discussed. For information regarding other activities, the reader is referred to the above manual or to the draft manual *Free-growing regeneration assessment manual for Ontario - draft* currently in preparation, which will soon replace the older manual. The purpose of these manuals is to ensure that the same methods and standards are used throughout the province, by both industry and government, to assess the success of regeneration.

The main objectives of regeneration assessment are to: i) determine the relative success of regeneration on any site; ii) provide resource managers with information to predict future stand development; iii) determine the need for future treatments on regenerated areas; and iv) allow for the comparison of different treatments that led to successful regeneration for various species and sites (Arnup and Rusnak, 1997). To achieve these objectives, a regeneration assessment is divided into three main categories:

stocking assessment; plantation survival assessment; and seeding assessment (Chaudhry, 1981).

Stocking¹ assessment is the first inventory of an area after harvesting or planting. The main purpose of stocking assessment is to determine the relative success of regeneration for an area according to prescribed stocking standards and to provide forest managers with basic information on stand establishment to predict future yields (Chaudhry, 1981). Regeneration success is judged on the basis of stocking, species composition and suitability of species to the site. A secondary objective of stocking assessment is to determine the need for future treatment, such as release, refill, re-treatment, insect and disease control, and assessment of free-to-grow condition². Timing is one major component of a stocking assessment. It is recommended that the timing window in northern Ontario be seven to eleven growing seasons after planting or harvest (Arnup and Rusnak, 1997). Assessment too soon after planting or harvesting increases the risk of declaring trees free-growing that may later be out-competed by other species. Exceptions to this timing window include: i) areas that have been carefully logged to protect advance growth, which can be assessed sooner than seven years; and ii) for chemically treated or manually tended areas, two full growing seasons must elapse after treatment before regeneration assessment.

¹ Stocking is defined as the frequency of occurrence of seedlings and advance growth of tree species of acceptable specifications, based on plots of a certain size as compared with the optimum number of evenly distributed trees that fully occupy a site (Chaudhry, 1981).

² Free-growing refers to the ability of a well-spaced crop tree to withstand critical competing non-crop vegetation through to maturity (Chaudhry, 1981).

Another component of a stocking assessment typically associated with naturally regenerating sites is determining if the crop species present is acceptable based on the ecology of the sites and the site-specific management objectives. Priority is given to conifer working groups compared to hardwoods, and only crop trees of acceptable species can be considered for well-spaced³ and free-growing status (Chaudhry, 1981). Stocking assessment is conducted by either an intensive systematic sampling or an extensive survey. Much of the emphasis during a regeneration survey is given to intensive systematic sampling. Surveys are conducted based on cover type: conifer, hardwood, and mixed. For the conifer cover type, emphasis is on stocking (Chaudhry, 1981).

The second and third categories of a regeneration assessment are plantation survival and seeding assessment. Plantation survival assessment involves a field survey where the survival data are recorded for every plot which has been regenerated by seedlings. In addition to determining the survival of the crop species, a competition index⁴ is determined. Recommendations are also suggested in the field. These can include: subsequent planting of seedlings, re-application of weed-control treatments, monitoring, or treatment for insect damage or disease. Recommendation of free-to-grow status is also made during the field survey.

³ Well-spaced refers to the distance between crop trees and reflects the potential growing space available to each of the crop tree through to maturity.

⁴ Visual estimate of the degree of competition based on over-head coverage of broad type competing vegetation (Chaudhry, 1981).

Seeding assessment is similar to plantation assessment; however, it deals with sites that are regenerating by seeding. A seeding assessment involves collecting information from the field on the germination, mortality, and survival of seedlings (Chaudhry, 1981). In addition, the crop species, competition index, and silvicultural recommendations are also determined in the same manner as the plantation survival assessment.

2.3 Potential for Remote Sensing in Forest Regeneration Assessment

To understand how remote sensing can be used as a decision-support tool in forest management, it is necessary to review past research that has investigated the use of remote sensing in forest regeneration assessment and the collection of plant information ordinarily collected through field investigations. Field investigations can be labour-, time-, and cost-intensive and can limit assessment by restricting the number of samples taken, the spatial and temporal coverage, and/or the amount of research that is conducted (Pitt and Glover, 1993). Remote sensing is seen as a method of obtaining additional data, as well as reducing errors associated with estimations, providing a more quantitative approach to regeneration assessment. Past research which has investigated the use of remote sensing has typically focused on large-scale aerial photography to obtain tree measurements, in attempts to reduce the need for field campaigns or to provide additional data to support field measurements.

Studies have investigated the use of large-scale aerial photographs to measure plant attributes during the regeneration phase of vegetation management. Aerial photographs were used to estimate pine density and competition conditions in young pine plantations by Smith *et al.* (1989). The study objective was to develop a system for estimating pine density and hardwood competition levels in 3-, 4-, and 5-year pine plantations from aerial photographs. The free-to-grow system was used as an indirect indicator of competition level, whereas pine density was determined by counting pines in rows, and between rows with comparable heights and crown sizes.

Aerial photographs were acquired in October using a standard 35mm camera with colour slide film. The photographs were acquired in October to maximize the contrast in foliage colour between the pines and hardwoods due to autumn colouration. Two scales were acquired with ground representation of 1:4000 and 1:6000. The slides were interpreted and acetate sheets containing the outline of pine and hardwood crowns were obtained, as well as the relative heights in comparison to surrounding vegetation. Crowns were then counted and a dot grid was utilized to obtain the relative percentage of cover for each category. Regression equations were developed to relate field surveyed pine density to the photo-based pine crown count. In addition, regression equations were used in prediction models for two different measures of competition level.

Results indicated a strong relationship between measurements made using field techniques and large-scale aerial photographs. The applicability of photo-based

prediction models in a practical decision-making situation was examined. Treatment decisions reached using the photos alone and the ground measurements were compared. Using either of the two photo scales, 78% of the plots produced the same decision as the ground measurements (Smith *et al.*, 1989). Results of the study indicated that photographs can be utilized to determine treatment decisions which are typically based on field measurements alone.

Pitt and Glover (1993) evaluated the use of large-scale aerial photographs in assessments of vegetation management research plots. The study investigated the degree to which large-scale photographs could be utilized to reduce the number of field plots needed to obtain estimates of response variables such as woody crown area per hectare and rootstock density. Woody crown area per hectare and rootstock density (number/ha) are two response variables used to evaluate competition levels in forest regeneration areas. Thirty-five millimeter photography was acquired from a small helium-filled blimp in July of 1990 and 1991, at scales of 1:828 and 1:414 respectively. Concurrent ground sampling was also conducted for ground truthing. The relationship between total plot crown area estimates on the ground and those manually measured from photos was strong ($r^2=0.97$).

The study concluded that, in addition, to effectively evaluating woody plant response variables, large-scale photographs, with some ground truthing, reduced total cost of the site survey by a minimum of 14% (Pitt and Glover, 1993). The study also outlined various advantages and disadvantages of large-scale photography. Advantages

included: providing a permanent record for future reference; utilization of photos by other groups to evaluate other effects of vegetation management treatments, such as on animals; ability for research and evaluation to be conducted over the winter months in preparation for the following field season; reduction in variation between sampling dates; and potentially more objective evaluation of treatment response variables (Pitt and Glover, 1993). Disadvantages include the potential loss of records due to equipment failure and the need for expertise in photo acquisition and measurement.

Another study conducted by Pitt *et al.* (1996) involved a two-phase approach to sampling of woody and herbaceous species attributes. The study was conducted over seven experimental treatments in the fall of 1992. Photography was acquired using a lightweight aluminum boom attached to a helicopter to obtain a scale of 1:366. The sampling objectives were to obtain estimates of crown volume index for woody species, as well as to estimate herbaceous percent cover. Sampling was conducted in two phases; phase one involved the evaluation of photographs to obtain crown volume index and herbaceous percent cover and phase two involved sampling the ground units to obtain field measurements of the crown volume index and herbaceous percent cover (Pitt *et al.*, 1996).

The statistical relationship was evaluated between phase one estimations and phase two estimations and used to correct phase one estimations for bias. Bias can be associated with photo interpretation and measurement and can include underestimation of smaller plants hidden by large plants and not detected on the photographs. Individual

woody species could be identified and measured on enlargements of the aerial photographs to a scale of 1:80. Through the use of regression equations relating the field-based measurement of woody crown volume index to the photo measurements, a 95.7% agreement was obtained. Results indicated that there were no differences between ground estimates, two-phase photo, and regression photo sampling methods with respect to the woody crown volume. However, the precision levels of the methods varied widely. Regression estimators were consistently more precise, with an average standard error 78% smaller than ground estimates and 65% smaller than two-phase estimates, while standard errors of two-phase estimates were 37% smaller than ground estimates. The presence of herbaceous vegetation increased the sampling errors of woody crown volume index estimates by an average of 39%, for both sampling methods.

The study determined that classification of herbaceous vegetation was successful, with the two-phase estimates and ground estimates producing similar results, while the two-phase estimates obtained better precision (Pitt *et al.*, 1996). The study concluded that if individual species or groups are well represented, large-scale photographs, in a two-phase sampling design, can be an effective tool for monitoring and quantifying vegetation structure in silvicultural and forest management field investigations.

Hall and Aldred (1992) outlined three objectives: production of maps to delineate unproductive areas, assess conifer stocking by species within a specified error, and evaluate the capability of large-scale photographs to reduce the cost of regeneration assessment using field measurements of stocking, density, species identification, and

percent detection by height class and species. Six cutover areas were selected in Saskatchewan and photos at a scale of 1:10 000 and 1:500 were acquired in May 1987. Field work was also conducted to evaluate the effectiveness of large-scale photographs as part of the third objective. The 1:500 scale photos were analysed in stereo and the assessment of the sites included percent conifer seedling estimation, species identification accuracy, stocking and density estimation, and the development of correction equations to adjust for systematic differences between photos and field measurements.

The identification of conifer species (jack pine and spruce) was correct 96% of the time for all seedling sizes. A higher rate of detection was obtained for trees greater than 30cm tall which were taller than the surrounding competition. Photo stocking estimates were considerably lower, by an average of 5% than stocking estimated by field measurements. A regression of density estimates between photo and field-based measurements produced a high regression coefficient. However, the resulting large standard error of estimate suggests that density estimates had low precision using large scale photographs. The study determined that large-scale photography was useful in assessing regeneration sites, nonetheless further investigations of various scales to better identify stocking levels are needed (Hall and Aldred, 1992).

The use of remote sensing, specifically large-scale aerial photographs, has been examined by several researchers and even put to operational use within the forest industry for certain objectives where it has been shown to be cost-effective. Research has begun to address the use of other sensors that can obtain large-scale images. Pitt *et*

al. (1997) outlined data requirements on the part of forest managers and resulting image requirements, which included the level of spatial detail resolved, coverage, timing, stereo requirement, spectral characteristics, and image format. Potential sensors were identified that could be used to meet the image requirements deemed necessary for forest vegetation management. These sensors included: optical satellites, radar, airborne line imagers, aerial photography, airborne videography, lasers, and digital frame cameras.

The required image spatial resolution is determined by the size of the vegetation of interest and the degree to which it has to be identified and measured. The spatial resolution requirement for trees less than 0.5 m tall was specified to be 1.6 cm for density, height, and plant conditions, whereas 8 cm was suggested for stocking assessments. In addition, it was recognized that for most sensors, the spatial resolution of the image decreases as the area of coverage increases. Therefore, the workshop recommended that the most cost-effective system that offers the largest image coverage with the desired spatial resolution be used. However, for investigations that focus on individual tree evaluations, an image coverage of at least 0.05 ha is required to ensure enough surrounding detail and aid in the location of plots (Pitt *et al.*, 1997). The timing of image acquisition relative to the vegetation phenology is also an important factor. Coniferous species are most visible in images acquired in early spring or late fall when the deciduous vegetation is leafless and the herbaceous vegetation is brown. Images should be acquired during the mid to late growing season if an evaluation of the non-

crop vegetation is to be conducted due to the difficulty in identifying deciduous woody vegetation in the leaf-off condition (Pitt *et al.*, 1997).

Stereo capability was discussed with the observation that stereo images do aid in manual interpretation of vegetation structure and type and are absolutely necessary for obtaining vegetation height data. Imagery which includes spectral resolution in the near infrared portion of the electromagnetic spectrum can enhance differences between healthy conifers and unhealthy or dead conifers and non-crop vegetation, aiding in the interpretation. In addition, for spectral-based computer classifications, colour infrared imagery may emphasize the difference in near infrared reflectance of vegetation (Pitt *et al.*, 1997). The format of the images was also discussed with an emphasis placed on the acquisition of digital imagery. Digital images can prevent the loss of spatial resolution that can result from the scanning of analog images and can also provide useful information within sunlit or shadow areas that photographs do not contain. Furthermore, images in a digital form can be stored, manipulated, analyzed, and interpreted through automated processes within a computer.

2.4 Other Forest Remote Sensing Research relevant to Regeneration Assessment

A large amount of research has investigated relationships between satellite or airborne image variables and mature forest parameters such as percent cover and LAI (Franklin *et al.*, 1997; Bulter *et al.*, 1995; Gong *et al.*, 1995). Leaf area index (LAI) is the projected leaf surface area per unit of ground area and is typically determined by

dividing the leaf area by the ground surface area (Price and Bausch, 1995). LAI is an indicator of the density of vegetation and can be used for estimation of forest canopy characteristics and determination of forest exchange rates of water, carbon dioxide, and oxygen (Gong *et al.*, 1995). Percent cover is defined as the percentage of the ground area which is covered with photosynthetic canopy materials, such as leaves or needles (Elvidge and Chen, 1995). LAI and percent cover are two vegetation structure parameters addressed in this thesis, and thus discussion of other remote sensing forest research be restricted to them and will not consider the many other forest attributes which have been studied.

Much of the research in modelling vegetation parameters is done within the context of radiative transfer modelling or determination of net primary productivity of an area. This has typically been conducted using satellite data. For example, Franklin *et al.* (1997) estimated forest LAI in an area of New Brunswick using Landsat TM data acquired in 1992. The normalized difference vegetation index (see 5.4.1) was calculated using TM data for three cover types: softwood, hardwood, and mixedwood and the overall relationship to LAI was weak (0.15) but statistically significant. The normalized difference vegetation index (NDVI) was calculated from the TM data was highly correlated with LAI for softwood (conifer) stands (0.93), but much less correlated in mixedwood (0.66) and hardwood (0.13) stands. The addition of stem density, measured from the TM data, with NDVI in a multiple linear regression improved the correlation with LAI for hardwood and mixedwood stands.

Other studies, such as the one conducted by Bulter *et al.* (1995) used higher resolution remote sensing data in estimating leaf area. Data from CASI were used to produce a forest leaf area map in Kananaskis Country, Alberta. NDVI was calculated for two bands (red and near infrared). Regression analysis was conducted to identify the relationship between field measured plot-level LAI and a plot-averaged NDVI for the same area. The relationship obtained between NDVI values and field measurements of LAI was weak (0.12) for all stands but was significant. The strength of the relationship increased with forest stratification by species to approximately 0.34 for white spruce (Bulter *et al.*, 1995). The study recommended that the key to LAI values using CASI data was to stratify the image into pure stands of different species. This improved the relationship from 20% correct to over 66% correct. The stratification method worked best for spruce, followed by pine, and then aspen stands. Variations in NDVI values were attributed to atmospheric effects, anisotropic reflectance, radiometric striping, and flight line differences, understory reflectance, and geometric errors in the data.

Another study was also conducted using CASI data to estimate LAI in a coniferous forest (Gong *et al.*, 1995). The two imaging modes, spectral mode (low spatial resolution, many spectral bands) and spatial mode (high spatial resolution few spectral bands) of the CASI sensor were implemented to determine which technique is more appropriate for coniferous LAI estimation and to compare the effectiveness of both. A regression analysis was conducted with LAI as the dependent variable and the spectral reflectance of each channel, its logarithmic transform and two vegetation indices

(NDVI and Simple Ratio Index) were defined as the independent variables for three methods (piece-wise, univariate, and vegetation index-based). Linear correlations indicated that RVI is more strongly correlated with LAI; NDVI was a better non-linear estimator of LAI than RVI for univariate regression and the vegetation index-based methods. For the spectral mode data the situation was reversed, with the piece-wise regression resulting in the largest prediction errors. The piece-wise method resulted in lower prediction errors than the other two methods using the spatial mode CASI data. The use of logarithmic reflectance in the multiple regression method produced better relationships with LAI and lower errors than did the use of the raw channels. This occurred for both the spatial and spectral mode data. The researchers also noted that different from the spatial mode, the near infrared channels of the spectral mode data made little contribution to LAI predictions with multiple regression. This was possibly due to the large pixel sizes in the spectral mode, and that the data only covered a portion of the study area, which lead to locational difficulties of LAI field measurement sites. The researchers recommended that spatial mode CASI data be used for LAI estimation because with the spectral mode, the LAI measurement sites were difficult to locate which can significantly affect the LAI estimates. Furthermore, they recommended that multiple regression analysis be used to further investigate the relationship between LAI and spectral reflectance data (Gong *et al.*, 1995).

The above examples of research to determine mature forest structure measurements using coarser resolution imagery can be adapted to high resolution

modelling of regenerating vegetation. In this thesis, the statistical methods and findings of these studies were applied in the design of the methodology given in Chapter 5.

2.5 Summary

There has been little research into the use of airborne digital cameras or other digital remote sensors in the assessment of regenerating conifer trees. The more commonly used aerial photography has proven useful in regeneration assessment. However, most of the methods of information extraction from the photographs are manual in nature leading to potential subjectivity on the part of the interpreter. Furthermore, these methods can also be time consuming for larger areas of study. Discussions and workshops on the use of remote sensing in forest vegetation management have reported that digital cameras could replace aerial photography within the next five years (Pitt *et al.*, 1997). This demonstrates that there is an interest in the use of airborne digital imagery within forest vegetation management which needs to be explored further. This research takes the aerial photography methods and moves them into a digital environment where automated processing can be exploited.

In addition to the use of airborne digital imagery as a means of assessing regeneration, this research assesses how well information related specifically to the vegetation of interest can be extracted from this type of imagery. Most of the research into the extraction of vegetation parameters, such as LAI and percent cover, has been limited to analysis of mature forest canopies using satellite data or high resolution

airborne sensors. The studies have found that the relationships of spectral reflectance and spectral transformations with parameters such as LAI are weak but statistically significant. Research has also examined how the selection of species cover types can improve the strength of the relationship. High resolution imagery, such as that used in this research, may provide the analyst improved species identification capabilities and eliminate the need to predict generalized LAI over large areas where there is more than one species present.

Chapter Three

Principles of Remote Sensing

3.1 Remote Sensing

Remote sensing is the science of obtaining information about certain features or phenomena through the use of recording devices or sensors that are not in direct contact with the area being studied. It allows for both spatial and temporal analysis and can be used to obtain information about large areas with a minimum amount of time and labour expense.

Coverage of areas using remote sensing can be more extensive and repeated in a more effective manner than in-situ investigations. This increased coverage can result in an extensive historical database that can simplify the assessment of long term trends and potentially improve methods of forest vegetation management and regeneration assessment. Furthermore, remote sensing can also be used to study areas where in-situ investigations are not feasible or are too costly. Once remotely sensed images have been obtained, information about certain features can be extracted through the use of manual or computer-aided techniques and used in various applications.

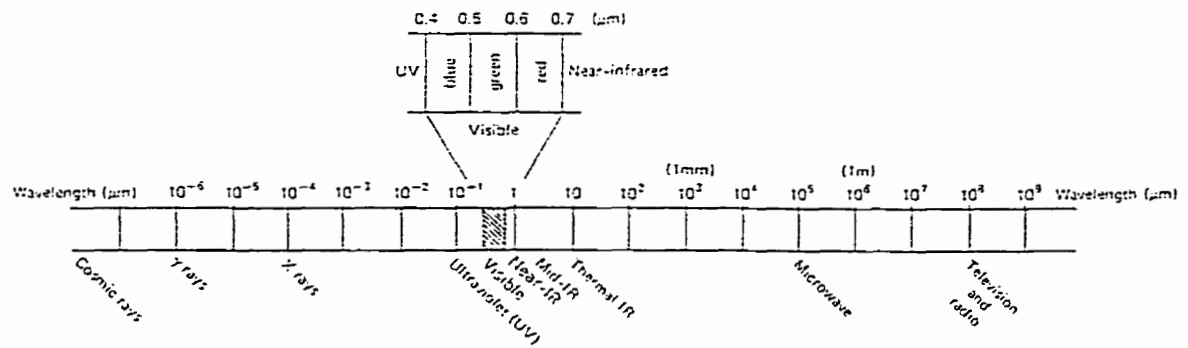
Currently, remote sensing within forest vegetation management has focused on the use of aerial photography to supplement field investigations. With an ability to provide information in a timely and effective manner, other sensors, both satellite and

airborne, could potentially play a larger role in forest vegetation management decisions and may reduce the need for in-situ investigations.

3.1.1 Remote Sensing Theory

Remote sensing can provide information about various surface and sub-surface earth features through detection of interactions which take place between the features and incident energy. These interactions typically produce variations in properties of the electromagnetic spectrum or other energy types. For the purposes of this thesis, only optical imaging of electromagnetic energy in the visible to short-wave infrared (400 - 2500nm) will be discussed. Remote sensing of other regions of the spectrum (thermal and microwave) as well as of other energy types (seismic, gamma, gravity, etc.) is not relevant to the thesis. The electromagnetic spectrum is composed of electromagnetic energy, characterized by wavelength (λ) or frequency (ν) (Figure 3.1), which travels at the speed of light (3×10^8 m/s). Energy travels from a source, the sun, and is either reflected or re-radiated by the target to a sensor. The interaction of this energy with the surface results in changes in the wavelength and intensity of the electromagnetic energy and provides a significant source of information to aid in the interpretation of features or phenomena from which the energy is reflected (Jensen, 1996). The electromagnetic energy is reflected to the sensor and is converted to an electronic signal whose voltage is in proportion to the amount of radiance. It should be noted in Figure 3.1 that the boundaries between regions are not discrete and are typically used for identification purposes only.

Figure 3.1
Electromagnetic Spectrum



(Lillesand and Kiefer, 1994)

All features or phenomena on the earth interact in a different way with incident electromagnetic energy. It is these unique interactions that facilitate the extraction of information about various features from remotely sensed images. Features like soil, vegetation and urban areas, all produce different spectral reflectance curves. Vegetation is the primary focus of this investigation and therefore only the interaction of vegetation with electromagnetic energy will be discussed.

3.1.2 Remote Sensing of Vegetation

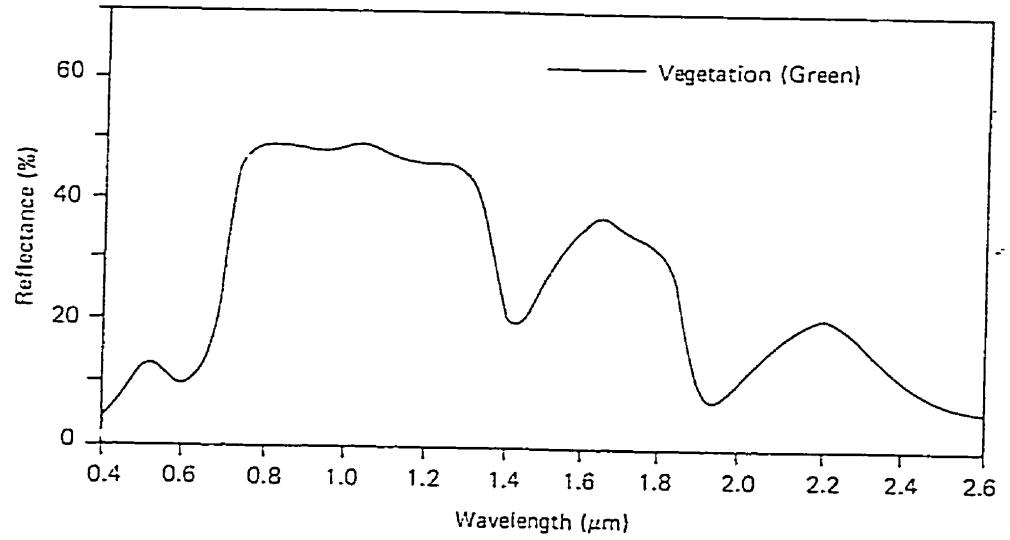
A leaf is built of layers of structural fibrous organic matter, with pigmentation, air spaces and water-filled cells (Curran, 1985). Each of these have an effect on the spectral reflectance, absorption, and transmission properties, which in turn affect the wavelength and intensity of electromagnetic energy that is detected by the sensor. Pigmentation in leaves, particularly chlorophyll, causes a high degree of absorption in the visible spectrum, with relatively more absorption in the blue and red, hence the green appearance of the vegetation to the human eye. The high reflectance in the near infrared is principally due to multiple reflections off of the nearly perpendicular cell walls. This is largely related to the amount of biomass and the turgor of leaves. In addition, there are numerous discontinuities within the leaf and areas of significant water absorption that characterize the reflectance of the vegetation within the near and short-wave infrared portions of the spectrum. The above factors combine to give vegetation low reflectance in red and blue wavelengths, slightly higher reflectance of green energy, high reflectance

of near infrared energy, and declining reflection in the short-wave infrared due to water absorption (Figure 3.2).

3.2 Image Classification

Classification analysis has long been a standard practice in remote sensing to produce thematic maps. There is a range of techniques that can be applied to classify an image; the most conventional ones including algorithms such as the Maximum Likelihood classifier (Peddle *et al.*, 1994). The classification process can be based on either intrinsic variations in brightness, (unsupervised cluster analysis), or based on a subset of samples of known cover types whose brightness characteristics are matched with those of the rest of the area (supervised classification). Unsupervised cluster analysis, in addition to being used as a classification method, can be conducted as a type of segmentation of the landscape, followed by a classification of those segments. Classifiers, such as the maximum likelihood, rely on a normally distributed dataset whereas some classifiers, such as a neural network, can incorporate data that are not normally distributed. Classification can also be conducted on a per pixel basis, where each pixel is analyzed and classified as an independent discrete entity, or on an object basis where the assignment of a pixel to a class is based on its spatial relationship with surrounding pixels (Lillesand and Kiefer, 1994).

Figure 3.2
Vegetation Reflectance Characteristics



(Lillesand and Kiefer, 1994)

Unsupervised Cluster Analysis

Unsupervised cluster analysis can serve two purposes. The first is as a preliminary step to supervised classification, or to aid the analyst in identifying land cover classes and training samples. The second purpose is as a form of classification with the production of a thematic map, of statistically discriminated clusters. Its primary advantage over supervised techniques is less user involvement as only a few input parameters are required. One of the simplest clustering algorithms is the K-means. The number of spectral clusters to be extracted from the data is specified and the algorithm then arbitrarily selects locations for the corresponding number of cluster means within the multi-dimensional image space (Lillesand and Kiefer, 1994). Each pixel within the image is then assigned to the cluster whose mean value is the closest through the use of a distance measure such as Euclidean distance. Once all of the pixels have been assigned a cluster, the algorithm recalculates the cluster means and the image pixels are again assigned to the nearest cluster. The process is iterated a specified number of times until there is either no significant change (the user may input the amount of change considered to be acceptable or the algorithm may use standard statistical values) in the location of the cluster means from one iteration to the next, or the maximum number of iterations specified is reached. The user must then determine the land cover class that is associated with each spectral cluster (Lillesand and Kiefer, 1994).

User Selection Of Training Samples in Supervised Classification

One of the first steps in supervised classification is the selection of sample training areas. The overall goal of training site selection is to assemble a set of statistics that represent the spectral response patterns of all the land-cover classes being used in the classification (Lillesand and Kiefer, 1994). Typically, training sites are selected following field investigations and are commonly selected on-screen through the delineation of polygons or individual pixels. The multispectral image data within the polygons are then extracted and summary statistics calculated for each polygon or for groups of polygons of a selected class. These statistical descriptions typically include the number of samples, the mean, standard deviation, variance, minimum value, maximum value, variance-covariance matrix, and correlation depending on the classification algorithm being used. They are used in subsequent separability analysis and classification.

Separability Analysis

A separability analysis of the sample spectral data is conducted as an indicator of the potential accuracy of the resulting thematic map or to aid in selection of a subset of spectral bands and other data layers to include in the classification process. It involves determining the statistical separation between spectral response patterns for all pairs of classes (Jensen, 1996). A range of statistical parameters can be used to measure separability, one of which is divergence, a covariance-weighted distance between the mean values of the classes (Lillesand and Kiefer, 1994). Transformed Divergence is one

of the most commonly used divergence measures, others include average divergence, Bhattacharyya distance, and Jeffreys-Matusita Distance (Jensen, 1996). For this research the Transformed Divergence separability measure was used. It gives an exponential weight to increasing distances between the classes; therefore, the larger the divergence, the greater the separability. Values of between 0 and 2000 are obtained, where 0 indicates very poor separability and a value of 2000 indicates excellent between-class separability (Jensen, 1996). The image analysis package EASI/PACE from PCI Geomatics Inc. used in this thesis scales the values by a factor of 1/1000 to between 0 and 2, where 0 indicates very poor separability and values of 1.9 to 2 indicate excellent separability. Separability analysis, as described above, can be used iteratively in training site refinement. If the separability between classes is poor, then the training polygons for those classes can be modified to improve it.

3.2.1 Image Classifiers

Maximum Likelihood Classification

The Maximum Likelihood Classifier (MLC) is a parametric technique that works by computing a mean vector, variance, and correlation matrix for all classes in the training data (Peddle, 1993). Sets of probability functions for all classes are estimated from the sample data. These functions are used to assign each image pixel to one of the classes (or to a null class) based on the relative likelihood that the pixel belongs to each class. The likelihood of pixels belonging to certain classes can be affected by *a priori* knowledge. In the software used, this knowledge is in the form of a bias factor which is

the value that allows determination of which class a pixel belongs to in the case of a tie between classes (PCI, 1996). Pixel assignment is also affected by the threshold value set for each class. The threshold is the number of standard deviations to be used to define the boundary in spectral space of each class. Beyond this threshold, a data point, or pixel, has such a low probability of inclusion in a given class that the pixel is excluded from that class (PCI, 1996).

The MLC assumes that the input data are multivariate normally distributed, independent, and have approximately equal variances. If these constraints are reasonably met, then the MLC is well suited for providing optimal classification accuracies using a limited number of variables (Peddle, 1993). The MLC is often used as a reference for classifier comparison because, if the class probability density functions are indeed Gaussian, it is the optimal classifier (Paola and Schowengerdt, 1995).

Neural Network Classification

Neural network classifiers are capable of incorporating non-normal data. They are commonly used in artificial intelligence applications and have become practical tools for use in many classifications, pattern recognition, optimization and forecasting applications (Miller *et al.*, 1995). Neural networks are modeled after the constructs of the human brain. Knowledge is stored in the form of weights that are applied to a node (inputs). A neural network can be used as a form of supervised classification where, instead of an algorithm that determines values such as in statistical classification, the network is presented with repeated examples of inputs and corresponding correct

outputs, and allowed to 'learn' what the correct classification process should be (Miller *et al.*, 1995). Human beings learn by experience; neural networks learn by setting weights that will produce a specified output.

Many variants of neural network algorithms can be used. Two types are the feedforward and back propagation. Forward feeding networks are two layer networks that are fixed in the number of units and connections. The input signals in a feedforward network are sent towards the intermediate hidden layer over connections that either attenuate or amplify the signal, with each hidden layer processing them in the same way. The signals are then sent to the output layer with no feedback loop back to the hidden layer (Gopal and Woodcock, 1996).

This is quite different from the back propagation network. The back propagation neural network typically has a three layer configuration with an input layer, an output layer, and a hidden layer (Paola and Schowengerdt, 1995). The input layer contains a node for each input band of multispectral imagery and the output layer contains a node for each desired class label. The hidden layer is needed to process the data which are not linearly separable (Miller *et al.*, 1995). Within the network, the signals between the layers are adjusted iteratively and different weights are applied to each connection of the hidden layer. These weights are adjusted in order to minimize the global error of the entire network. To achieve the lowest possible global error, the iterative adjustment of weights should be very small. However, this would result in an excessive amount of time required to train the network. This is overcome by specifying a learning rate. The

learning rate represents the percentage of the step towards the global error (Paola and Schowengerdt, 1995). A larger learning rate can speed up training although there is an increased risk of oscillation or non-convergence of the segment. Furthermore, with a small learning rate, the network may require more training iterations to reach the minimum acceptable error.

During training, the network will take the steepest descent from one position to the next position to achieve a lower error. Along the way the network can encounter valleys or local minima. This can cause the network to become stuck and the error will not decrease to the global error. The network can also oscillate between a local minimum and the global error (Paola and Schowengerdt, 1995). These problems can be eliminated with the specification of a momentum parameter which is set at the beginning of the training phase. A larger momentum rate can allow for an increase in the learning rate without the risk of oscillation or non-convergence, however, the global error may not be reached because larger steps are taken between the iterations.

Neural networks have been compared to MLC and proven useful with a minimal training set (Miller *et al.*, 1995) additionally, other research by Foody *et al.* (1995) indicated that the classification accuracy was increased significantly as a result of increasing the number of training cases.

Contextual Classification

A context classifier is different from conventional per pixel classifiers because it uses not only the spectral information at each pixel, as do other classifiers, but it also

uses the spatial features derived from spectral information (Gong and Howarth, 1992). The spatial information is derived from a sample window of several pixels, where the neighbours of the central pixel are considered in the classification.

The classifier that was used in this research involved grey-level reduction of the data and a frequency-based contextual classification (Gong and Howarth, 1992). In order to process large amounts of data in contextual classification, the number of grey-level vectors in multispectral space is reduced. This is achieved through grey-level vector reduction such as an eigen-based method involving principal component transformations. Occurrence frequencies, the number of times that a pixel value occurs in a specified window, are determined to generate a table for every pixel in the image (Gong and Howarth, 1992). A minimum distance classification is then applied to the frequency tables. For given mean histograms of all land-use classes the distances are compared by the classifier against the histogram of a given window, based on the frequency table, and the centre pixel of the window is assigned to the class which has a minimum distance (Gong and Howarth, 1992).

3.3 Textural Analysis

Image texture refers to the frequency of change and arrangement of tones (Jensen, 1996), which takes into account the variability of the grey values within a region of an image or over the entire image (Augusteijn *et al.*, 1995). One of the most common uses of texture analysis is to incorporate spatial information in classification of images.

Classification is typically based on spectral information only, although, researchers have begun to include texture measures in the classification of images (Augusteijn *et al.*, 1995; Carr, 1996; Palubinskas *et al.*, 1995). Through the addition of the texture of image features, the accuracy of the classification can be increased (Peddle and Franklin, 1991).

Two common approaches to texture classification involve first-order statistics and second-order statistics. A third texture approach, Fourier power spectrum texture measures, is not considered as this approach is generally inferior to the statistically based measures (Jensen, 1996). First-order statistics involve measures derived from the raw image data, such as means, variances, skewness, and kurtosis. For example, the standard deviation of brightness values within a window of specified size, moved over an entire image, provides a measure of the spectral variability over short distances and, as such, is a measure of local texture (Campbell, 1987).

More sophisticated measures include second-order texture measures, which are derived from a dataset which itself was extracted from the raw data. Co-occurrence texture measures are one set of second-order measures which calculate a set of features based on the co-occurrence of grey levels in pixel pairs with a specific orientation to one another. A matrix is calculated giving the frequency of occurrence of all pairs of grey levels in the specified image area. High frequencies of occurrence on, or near, the diagonal of the matrix indicate smooth or uniform texture as many adjacent pixel grey levels are similar. High frequencies farther from the diagonal indicate rougher textures. From the co-occurrence matrix, many measures of texture can be derived. They include

entropy, angular second moment, contrast, mean, and correlation (Peddle and Franklin, 1991). Each is designed to extract a particular characteristic of the spatial information. For example, the contrast measure sums the frequencies at each position in the co-occurrence matrix times the grey level difference so that off-diagonal occurrences (higher texture) are weighted more (Carlson and Ebel, 1995). Several comparative studies have found that co-occurrence measures of texture are superior to other texture measures in increasing classification accuracy (Augusteijn *et al.*, 1995).

3.4 Vegetation Indices

Vegetation indices are mathematical image transformations that are designed to be sensitive to plant health. They are generally divided into two categories, ratios and orthogonal indices, the ratio indices being the most commonly used and typically being derived from red and near infrared spectral data (Elvidge and Chen, 1995). They work by contrasting the intense chlorophyll pigment absorption in the visible (usually red) against the high reflectance by plant material in the near infrared. Their use in estimation of vegetation variables such as percent cover, leaf area index, and absorbed photosynthetically active radiation has been investigated for modelling of vegetation parameters and processes as discussed in section 2.4.

Ratio vegetation indices include among others, the simple ratio index (SRI) (see 5.4.1) and normalized difference vegetation index (NDVI). These two indices take advantage of the complementary reflectance of red and near infrared energy. Variations

of ratio indices, such as the soil adjusted vegetation index (SAVI) (see 5.4.1) incorporate factors such as reflectance of background properties like soil and rock material. These factors can affect the indices particularly when there is a low level of vegetation cover (Elvidge and Chen, 1995). Orthogonal vegetation indices use the distance from a soil line, defined by samples of bright and dark soils, as a measure of the amount of vegetation (Elvidge and Chen, 1995). They include the perpendicular vegetation index (PVI) and the difference vegetation index (DVI).

There are several ways in which background properties such as soil and rock can affect vegetation indices. For example in a simple ratio of NIR to Red, soil, with a greater reflectance than vegetation in the red, increases the denominator while its lower near infrared reflectance decreases the numerator, causing a significant decrease in the ratio. In addition, vegetation over a bright background will result in a lower vegetation index than for the same vegetation over a dark background (Elvidge and Chen, 1995).

Another influence of the background materials on vegetation indices is the mixing of background and canopy reflectance, a process which is most significant in the NIR as a high proportion of this energy is transmitted through the canopy to the ground. Near infrared radiation transmitted through the canopy can either be reflected or absorbed by background materials. For bright backgrounds, there is an increase in near infrared radiation due to reflectance of the transmitted radiation by the background. The magnitude of mixing between the plant canopies and the background material is directly related to the brightness of the background and the wavelength-dependent transmission

of light through the canopy (Elvidge and Chen, 1995). This effect of mixing can lead to higher vegetation index values over brighter backgrounds, which is opposite to the influence described above and thus, the background effects may be somewhat moderated.

Chapter Four

Study Areas, Image Acquisition and Field Data

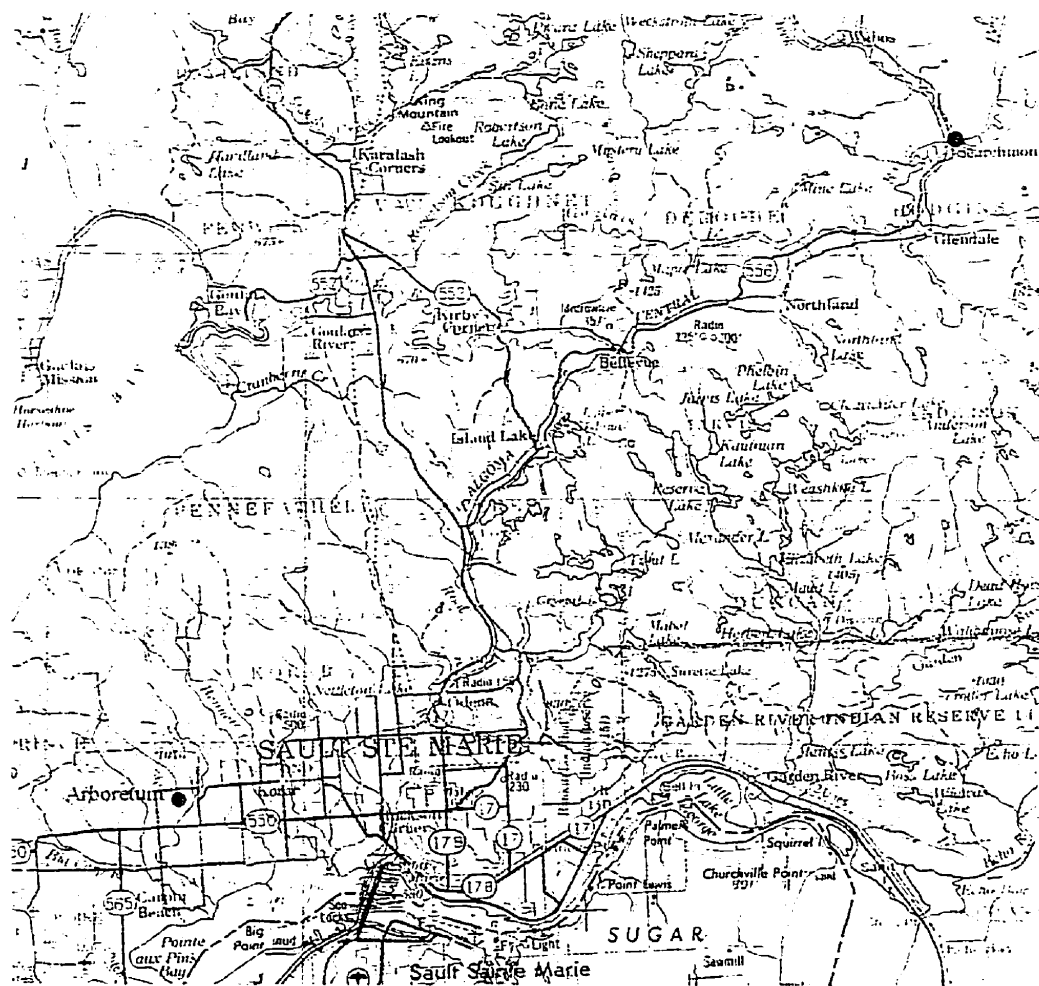
4.1 Location and Description of Study Areas

The study areas consist of two regeneration sites located in west-central Ontario near Sault Ste. Marie (Figure 4.1). The first site is a forest tree nursery (arboretum) located in the west end of the city. The second site is a natural clearcut situated north-east of the city in the Searchmont area. The Ontario Forest Research Institute (OFRI) operates and maintains both sites.

The arboretum contains three blocks (loam, sand, and clay), which are identical in layout and plant setup. There are eleven, 14m x 28m plots at each block, each containing the crop species jack pine (*Pinus banksiana*) and black spruce (*Picea mariana*) and one competition species. The competition species are as follows:

Trembling Aspen	(<i>Populus tremuloides</i>)
White Birch	(<i>Betula papyrifera</i>)
Green Alder	(<i>Alnus crispa</i>)
Upland Willow	(<i>Salix humilis</i>)
Red Raspberry	(<i>Rubus idaeus</i>)
Fireweed	(<i>Epilobium angustifolium</i>)
Large-Leaved Aster	(<i>Aster macrophyllus</i>)
White Clover	(<i>Tifolium repens</i>)
Braken Fern	(<i>Pteridium aquilinum</i>)
Blue-Joint Grass	(<i>Calamagrostis canadensis</i>)

Figure 4.1
Location of Research Study Areas

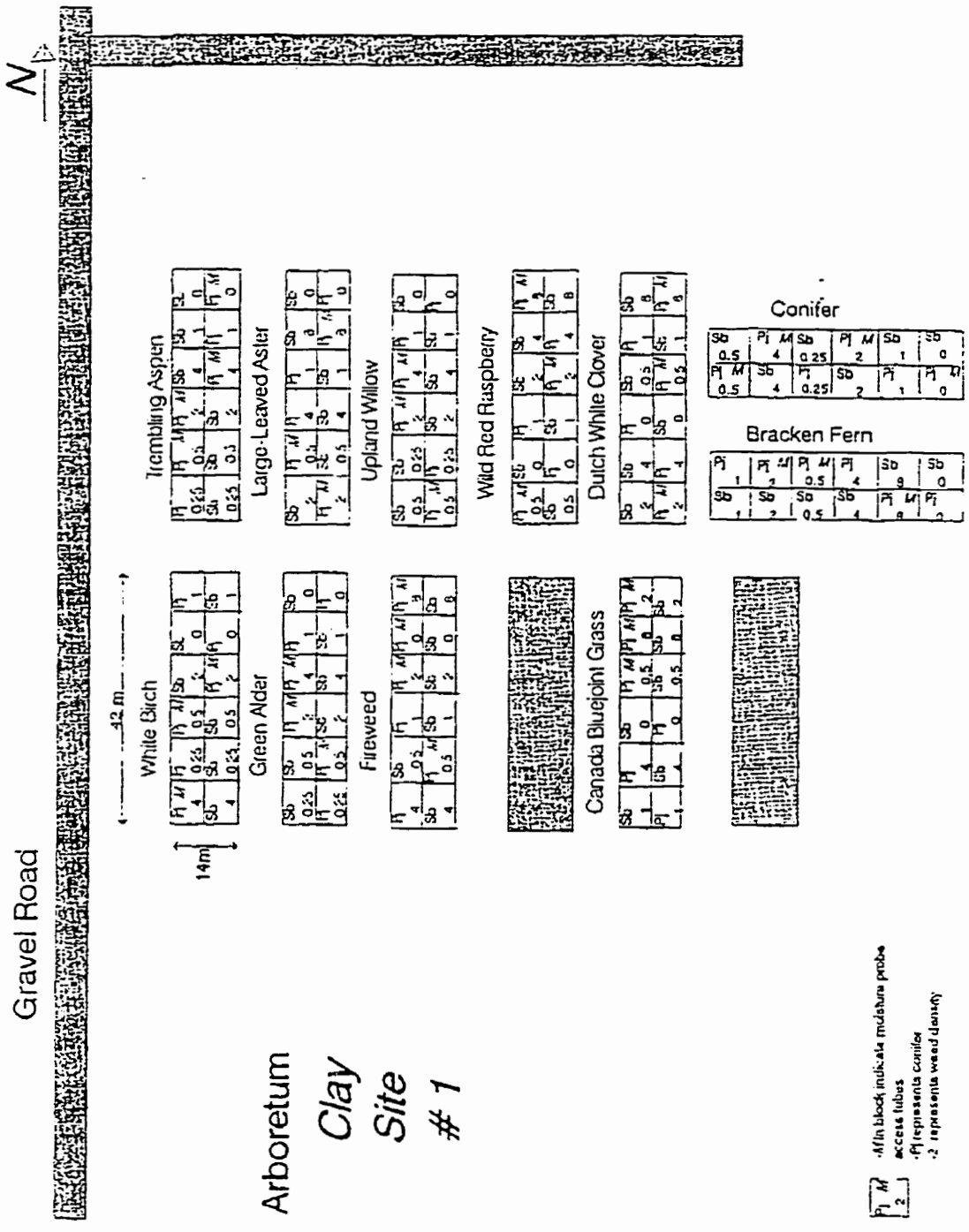


Adapted from Natural Resources Canada (1983) - NTS Map Edition 2, scale reduced to 1:312,500

There are twelve, 7m x 7m experimental units within each plot, each containing either jack pine (Pj) or black spruce (Sb) and one competition species at a specified density, with the crop trees planted every metre. Densities of selected competition for raspberry, bracken fern, fireweed, aster, clover, and blue-joint grass are 0, 0.5, 1, 2, 4, and 8 plants per metre square. For the remaining competition species (trembling aspen, white birch, green alder, upland willow, and conifer trees planted in competition with each other), the plant densities are 0, 0.25, 0.5, 1, 2, and 4 plants per metre square. Competition species' densities are allocated to experimental units in a randomized block design. To maintain a single competition species and specified plant density, plots have been hand-weeded. The study has been in place since 1994. Figure 4.2 shows the set-up of the clay plot.

The Searchmont site contains four, 28m x 28m plots, with ten 7m x 7m experimental units. Each unit contains four coniferous species: red pine (*Pinus rubens*); white pine (*Pinus strobus*); jack pine; and black spruce, with natural herbaceous competition. A herbicide program with ten different treatments has governed the growth and amount of competition on each plot. Treatments were applied in a sequential pattern for the first five years after tree planting: no vegetation removal, annual vegetation removal, 1, 2, 3, and 4 years of consecutive removal, and waiting 1, 2, 3, and 4 years before annual removal was initiated. The study has been in place since 1992 and ended when all treatments were applied in 1996. Figure 4.3 shows an airphoto with a plot layout overlay.

Figure 4.2
 Plot, Density and Conifer Layout Based on Competition Species
 of the Clay Site at the Arboretum



4.2 Data Acquisition

The image data for this research were obtained in August, 1996, using the Kodak Digital Camera Series (DCS) 420IR colour infrared camera which was graciously provided by the Kodak Eastman Company of Rochester, New York. The DCS 420ir consists of a Nikon N90 camera body with a 28mm lens, which focuses the image onto a charged couple device (CCD). A CCD is a solid-state chip containing a series of light sensitive photosites. The CCD in the DCS 420ir camera is of medium format, containing 1524 by 1012 pixels for a total of 1.5 million light sensitive pixels (Omer, 1997). This provides a chip resolution that approaches that of standard 35mm colour slide film; however, the 35mm slide film covers 2.6 times the ground area of the digital camera images for a given lens focal length (Greenfield and Maus, 1997). Digital images are obtained from the photosites which convert the incoming spectral energy into electrons. Electrons pass through an analog-to-digital converter and a file of digital information is produced in which bits represent colour and tonal values of a target. Photosites within the CCD are square, resulting in an image with square pixels and equal resolution in both directions.

The three different wavelengths, in this case the green (500-600nm), red (600-700nm) and near infrared (700-800nm), are captured in a single, full frame. A filter is placed over each photosite in the sensor chip, giving it the ability to capture green, red, or near infrared information. Thus, only one of the three wavebands is actually acquired at each photosite. As a result, the spatial resolution is degraded to approximately 80%

of the resolution of a panchromatic DCS camera (King, 1995). Each image in this raw format is stored on a removable hard disk within the camera. The hard disk used in this research could hold up to 105 images. The images can be downloaded and stored in a computer in their raw format. However, for display and analysis of three-band data, the other two wavebands at each pixel must be derived. This is conducted through a Kodak proprietary interpolation process where, at each photosite, digital numbers for the two bands which were not sensed are calculated using weighted averages of their values from the closest photosites which contain those bands. This procedure is automatically conducted upon opening an image file with a computer program such as Adobe Photoshop using a Kodak driver. It produces full three-band images which are three times the size of the raw image format.

The flights were carried out with the assistance of the Canadian Forest Service. A mount was constructed for the digital camera which was placed in the hopper of a Cessna 188 "Ag-Truck" single person agricultural spray aircraft. The pilot operated the digital camera through a remote trigger, with the aid of a real-time video image displayed on a small monitor. Forty digital images were obtained from nominal altitude of 80 m (250') above ground over the arboretum. Ground pixel size was approximately 2.5 cm. At an aircraft speed of about 45 m/s, to obtain about 50% overlap between images, the images had to be acquired using the camera's burst mode. In this mode, 5 images can be acquired into the camera's RAM in about 2.25 seconds, but after this, a period of about 12 seconds is required to download the images to the camera's hard disk. As such,

abilities at such low altitude. The shutter speed of the camera was set to 1/4000s to optimize the trade-off between image motion during exposure and the exposure level. At this setting there was approximately 1 pixel of image motion and the exposures generated typically consisted of about 120 grey levels. An exposure of 1/8000s (the fastest available) was more desirable, but test images showed that there were too few grey levels for adequate classification and statistical analysis. The image motion and limited range of grey levels had to be accepted due to the type of aircraft that was used. A slower aircraft is more appropriate for operational situations and would result in a decrease in image motion to suitable levels of less than half a pixel and allow for improved exposure settings.

Each acquired image covers an area of 38.1 m x 25.3 m, or approximately 964 m². Images were acquired for each of the three blocks at the arboretum and for two of the plots at Searchmont. Data were also obtained with a ground pixel size of 5cm as a backup in case the image motion was excessive in the higher resolution data. However, due to the scale of the features being studied, only the 2.5 cm data were utilized. Figures 4.4 and 4.5 show mosaics of the arboretum and Searchmont images.

Investigation of the arboretum image data revealed that the most complete coverage was obtained for the clay and loam blocks. The amount of data obtained for the clay plot was greater than the loam block, as whole plots with full ranges of densities for three competition types had been imaged. Consequently, the clay block was used more extensively in this research. The Searchmont data were obtained for two of the

plots and were incorporated in the first objective as an 'operational' test of the classification which obtained the highest accuracies at the arboretum site. The limited coverage of the digital imagery was a result of navigational difficulties at the Searchmont site, (due to surrounding hills), and the early termination of the flights over the arboretum site (due to complaints about noise filed by neighbouring residents).

For comparative purposes, 35 mm colour and colour IR slides and prints were also obtained for scales equivalent to the 2.5 and 5 cm digital data. The scales for the photos and slides were calculated to give approximately the same spatial resolution, in line pairs millimeter, as the digital camera imagery. Flight parameters were then established based on the desired resolution and camera attributes (focal length, shutter speed, etc.). These photographs were acquired for comparison of visual interpretation, as backup in case the digital imagery was not sufficient, and to assist in identification of the location of the digital images as a result of the greater coverage by the 35 mm photographs. Locational identification of the digital images was also facilitated by the plot labels that were set out at both ends of the plots by the Canadian Forest Service.

Vegetation measurements, acquired by the OFRI as part of their field research, were obtained for the arboretum, specifically the clay block and the Searchmont site. These measurements included conifer survival, percent vegetation cover, and leaf area index. Measurements of percent cover and leaf area index at the arboretum site had been sampled for the competition species on jack pine experimental units only. Searchmont field measurements were not used in this research.

Figure 4.4
Mosaic of Digital Camera CIR Imagery
for Arboretum Site

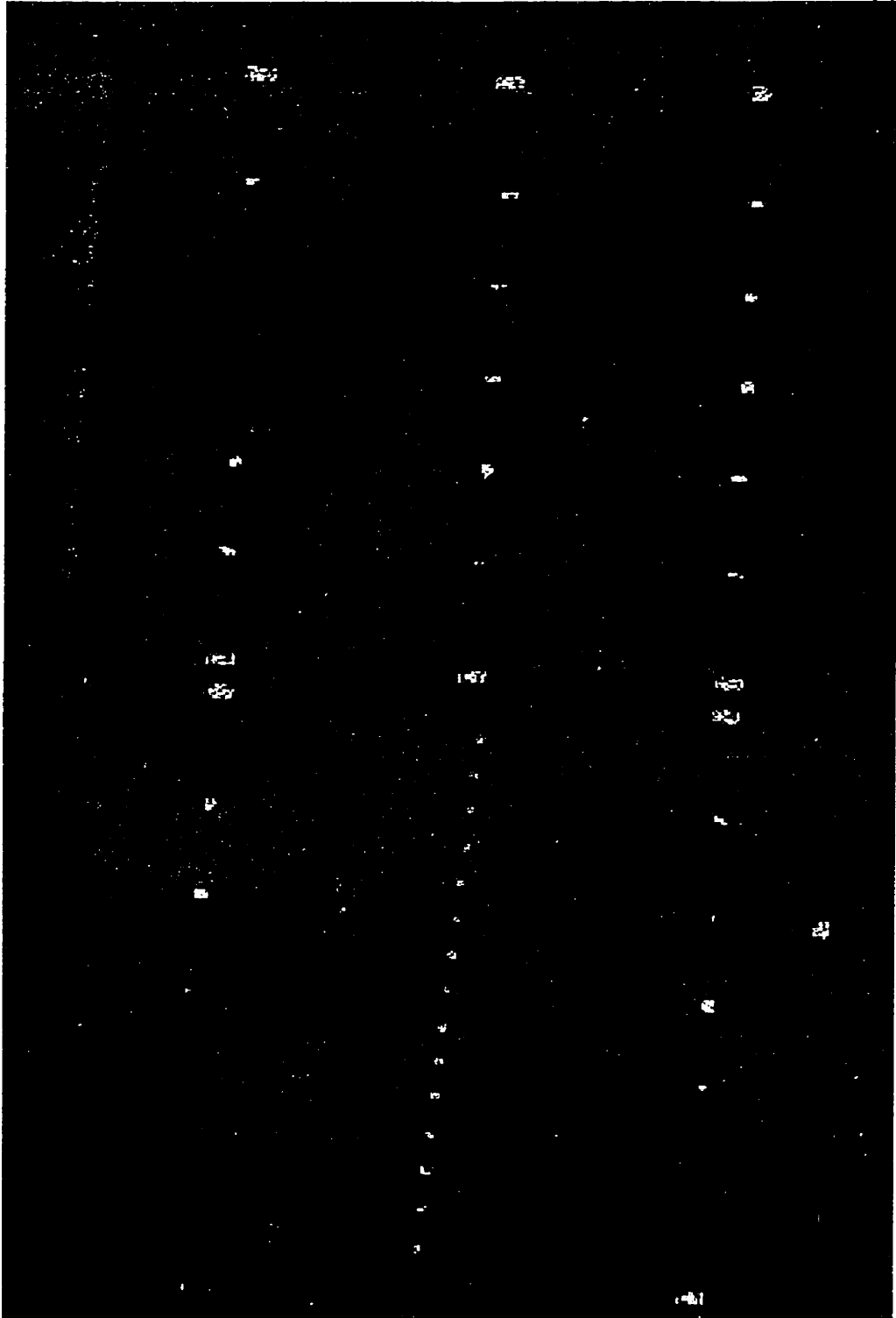


Figure 4.5
Mosaic of Digital Camera CIR Imagery
for Searchmont Site



Chapter Five

Methodology

5.1 Introduction

There were two phases to this research, reflecting the two objectives. The first involved evaluation of conifer and competition species identification through automated classification procedures and the production of thematic maps of the regeneration site. The second phase involved assessing whether field measured values of selected vegetation parameters (leaf area index (LAI) and percent cover) could be related to statistical analysis of grey level values extracted from the imagery.

The underlying approach to this research was to work within a digital environment, thereby providing a feasible methodology that could be readily transferred to an operational setting. A PC platform was utilized, representing a minimal operational investment as opposed to a higher-end workstation or UNIX platform. Commercially available image analysis software (PCI EASI/PACE) was used to conduct all image analysis for this research. Statistical analysis was conducted using a SPSS statistical software. This chapter describes the methods used in phases one and two.

5.2 Data Preparation

To conduct computer analysis of the acquired digital imagery, the first step involved extraction of the data from the camera's hard drive. Images were downloaded

to a Macintosh computer and were expanded to their final format using the Macintosh Kodak driver for Adobe Photoshop. Images were then saved in a "TIFF" format and imported into PCI's EASI/PACE image analysis software. This original, unenhanced data were used in subsequent analysis.

5.3 Phase 1

5.3.1 Separability Analysis

Preliminary investigation of the image data was conducted on single images from the clay and loam blocks at the arboretum. Spectral data were extracted for a subset of competition species that were available in the imagery, namely: trembling aspen; upland willow; red raspberry; fireweed; large-leaved aster; braken fern; and blue-joint grass. Two approaches were undertaken in the selection of sample polygons. The first approach involved establishing a reference separability. Spectral data were generated for the conifer trees, jack pine and black spruce, and each of the competition species in areas of the image where no direct competition between conifers and competition was present. Analysis of the statistical separability of the conifers from the competition in this case gave an indication of the spectral distinction between classes, given that there were no mixed pixels. The second approach involved determining separabilities of the conifers from the selected competition at the various competition densities available.

Polygon training areas were visually delineated on the image for each conifer and competition species, for both reference and density dependent separabilities. Illuminated

(direct and diffuse) portions of the conifer trees and competition were selected at a maximum of 30 pixels per tree or plant. A total of between 150 and 300 pixels were sampled for each species in all paired separability tests. Image data were not limited to only the most sunlit portion of the trees or competition plants to represent a more operational approach. However, in polygon delineation, shadows were avoided as they can severely increase spectral data variance for any vegetation class. The decision to extract image data from a wider portion of the crowns of trees and plants was based on previous research by Gougeon (1995) which indicated that typical multispectral mean values of tree crowns, where the sampling was not restricted to the sunlit portion only, produced one of the most accurate classifications (~72%) in comparison to classifications using only the sunlit portions of the training data.

A separability analysis was then conducted using the spectral data extracted from the images for each training polygon. Transformed Divergence was calculated, with a value of greater than 1.9 indicating good separability, values between 1.7 and 1.9 indicating average separability, and values less than 1.7 indicating poor separability (Lillesand and Kiefer, 1996). This initial investigation was followed by a test classification using the maximum likelihood algorithm to investigate how the classes with poor separabilities would be represented within the classification.

5.3.2 Production of Mosaic Image for Further Analysis

After the preliminary separability analysis, images from the clay block were combined to form a mosaic image which provided a full range of densities for selected

competition species. Starting with mosaic production from two adjacent images, additional images were added in an iterative procedure. Ground control points (GCPs) were manually selected from the overlap area between the two images being joined. GCPs are required in order to rectify one image to another. Four GCPs were selected in each pair of images and were used in a first-order, nearest neighbour transformation. GCPs such as tree crowns, dead trees, plot edges, plot markers, and a person's sneakers were used. A total of 12 images from the clay block at the arboretum and 9 images from the Searchmont site were mosaiced into single images. The mosaics for both the arboretum and Searchmont site are in Figures 4.4 and 4.5, respectively. The images have been re-sampled for reproduction purposes, therefore, the resolution has been significantly degraded.

The creation of a complete image mosaic for the clay block allowed easier extraction of spectral data, classification, and analysis of results. This mosaic image was then used in an unsupervised classification as well as three different supervised classifications.

5.3.3 Evaluation of Automated Classification Methods

Unsupervised Classification

The first classification was conducted using an unsupervised K-means classifier on the mosaic image with all three spectral bands (green, red, near infrared) as input information. An output of eleven clusters was specified with a total of twenty iterations run. Eleven clusters were specified to correspond to the vegetation and land cover

classes visually identified in the imagery. A seed file was not specified; therefore, the algorithm arbitrarily selected the location of the initial mean vector.

Supervised Classification Training

Since the initial separability analysis (5.3.1) had been conducted on an image-by-image basis, new polygons were delineated for spectral data extraction from the mosaic. Eleven classes were identified: conifer trees (jack pine and black spruce), fireweed, upland willow, raspberry, blue-joint grass, large-leaved aster, soil, grass, shadows, and a null class.

Maximum Likelihood Classification

The second classification procedure was the Maximum Likelihood Classification (MLC). The classification was applied to the three spectral bands using the eleven classes, with threshold and bias values for all classes of 3 and 1, respectively. A threshold value of 3 standard deviations was selected for all classes because knowledge of the site was extensive, and therefore the chance of incorrectly selecting training pixels not representative of a given class was very limited. All classes were given an equal bias value because a change in bias would have subjected the classification to *a priori* knowledge on the part of the user, and would unjustifiably give more weight to specific classes.

Neural Network Classification

The third classification conducted was an artificial neural network (ANN). The first step in applying the neural network to the image was to create a neural network

segment using the three spectral bands and the eleven class signatures. This segment was then used to train the neural network with 10,000 iterations and a learning rate and momentum of 0.1 and 0.9, respectively. The learning and momentum rates affect how quickly the neural network reaches the global error set at 0.01. Arbitrary variations of the momentum and learning rates were investigated and the lowest error was obtained for the values listed above. The trained neural network segment was then used to classify the image and create a thematic map.

Context Classification

The fourth classification that was conducted was a context classifier. A context classifier takes into consideration the pixels surrounding a location as opposed to conventional classifiers such as the MLC and ANN which conduct a per-pixel classification and consider pixels in isolation (Gong and Howarth, 1992). In order to implement the context classifier, the spectral dataset was reduced from multiple input bands (green, red, near infrared), to one information band using an eigen-based grey-level vector reduction method (Gong and Howarth, 1992). The context classification was then conducted on this single information band using the eleven class signatures and a pixel window size of 9 by 9. This window size was selected after investigation revealed that other window sizes did not identify the planting structure of the plots as well and certain classes were not correctly identified.

5.3.4 Texture Analysis

The third step of the first phase involved incorporation of the spatial information in the image through the use of texture measures. Two co-occurrence texture measures, Standard Deviation and Variance, were implemented on the red spectral band. The Standard Deviation texture measure is calculated by using the co-occurrence matrix to obtain the frequency of occurrence of a given grey level pair. This frequency is multiplied by the squared difference between the given raw grey level and the mean grey level of the matrix. This is conducted for all matrix cells and the result is summed and the square root taken. The resulting value becomes the new grey level value of the centre pixel in the moving window. This process is repeated at each iteration of the moving window (PCI, 1996). The variance texture values are calculated in a similar manner to the standard deviation; however, the square root is not taken. The red band was used because of the distinct visual difference in grey levels between vegetation and soil, which was judged to provide better potential for representation of the spatial information using the texture measures.

Other co-occurrence (Homogeneity, Contrast, Dissimilarity, Mean, Angular Second Moment, Correlation, and Entropy) and grey level vector difference (Mean, Angular Second Moment, Contrast, and Entropy) texture measures, a variety of window sizes (5 x 5, 7 x 7, and 9 x 9) and spatial sampling directions (one pixel to right, one pixel up, one pixel up and to the right, and an average of all spatial directions) were also investigated. However, the two co-occurrence texture measures selected with a pixel

window size of 3 by 3 and a spatial sampling direction of one pixel below the centre pixel provided the best visual texture representation. The other texture images did not identify the change in texture from the crowns of vegetation to the soil as well as the two co-occurrence texture measures chosen. Other quantitative evaluation methods, such as determination of the correlation of the texture measures with the spectral band that was used to derive the texture information and selection of the least correlated texture measure, or evaluation of correlations of each texture measure with the biophysical parameters of interest, (Olthof and King, 1997) were not conducted due to the large amounts of data processing that would be required to test all of the co-occurrence and grey level vector difference texture measures.

The resulting texture images were extracted into a 32-bit data channel and then scaled to 8-bit for inclusion in the classification process. The four classifiers: unsupervised, maximum likelihood, neural network, and context, were all conducted twice more, using the same parameters discussed above on combined data sets consisting of the three spectral bands and one of the texture measures.

5.3.5 Accuracy Assessment

The final step of the first phase involved an accuracy assessment of the classified images. Upon determining that per pixel separability between conifer trees and competing species was quite low, and that the potential per pixel accuracy of any thematic classification was low, an alternative approach to accuracy assessment was developed. Since the primary focus of the phase 1 research was the classification of

objects (trees), an object oriented approach was taken to conduct the accuracy assessment. For the assessment, only the competition plots that contained a full range of plant densities were considered. These included: fireweed, upland willow, and red raspberry. Other plots with blue-joint grass, large-leaved aster, and Dutch clover, were not used for two reasons: either they did not have a full range of densities or they were in a poor state (e.g., excessive weed growth).

Experimental units for the three full density plots were divided into separate images based on density. The resulting sixteen images contained the unsupervised, maximum likelihood, neural network, and context classifications for the spectral information alone, and the same classifications with the inclusion of the two texture measures. Bitmaps of the two conifer classes were extracted from the classification images and a graphical mask was applied to the experimental units to eliminate all areas outside of the plot. Next, polygons were numbered within each of the experimental units to identify each polygon that was classified as a conifer. The number of pixels which should be taken to represent only the core of a conifer seedling was not known so for the given pixel size (2.5cm) and typical tree height and diameter, empirical testing of polygon sizes between 9 and 20 was conducted. The polygon sizes are based on the size of the core area of the crown and do not represent the whole crown which would be greater in size. Only the core of the crown was used in determination of the polygons sizes as the test classifications showed that the outer portions of the conifer crowns were not being identified as coniferous.

The total count of conifer cores for each experimental unit was used to conduct an initial accuracy investigation. These counts were compared to the actual number of conifers for each experimental unit and a value representing the percentage of over-estimates (positive number) or under-estimates (negative number) of the number of trees was obtained and graphed. These values were used to determine the best five classification combinations. A more comprehensive accuracy assessment was then conducted for the best five classifications to determine the errors of omission and commission for the experimental units where no competition was present.

The omission and commission errors were used in the calculation of the User's and Producer's accuracy for each of the plots. User's accuracy represents the probability that a tree classified on the map is actually that tree class on the ground and is determined as 100% minus the errors of commission (trees classified which do not exist) (Jensen, 1996). The Producer's accuracy indicates the probability that a known tree was correctly classified and is determined as 100% minus the errors of omission (existing trees that were incorrectly classified) (Jensen, 1996).

5.3.6 Evaluation of Classification using Searchmont Image Data

To determine how well the classification of a controlled vegetation complex, such as the arboretum site, would perform in an operational setting, the classification method that produced the highest accuracies for all three plots was implemented on the Searchmont study site data. The four conifer classes were extracted out of the classification and individual polygon identification labels were created for all those

polygons with greater than 100 pixels. A threshold of 100 pixels (625 cm²) was chosen for the Searchmont site as opposed to the range of 9 to 20 pixels used for the arboretum accuracy assessment because the trees at the Searchmont site are older and therefore the diameter of the core area of the crown is larger.

Two of the three plots (3-6 and 4-10) in the Searchmont image were used to conduct an accuracy assessment (see Figure 4.3). This assessment involved determining errors of omission and commission, and determination of User's and Producer's accuracy for each of the plots.

5.4 Phase 2

The purpose of the second phase of the research was to assess whether statistical analysis of grey level values extracted from the imagery could be statistically related to corresponding field measured values of leaf area index (LAI) and percent cover. The methods used to conduct this phase of the research are outlined in the following sections and were conducted using spectral image data, spectral transformations, and texture data derived from the digital imagery.

5.4.1 Vegetation Indices

Three vegetation indices were derived using the red and near infrared spectral data. The first two are standard indices; a ratio vegetation index (RVI) which is derived by simply dividing the measured brightness of the near infrared band by the brightness of

red band (Equation 5.1) and the normalized difference vegetation index (NDVI) (Equation 5.2).

$$RVI = \frac{NIR}{Red} \quad 5.1$$

$$NDVI = \frac{NIR - Red}{NIR + Red} \quad 5.2$$

The third vegetation index that was used in this research was the soil adjusted vegetation index (SAVI). This index takes into account the spectral properties of the background soil which can have adverse effects on such indices, especially when there are low levels of vegetation present. A soil adjustment factor (L) is added into the equation (5.3) and is typically set to 0.5 (Elvidge and Chen, 1995).

$$SAVI = \frac{NIR - Red}{NIR + Red + L}(1 + L) \quad 5.3$$

The index values generated were left as 32-bit data to maintain the resulting data range and precision; if the index values were scaled into 8-bit values, then the grey level values would be similar for all the vegetation indices. Such a loss in precision would negate the purpose of exploring different types of indices.

5.4.2 Statistical Database Compilation

To conduct statistical analysis on the grey level values, they needed to be extracted from the imagery at the same location as the field samples on only the experimental units of jack pine trees; field measurements were not conducted on black

spruce units. Graphic polygons were delineated over the conifer trees in the image at the three field sample locations for each of the density plots.

Polygons covered an area of one metre square (approx. 1936 pixels) and were centred on each jack pine tree. Grey level values were obtained for the raw spectral bands, both texture measures identified in phase one, and all three vegetation indices. The mean and variance of the grey level values for each of the variables were extracted and placed into a statistical package with the field measured values for LAI and percent cover. All remaining statistical analysis was conducted using the image and field information contained in this database.

5.4.3 Statistical Analysis

Tests for normality using skewness and kurtosis were conducted on the database. Those data which were not normally distributed were transformed using a logarithmic transformation to achieve a normally distributed dataset.

Linear, bivariate correlations were conducted separately using the mean and variance of each image variable against each field variable to determine the strength of their relationships. Probability values were also calculated to determine the significance of the correlation values obtained. Investigation of the correlation analysis results involved not only examination of the strength and significance of the correlations for each variable pair, but also comparison of the r-values obtained for the 1st order measurements (grey level values for the spectral bands) to those r-values obtained for the 2nd order measurements (co-occurrence texture measures). Furthermore, the r-values

obtained for the 2nd order co-occurrence texture measure, Variance, were compared to those obtained for the statistical variance derived from the raw imagery and the spectral transformations, which can be considered as 1st order texture measures.

A forward stepwise multiple-regression analysis was conducted separately for the mean and variance of all image variables against the field measured values of LAI and percent cover in order to determine how well spectral and textural information obtained from the digital images could predict the field measures. Regression coefficients, standard errors, and F-statistics were calculated to determine the strength of the relationships, the level of significance, and the contribution of each of the variables to the regression equation.

Chapter Six

Results and Discussion

6.1 Introduction

Results of analyses that were conducted during this research are presented and discussed in the following sections. The initial separability analysis that was conducted will be discussed first, followed by the classification and accuracy assessment results. The final portion of this chapter will discuss results of the statistical analyses that were conducted as part of the biophysical modelling.

6.2 Separability Analysis

Results of the initial per pixel separability analysis were originally presented in Haddow *et al.* (1997). Tables 6.1 and 6.2 show the reference separabilities for the competitor and conifer species (jack pine and black spruce) that were considered 'good' (greater than 1.9) and 'poor'. Good separabilities, with values ranging from 1.90 to 2.00, were obtained for large-leaved aster, upland willow, red raspberry and fireweed from both conifer species. Large-leaved aster and fireweed were both flowering at the time of image acquisition, contributing significantly to their 'good' separabilities. As a result, timing of image acquisition should play an important role in obtaining images for spectral analysis and classification of various species. However, this may present difficulties when there are a number of different species that have to be taken into

consideration, as flying at different times for different stages of growth would be costly and lead to difficulty in combining the data for proper analysis. As numerous studies have found (e.g., Pitt *et al.*, 1997; Hall, 1984), if identification, counting, and measurement of coniferous species is the objective, then acquisition of data should be during leaf-off periods of the competing deciduous vegetation (i.e., spring and fall). However, to assess the type and amount of competition acquisition of images must be conducted when there are leaves present on the trees.

Poor separabilities were obtained for the remaining competitor species; blue-joint grass, braken fern, and trembling aspen. In addition to the separabilities between conifers and the competition species, an analysis of the separability of jack pine from black spruce was conducted when they were not in competition with each other. The results indicated that the two conifers species had essentially similar spectral characteristics in this imagery, with a poor separability of 1.27. Several factors may explain such poor results. First, at most densities, the background reflectance of the soil contributed significantly to the image brightness, thereby producing a similar spectral response for each pair of classes. Secondly, sampling of individual conifer tree crowns at medium to high competition densities was very difficult and locational errors could have resulted in the incorporation of additional spectral information from the surrounding competition. Conifer crowns were undetectable at densities as low as 2 competitor plants per metre square for plots where blue-joint grass and red raspberry were in competition with the conifers. A third factor involves the sensor used to collect the data.

The low separabilities could be attributed to the fact that the DCS420 CIR camera has wide spectral bandwidths. The use of narrower bandwidths may improve separabilities. Furthermore, the dynamic range of the imagery was not very high, being only 120 digital numbers. In-flight investigation revealed that increasing the exposure resulted in either saturation of trees in the near IR or too much image motion. Therefore, the exposure settings used represented a compromise between these factors. Image motion was about 1 pixel with the aperture fully open. Two factors could have been corrected to reduce image motion: 1) fly at a slower aircraft speed, which was not possible with the aircraft available, or 2) increase the shutter speed to 1/8000 sec but this would have reduced the dynamic range even further.

Most of the factors discussed above are related to the technical performance of the camera. In order to obtain 2.5cm pixel imagery the camera was pushed to the limits of its capabilities. The small pixel size was necessary to assess regenerating trees less than 1m in height. Radiometric response improvements of digital cameras such as the DCS420 CIR should improve their use in automated spectral classification of regenerating sites. However, the first two factors noted above, spectral contribution of non-crop species and locational errors in sampling, are more difficult to overcome. They limit capability at moderate to high competition density for both visual interpretation and automated spectral classification because, in many cases the conifer trees were completely obscured by the competitor species (Haddow *et al.*, 1997). The situation is different when the species of interest are the competition. Visual identification is easier

because the competition typically is not obscured to the same degree as the conifer seedlings.

Transformed Divergence separabilities for a full range of densities of two competition species, trembling aspen (Figure 6.1), and upland willow (Figure 6.2) were also obtained. Partial sets of densities were obtained for large-leaved aster and blue-joint grass and are located in Table 6.3. All data showed an inverse linear relationship between separability and density (Haddow *et al.*, 1997). The detrimental effect of competition density on spectral separability of conifers and competitor species is evident. As competition levels increase, separability decreases. This relationship can be attributed to the factors that were discussed above in relation to the reference separabilities that were obtained.

The ability to identify the conifer trees at various densities is also dependent on the types of competition that surrounds the trees. For example, conifer trees were visible at all densities of large-leaved aster, due to the distinct spectral difference between the two because the competition was flowering (Table 6.3). Therefore, a density threshold for conifer identification could be as high as eight competition plants to one conifer as long as the aster is flowering at the time of image acquisition. However, conifers were difficult to identify at all densities, even very low densities, for other competition species such as trembling aspen and blue-joint grass (Table 6.2). The separabilities when there was no competition were 'poor' to begin with and decreased as the level of density increased. A threshold for these types of competition might be set as low as one

competition plant for every two conifers or require that these species not be present at all. This assignment of a density threshold beyond which conifer seedlings cannot be accurately identified will be difficult to determine in a more operational setting when different competition species are growing together in a single plot.

Initial test classifications using a maximum likelihood classifier were conducted for competitors which had 'poor' separabilities with the conifer species (Table 6.2) to test the worst case scenario for thematic mapping. Contrary to expected results, the thematic maps showed very clearly the planting pattern of the experimental units for conifer and competition species. Therefore, although the separability of each pair of competition and conifer classes was 'poor' in these tests, the presence of trees were well identified by the classifier. Examples of such thematic maps can be found in Appendix C. The reason for this apparent discrepancy is that, on a per pixel basis, there were many pixels in error, particularly near the edges of seedlings where soil background and/or overlapping competition contributed most to pixel brightness. Thus, low separabilities translated into low per pixel classification accuracy. However, with a central portion of each conifer or competition plant classified correctly, the output map showed their planting patterns very well (Haddow *et al.*, 1997). This indicated potential for production of such thematic maps for use in tree counting and regeneration success measurement despite the poor per pixel separability.

Table 6.1
Crop and Competition Reference Separabilities
which were 'Good'.

	jack pine	black spruce
large-leaved aster	2.00	2.00
upland willow	1.91	1.96
red raspberry	1.94	1.90
fireweed	2.00	1.91

Table 6.2
Crop and Competition Reference Separabilities
which were 'Poor'.

	jack pine	black spruce
blue-joint grass	1.44	1.11
bracken fern	1.07	1.03
trembling aspen	1.20	1.44
conifers	1.27	

Table 6.3
Partial Density Dependent Separabilities for
Large-Leaved Aster and Blue-Joint Grass

Density (plants/m ²)	jack pine	black spruce
large-leaved aster		
0	1.99	1.99
1		1.99
4		1.99
8	1.95	
blue-joint grass		
0	1.44	1.11
0.5	1.21	1.38

Figure 6.1
Transformed Divergence of Trembling Aspen Competition and Two
Conifer Species at Various Competition Densities.

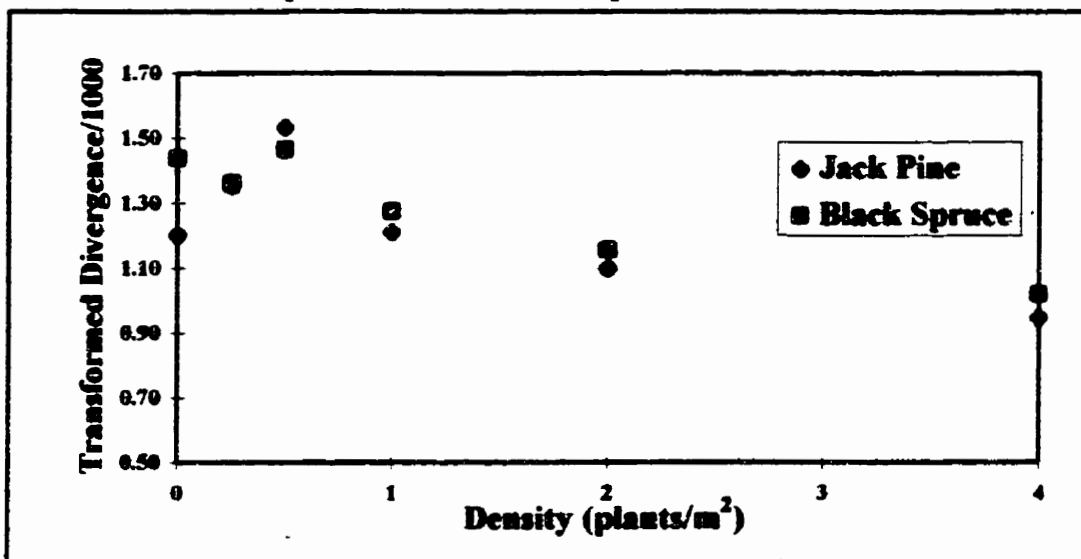
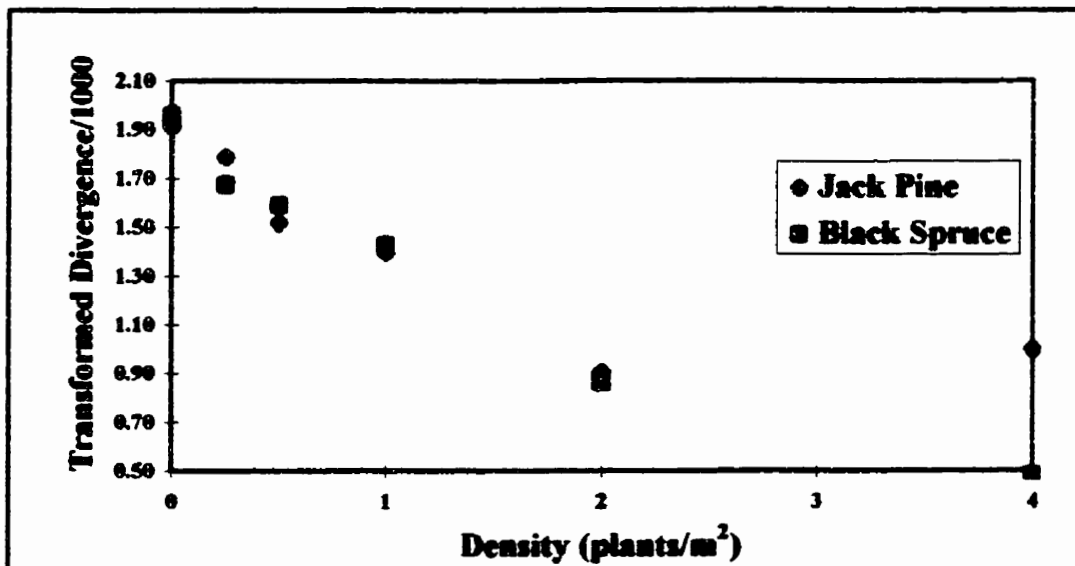


Figure 6.2
Transformed Divergence of Upland Willow Competition and Two
Conifer Species at Various Competition Densities



6.3 Evaluation of Automated Classification Methods

6.3.1 Image Statistics

Spectral Training Sample Statistics

Eleven land cover classes were used in the training of the supervised classifications. They included: jack pine, black spruce, fireweed, upland willow, red raspberry, blue-joint grass, large-leaved aster, soil, grass, shadows, and a null class. The latter was included to account for the area in the mosaic that did not contain any data, such as the area on the red raspberry plot where the flight lines did not provide enough overlap. These classes were selected using the plot map (Figure 4.2) that was provided by the Canadian Forest Service as a reference. The mean and standard deviation for the training samples of the eleven classes used in the production of the thematic maps using the spectral data for the arboretum site are located in Table A-1 of Appendix A.

Spectral Separability Analysis

Training samples' statistics demonstrate why the separabilities between the vegetation classes are low, as the separabilities are affected by mean and standard deviation values of the competition and conifer classes. Upland willow, red raspberry, and large-leaved aster have some of the better separability values with the conifers, 1.42, 1.25 and 1.99, respectively for jack pine and 1.33, 1.36, and 1.99 for black spruce. The mean values of these classes are quite different from the means of jack pine and black spruce for more than one band. However, high standard deviations affect the separabilities as well.

Standard deviation values obtained for the classes range from 4.3319 to as high as 13.5951. These high values can be associated with locational error in polygon sampling for the vegetation. Furthermore, some of the highest standard deviation values, greater than ten, were obtained for vegetation that was flowering such as fireweed and large-leaved aster, because not only were the leaves selected for classification, but the flowers were also included, which is necessary if the entire plant is going to be classified correctly. The timing of acquisition again plays an important role, not only with the vegetative state, but also with the condition of the soil. Image acquisition when the vegetation contains no leaves would eliminate variations in grey levels within herbaceous species, thereby reducing the standard deviation. The soil class also exhibited high standard deviations. These values can be associated with the tilling of the soil which can cause variations in the soil moisture within and between plots. In addition, images should be acquired when there is a greater chance of uniform soil moisture. However, as discussed earlier, if the level of competition is being measured, avoiding high standard deviations may be difficult because the images need to be acquired when there are leaves on the competition.

When the standard deviations are applied to obtain data distribution ranges, most of the vegetation classes overlap. For example, jack pine and black spruce have mean values of 90.35 and 87.82, respectively, in the green band. For respective standard deviations of 7.56 and 7.57, the full distributions ($\pm 3s$ from mean assuming normality) for the two classes range from 67.67 to 113.03 for jack pine and 65.11 to 110.54 for

black spruce. This represents an overlap of approximately 42 grey levels or 94%. Such overlap of grey level values also occurs for the other spectral bands and texture measures, explaining why the separability between the two conifer species is poor. Other vegetation classes also exhibited overlap between data distributions. If the standard deviation values were lower for those classes where overlap occurs and the data had a greater range of grey level values (> 120), this would result in a greater separation between mean values and the amount of overlap between distributions would be decreased. This would certainly lead to an improvement in the separability between the vegetation classes.

Table A-2, Appendix A contains the separabilities for the eleven classes based on the incorporation of the spectral information only. These results repeat what was discussed above for the initial separability analysis. The conifers again exhibited poor separability of 1.13, which is less than the value obtained in the initial analysis. Separabilities between the competition classes were also low as is the case with the very poor separability of 0.29 that was obtained between upland willow and red raspberry. The four competition species (large-leaved aster, upland willow, red raspberry, and fireweed) which obtained high separability with the conifer species in the initial separability analysis produced lower separabilities in this analysis. Large-leaved aster was the only one to maintain a 'good' separability (1.99), while the other fell to 1.42 for upland willow, 1.25 for red raspberry, and 1.66 for fireweed. For the competition species, the highest separabilities were obtained between vegetation that was flowering

and that which was not, and also between land cover classes that were distinctly different such as vegetation and soil or vegetation and shadow. Reasons for the poor separability results were discussed above with respect to the initial separability analysis and applied to the results obtained during the evaluation of automated classifiers.

The reduction in separability from the initial values can be associated with the mosaic image. The initial separability analysis involved selection of polygons in a single image for each of the competition species. However, in order to obtain an image that was representative of the entire plot, the mosaic was compiled. Since no radiometric corrections or colour matching were applied to the image when they were incorporated into the mosaic, spectral differences for the same species between images due to optical lens effects and bi-directional reflectance variations may have been significant. Attempts were made to restrict sampling to the centre of the images and reduce the influence of these effects, except the vegetation being sampled did not always fall within the centre of the images. Furthermore, small changes in brightness between some images add to the variance for those classes that were sampled from more than one image within the mosaic. These factors not only influence the separability between classes, but also the mean and standard deviation statistics that were obtained for the land cover classes.

6.3.2 Image Classification of Conifers from Spectral Data Alone

The purpose of evaluating the various classification methods was to determine if an automated classification process could provide accurate identification of conifer

seedlings for species composition assessment and for measurement of other attributes that require seedling counts.

Unsupervised Clustering with Spectral Information

Unsupervised clustering resulted in the production of a thematic map with eleven spectral clusters. The mean and standard deviation statistics that were produced for the spectral classes are located in Table A-3 of Appendix A. An example of the spectral cluster map (Figure C-2) produced by the K-means clustering is located in Appendix C. The mean and standard deviation values obtained for the eleven classes for the supervised training samples were used in addition to visual inspection of the thematic map and knowledge of the location of planted conifers to determine which spectral cluster(s) corresponded to the conifer species on the ground. Clusters 4 and 5 were identified to be conifer species and were used in tree counting assessment. The other clusters were not assigned land cover class labels as they were not required for this process.

Supervised Classifications with Spectral Information

In classification of images using neural networks, errors in the network training stage are output for assessment before the classification is conducted. The global error reached during training of the neural network for the spectral information alone was 0.44. The specified default error of 0.01 was not reached, yet the neural network was considered to be "trained" and the error was accepted. Variations in the number of iterations, learning rates and momentum rate were investigated, but the global error was

consistently greater than the software maximum default error mentioned above. Although the final training parameters of 10,000 iterations, learning rate of 0.1 and a momentum of 0.9 did not reach the specified error of 0.01, they were accepted for classification, as the specified error would not have been reached because the neural network was oscillating. Even with changes in the learning rate and momentum oscillation still occurred. This oscillation and high global error could be a result of the poor separability between most classes, which can lead to confusion between classes or because there are too few input channels. Improvements in the spectral separability between the classes could lead to a lower total error produced.

The thematic maps produced by the maximum likelihood, neural network, and context supervised classifications for the spectral data are located in Appendix C and are figures C-3, C-4, and C-5, respectively. The images located in Appendix C represent an example of the thematic maps generated for the arboretum site for all of the classifications conducted as part of this research. Due to the similarities of the maps, others produced at later stages are not included. The thematic maps clearly demonstrate the ability of the classification algorithms to identify the planting structure of the experimental units, discussed above. The unsupervised cluster map, maximum likelihood, and neural network thematic maps all appear similar, with a very jagged appearance to boundaries and more noise than the context thematic map. The amount of noise within classes was less for the context thematic map and it had a more visually pleasing and interpretable appearance. There were no harsh edges within the context

map compared to the other thematic maps, where the edges of plots, targets, and field markers were more distinct. The context classification resulted in a more generalized appearance in the land cover classes. However, the generalized appearance of the context thematic map also resulted in loss of detail at this resolution as groups of individual trees were often combined into a single polygon and represented as a single tree. The map may give a false impression regarding the condition of the site. For example, such groupings of trees may lead to an under-estimate of stocking levels because only one tree might be identified when there are actually more than one present on the ground.

6.3.3 Image Classification of Conifers from Textural and Spectral Information

Texture Training Sample Statistics

The mean and standard deviation (Table B-1, Appendix B) for the Standard Deviation and Variance co-occurrence texture measures exhibit a degree of overlap between class distributions. Instead of overlapping by 94%, the distributions of jack pine and black spruce only overlap by 82% for the Standard Deviation measure and 84% for the Variance measure from the spectral distribution. This decrease in overlap with the addition of a texture measure, Standard Deviation or Variance, was expected to improve the separabilities between the land cover classes when the texture band was added to the three spectral bands.

Texture Separability Analysis

The separability values obtained for the training polygons from the combined spectral/texture information are summarized in Table B-2, Appendix B. With the addition of the texture information, the separabilities between land cover classes improved slightly. However, the improvement was not sufficient to obtain good separabilities between classes like jack pine and black spruce. The separabilities between jack pine and black spruce increased from 1.13, to 1.23 with the addition of the Standard Deviation texture information and to 1.17 with the Variance texture information. This improvement is not significant, as the separability between the two classes is still 'poor'. More significant is the improvement in separability between coniferous species and deciduous species. The separability between jack pine and fireweed increased from 1.66 to 1.83 and 1.77 with the addition of Standard Deviation and Variance texture measures, respectively. In addition, the separability between jack pine and upland willow increased from 1.42 to 1.51, with the addition of the Standard Deviation texture measure and to 1.57, with the Variance texture measure. Separabilities between black spruce and the various competition species demonstrate similar increases.

Separabilities for land cover classes that were distinctly different, such as vegetation and soil, remained similar even after the addition of spatial information. The separabilities between some of the competition species increased with the addition of spatial information. The competition with the lowest separability using only spectral information (0.29) between upland willow and red raspberry, was improved somewhat to

0.35 with the addition of Standard Deviation texture measure and to 0.40 with the addition of Variance texture measure. The addition of texture appeared to have a greater effect on the separability between competition than between vegetation and other land cover classes such as soil and shadow. There was little improvement in the separabilities between vegetation classes and soil and shadow because they were already very high. The improvement in separability for vegetation classes can be attributed to the fact that there is more spatial information present within vegetated areas than there is for soil or within areas of shadow.

Unsupervised Clustering with Spectral/Texture Information

The spectral classes that were generated with the addition of the texture measures by the K-means algorithm were similar to those generated with the spectral data only. Clusters 4 and 5 were identified for use in the accuracy assessment in both the clustering using the Standard Deviation and Variance texture information. These clusters were identified in the same manner as those for the spectral data only.

Supervised Classification with Spectral/Texture Information

The total errors that were obtained for the neural network training phase for the classifications of spectral data plus either Standard Deviation and Variance texture measures were 0.36 and 0.37, respectively. However, in order to obtain good accuracy, the neural network must be adequately trained and a low global error reached. In this case, the error achieved was accepted and the image was classified using the neural network. The addition of the co-occurrence texture measures decreased the global error

and improved the training of the neural network slightly over the spectral data alone (0.44).

6.3.4 Accuracy Assessment of Conifer Seedling Counts

Thematic maps produced by each of the classification techniques were used to obtain conifer seedling maps by masking out all other classes. These conifer seedling maps (Figure C-1) were then used to conduct an accuracy assessment of automated seedling counting. Note that in the tables and graphs presented in the following discussion, plots are identified by the competition species that are growing in each. Thus, the accuracy assessment was conducted for each individual plot where conifers were planted with a competition species at a given density. Appendix D contains graphs representing the percent over- and under-estimates for counts of conifer seedlings obtained during the initial phase of the accuracy assessment. Each graph represents the conifer counts expressed as a percent over- or under-estimate of the actual field count, for all densities of the three plots (fireweed, upland willow, red raspberry) based on the range of pixel sizes specified. As outlined in the methods, the range of pixel sizes used represents the possible size of the central cores of conifer seedlings and does not reflect the size of entire crowns.

Figures 6.3 through 6.7 represent the best five classifications that were chosen out of the twelve that were conducted. These include: a neural network with spectral and Standard Deviation texture information; a context classifier with spectral and Variance texture information; and three unsupervised clustering maps, one with the

spectral information only, one with the addition of the Standard Deviation texture measure, and the third with the spectral and Variance texture information. Figure 6.8 represents one, for comparison purposes, of the classifications that was not chosen due to the high percentage of errors that it produced. The five best classifiers (Figures 6.3 to 6.7) represented the classifications with the lowest percentage of error from the actual number of trees in each plot. The graphs demonstrate that the error curves for the five classifications were much closer to 0% error than those that were not chosen such as Figure 6.8.

The accuracy of each classifier depended on the competition species. For example, the fireweed plot seemed to have the greatest amount of over-estimates for all classifications except for the context classification where it produced under-estimates. In the case of the context classifier, the raspberry plot produced the greatest over-estimates. Upland willow consistently produced the least amount of over and under-estimation and was generally grouped together over the range of densities in that plot, with less than 100% error. Classifier accuracy was also dependent on the density of competition. As expected, the lower densities of the various plots produced the lowest percentage of over and under-estimates. As the density of competition increased, the amount of over and under-estimation increased, with the higher densities (eight competition plants to one conifer) typically producing the greatest amount of over and under-estimation for each plot. Thus, as density increased, the percent error in conifer counting increased.

The effect of changing the minimum acceptable number of pixels to define the core of a conifer seedling, was most prevalent for the fireweed plot. As the number of pixels increased from 9 to 20, the amount of over-estimation decreased. This was seen for all of the classifications except for the context classifier which remained the most constant in counting errors for the entire range of pixels for all densities and plots. For the other plots, upland willow and red raspberry, the decrease with number of pixels was not as pronounced as for fireweed. As a result, it is difficult to suggest a single number of pixels to be used as different trees have different diameters.

The effect of pixel size is also dependent on the type of species. Determination of a correct number of pixels may not be as important for upland willow and red raspberry as they remained relatively unaffected by the change, but determining the appropriate number of pixels for fireweed may reduce the amount of error in the conifer counts. Determination of a single number of pixels is limited by the features under study and therefore should be chosen based on the features, and not on which one produces the least amount of error in the conifer counts. However, the downward trend of the curves does indicate that the x-axis intercept may actually be close to the whole tree size as opposed to the core area of the conifer crown. This value could be used as an optimal number of pixels to represent a seedling.

The neural network appeared to have performed the best overall, with the lowest percentage of over and under-estimates. The unsupervised clustering for all three variations produced similar results with the upland willow and red raspberry plots all

concentrated between approximately 100% and -50% and the fireweed around 300% except when there was no competition present. The context classifier had a greater balance between over- and under-estimates but like the other classifiers produced high over-estimates for the fireweed plot. These errors are very high and demonstrate that when all but the lowest densities are present, automated conifer counting using these methods is feasible.

Both over-estimation or under-estimation of conifer counts affect decision making. The worst case scenario is if the area is actually understocked, but the conifer counts are over-estimated from the thematic maps and indicate a well stocked area. This may lead a forest manager to believe the plot does not require treatment to improve stocking with the long-term consequence of insufficient yield or harvest. Conversely, if the plot is actually overstocked, and an under-estimate is made from the map, a decision not to treat the plot may be made. Such overstocking may lead to growth problems as the trees may compete with one other, decreasing potential total yield. Short-term costs can also be affected by the conifer estimates. This situation can arise if a plot is actually at an acceptable stocking level, yet a forest manager believes the plot is understocked because the conifer count from the thematic map was under-estimated. The short-term costs involve conducting field surveys to determine which silvicultural practices may be required to increase the number of conifers and ensure a well stocked plot when it is time to harvest. The expense of the field survey is actually wasted because there is no requirement to improve the stocking of that plot.

Figure 6.4
Conifer Counting Error (%) for Context Classifier with Spectral and Variance Texture Data as a Function of
Competition Species and Density, and the # of Pixels Defining a Seedling

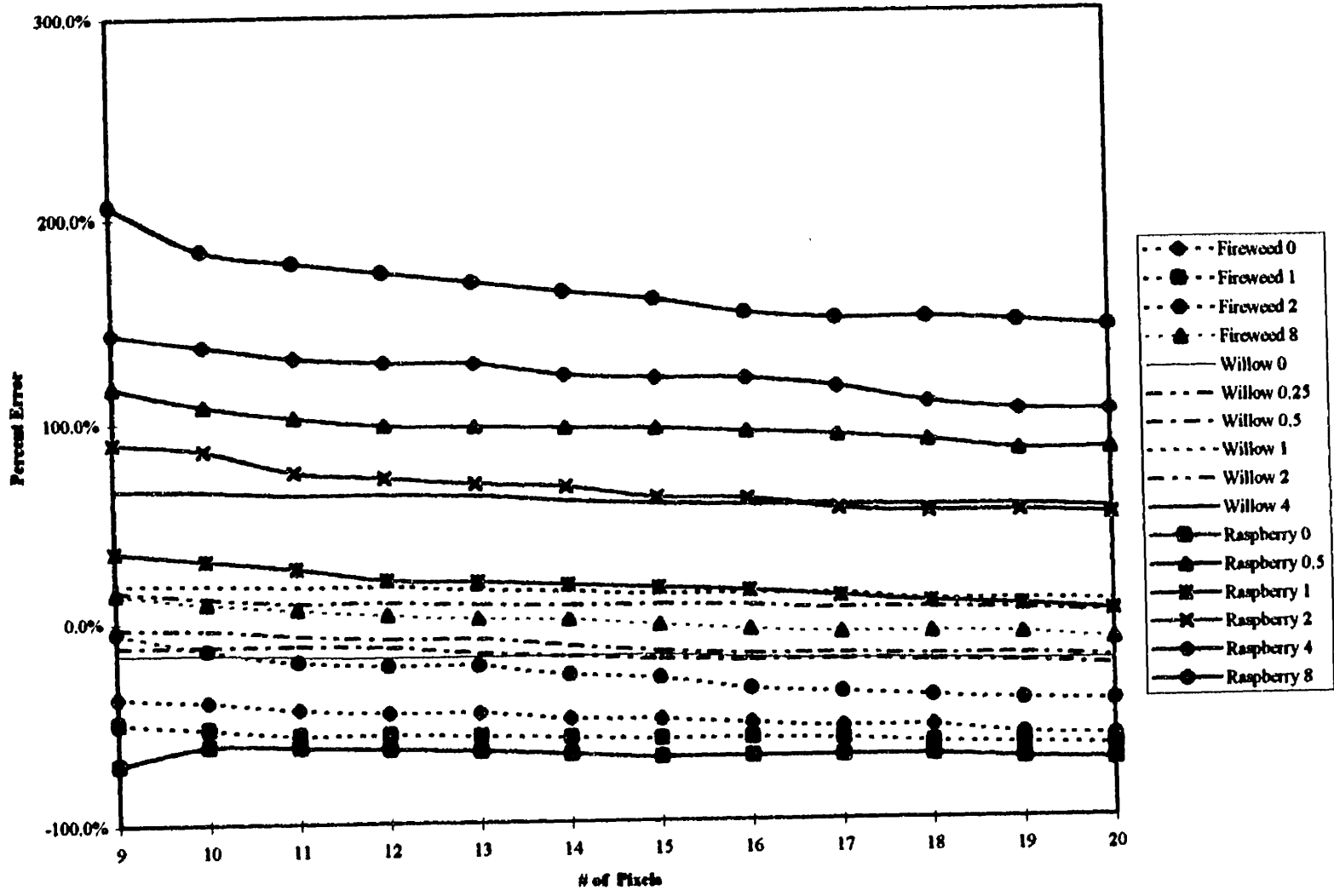


Figure 6.6
 Conifer Counting Error (%) for Unsupervised Clustering with Spectral and Standard Deviation Texture Data as a
 Function of Competition Species and Density, and the # of Pixels Defining a Seedling

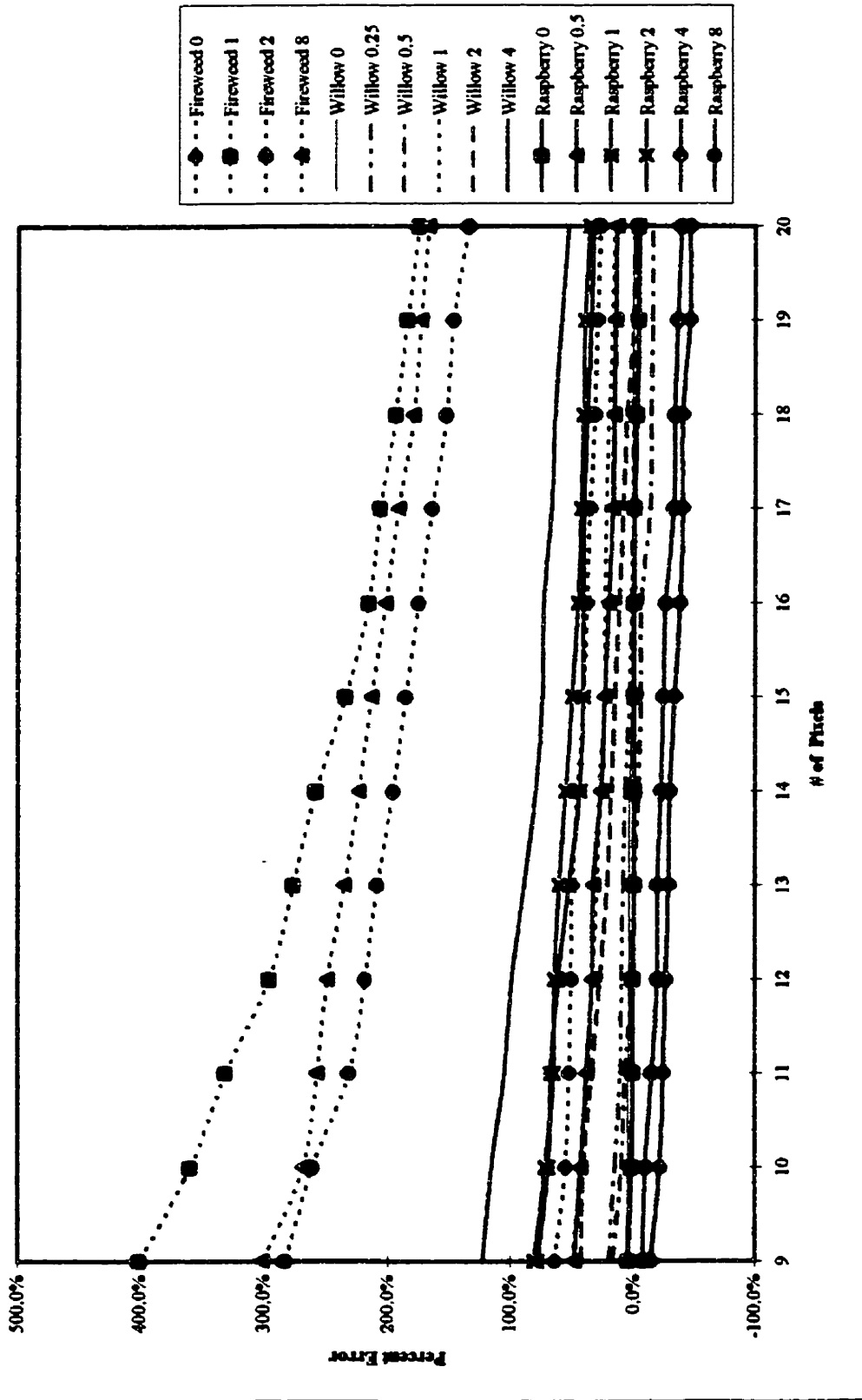


Figure 6.7
 Conifer Counting Error (%) for Unsupervised Clustering with Spectral and Variance Texture Data as a Function of
 Competition Species and Density, and the # of Pitches Defining a Seedling

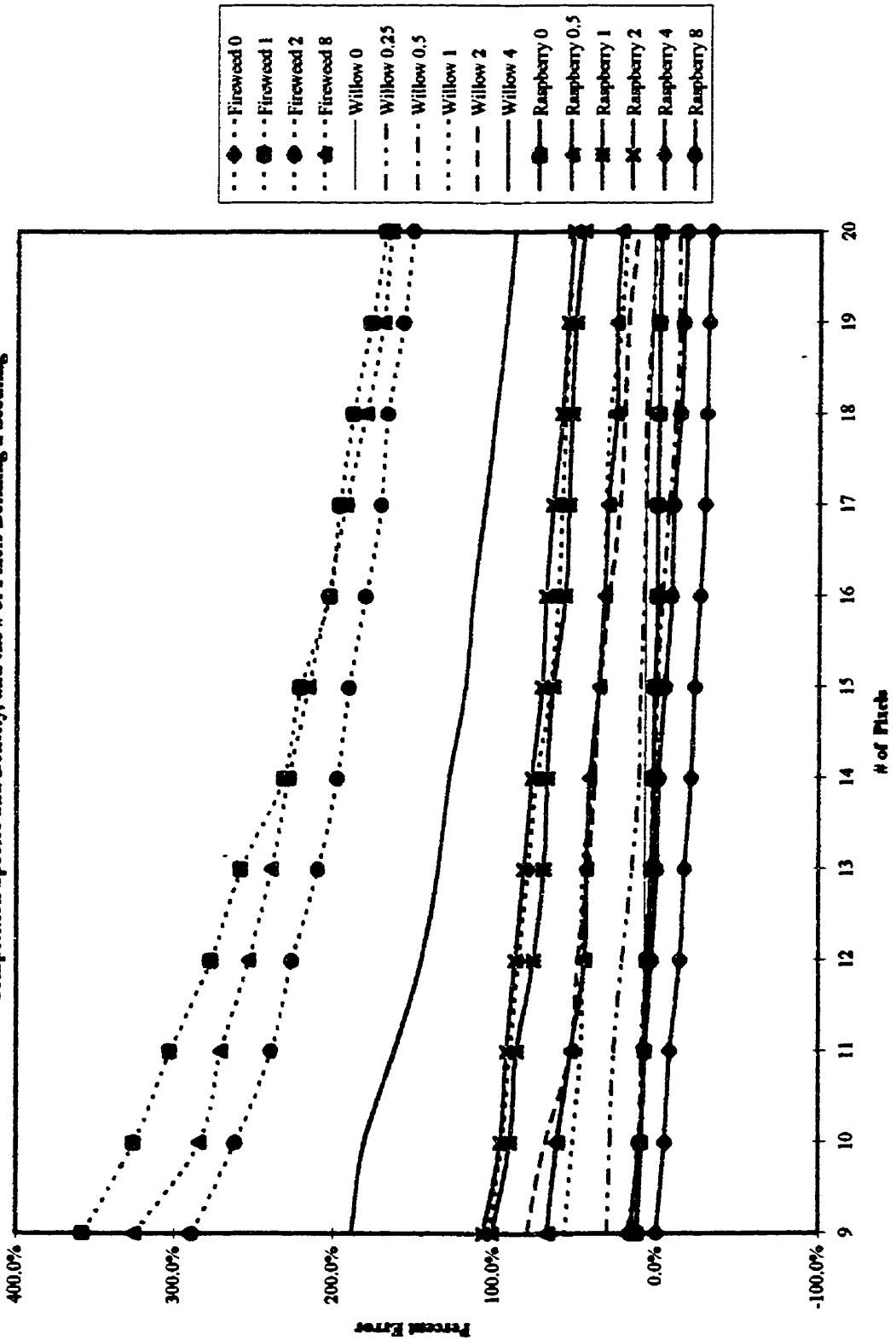


Table 6.4 identifies the errors of omission and commission for the five classifications that were identified as performing well. Errors of omission resulted when a conifer existed in the field but was not identified on the map. Errors of commission resulted when a conifer was identified on the map but it did not exist on the ground at that location. The values were obtained on conifer experimental units where there was no competition present. These plots were chosen because the separabilities between the conifers and the various competition species would result in excessive errors of commission as the density of competition increased. In addition, these plots simulate the leaf-off condition which is more reasonable for counting trees. A grouping of pixels was considered if there were more than nine pixels present. Those that had less were disregarded because they did not constitute a tree by definition.

It can be seen that the context classifier has a high occurrence of errors of omission for all plots. The unsupervised clustering had high errors of commission for only the fireweed plot as well as a high occurrence of errors of omission for the clustering with the addition of the Variance texture measure. Of all plots, fireweed produced the highest number of commission errors for all classifications. This could be associated with the greater amount of weeds that were present at this plot than were present in the other two.

From the errors of omission and errors of commission, User's and Producer's accuracies were determined for each of the classifications (Table 6.5). The highest accuracies were obtained for the neural network with the Standard Deviation texture

information added to the spectral data. This classification obtained both the highest User and Producer accuracies out of the five classifications for all three plots. An interesting note is that the unsupervised clustering, both with only spectral information and the addition of texture information, performed reasonably well in comparison to the supervised methods, especially the context classifier. The context classifier performed the poorest, obtaining the lowest accuracies of all the classifiers. The User's accuracies obtained by the neural network are similar to those obtained by Hall and Aldred (1992) for jack pine trees, where 96% accuracy was obtained in identification of conifer seedlings through manual interpretation of aerial photographs.

6.3.5 Assessment of Classification on Searchmont Data

Appendix C also contains an image of the neural network classification with spectral data and Standard Deviation texture information that was conducted for the Searchmont mosaic (Figure C-6). The minimum total error reached after 10,000 iterations of training was 0.11. The target maximum total error (0.01) was not reached, although, the error achieved at the Searchmont site was better than the error that was achieved at the arboretum site (0.36) for the same combination of spectral information and the Standard Deviation texture information.

In addition to achieving a lower total error during the training, the neural network for the Searchmont site trained in a little over half the time that was required to train the arboretum neural network. File size could have played a role in this, yet the difference between the two files was not that great to produce the significant reduction in

training time. Another factor that could have played a role in the reduction in training time is the smaller number of classes (five) at the Searchmont site than the arboretum site (eleven). The method used in this research was that the number of hidden layers corresponded to the number of classes used in the training phase. As a result there were fewer hidden layers, therefore, fewer connections between the nodes. This can reduce the amount of computation that occurs at each iteration to adjust the weights that are applied to each node in an attempt to achieve the total error specified.

The errors of omission and commission that were obtained for the three Searchmont plots are given in Table 6.6. Plot 3-3 was not included in the assessment due to the excessive amount of competition that prevented accurate visual identification of conifer trees. Furthermore, in Plot 3-3 the competition was so heavy that when polygons were generated to count the errors of omission and commission the majority of the plot was identified as being one polygon. The User's and Producer's accuracies were obtained from the omission and commission errors. The user's accuracies that were obtained for plots 3.6 and 4.10 were 77.6% and 21.8%, respectively. The results indicate that the user's accuracy was significantly affected by the density of the competition at each of the plots with plot 3.6 visually having a lower level of competition than plot 4.10. The producer's accuracy for both plots was 100% since there were no errors of omission for either plot.

Table 6.4
Errors of Omission and Commission in Counting Conifer Trees
for Arboretum Plots: when no competition present

	Fireweed Plot		Red Raspberry Plot		Upland Willow Plot	
	Plot Conifer Total = 98		Plot Conifer Total = 84		Plot Conifer Total = 94	
	Omission	Commission	Omission	Commission	Omission	Commission
Neural Network Standard Deviation	1	49	6	1	1	5
Context Variance	42	9	59	1	20	5
Unsupervised Spectral	1	68	3	3	1	6
Unsupervised Standard Deviation	1	70	2	1	1	9
Unsupervised Variance	37	11	3	3	1	8

Table 6.5
User's and Producer's Accuracies for Each Plot When No Competition Present at
the Arboretum Site Based on Errors of Omission and Commission

	Fireweed Plot		Raspberry Plot		Upland Willow Plot	
	Producer's	User's	Producer's	User's	Producer's	User's
Neural Network Standard Deviation	99.0%	66.4%	92.9%	98.7%	99.0%	94.4%
Context Variance	57.1%	93.2%	29.8%	96.1%	78.7%	74.7%
Unsupervised Spectral	99.0%	58.8%	96.4%	96.4%	98.9%	93.9%
Unsupervised Standard Deviation	99.0%	58.1%	97.6%	98.8%	98.9%	91.2%
Unsupervised Variance	62.2%	84.7%	96.4%	96.4%	98.9%	92.1%

Table 6.6
Errors of Omission and Commission in Counting Conifer Trees
for Searchmont Plots

	Plot 3.6		Plot 3.3		Plot 4.10	
	Plot Conifer Total = 125		*		Plot Conifer Total = 87	
	Omission	Commission	Omission	Commission	Omission	Commission
Neural Network Standard Deviation	0	36	*	*	0	312

* Unable to count errors in Plot 3.3 due to excessive competition growth, see following text.

6.4 Biophysical Modelling Statistical Analysis

Appendix E contains the mean (Table E-1) and variance (Table E-2) statistics for the grey level values that were extracted for the jack pine trees measured in the field for LAI and percent cover. LAI and percent cover field values are also listed in the tables. The tables contain both the original data and the normalized data. A power transformation was applied to the mean dataset, while a logarithmic transformation was applied to the variance dataset. Those variables that were transformed to obtain normality are indicated by an asterisk (*) after the variable name. It is these variables that were used in the analysis in place of the non-normal original data. Kurtosis and skewness values that were obtained for all of the variables are also listed in Appendix E for the mean and variance statistics, tables E-3 and E-4 respectively.

6.4.1 Correlation Analysis

The correlation values (r) and corresponding significance values (p) obtained for the mean and variance datasets are located in Tables 6.7 and 6.8, respectively. Correlation values that are discussed in the following sections are indicated in **bold**. Significance level was measured with a 95% confidence interval. Therefore, a p -value of 0.05 or less indicates a significant correlation. Results of the correlation analysis using the mean of the variables will be discussed first, followed by the variance.

Correlation Analysis using Mean of Variables

Table 6.7 indicates the r values obtained for the mean dataset. Overall, the values obtained for LAI were weak, and not statistically significant. The highest r value

obtained was with near infrared reflectance (-0.31). The negative relationship is contrary to what would typically be associated with the two; as NIR reflectance increases, the LAI should increase because there is more vegetation present. This may be due to the NIR spectral bandpass of the camera which includes a significant amount of red spectrum transmission. The red band, produced a correlation of -0.31 ($p=0.06$). The negative relationship is expected, as red reflectance decreases, the absorption by the plant increases, suggesting that there is an increase in the amount of vegetation and, therefore, LAI.

The Standard Deviation texture measure has a negative relationship (-0.30) with LAI. This suggests that as the amount of texture decreases, the area becomes smoother, resulting in a more homogeneous land cover; in this case vegetation. This would be indicative of an increase in the LAI.

Percent cover produced similar relationships with the image variables as LAI, since the two are positively correlated (0.86). Correlation coefficients obtained for percent cover with the variables discussed above were higher than those with LAI and also more statistically significant. For example, the correlation between red and LAI was -0.31 ($p=0.06$), yet, the correlation between red and percent cover was -0.40 ($p=0.01$). All three of the vegetation indices produced significant correlations with LAI and percent cover, yet they were 'weaker' than either the red or NIR spectral data.

Table 6.7
Correlation Coefficients and P-Values for Mean of Image and Field Variables

	Green	LAI	NDVI*	NIR	Percent Cover	RVI*	Red	SAVI*	Standard Deviation	Variance
Green	1.00 P= .									
LAI	.26 P= .11	1.00 P= .								
NDVI*	.44 P= .01	-.22 P= .18	1.00 P= .							
NIR	.61 P= .00	-.31 P= .05	.53 P= .00	1.00 P= .						
Percent Cover	.24 P= .14	.86 P= .00	-.34 P= .03	-.41 P= .01	1.00 P= .					
RVI*	.43 P= .01	-.21 P= .20	.99 P= .00	.51 P= .00	-.33 P= .04	1.00 P= .				
Red	.56 P= .00	-.31 P= .06	.38 P= .02	.99 P= .00	-.39 P= .01	.36 P= .03	1.00 P= .			
SAVI*	.45 P= .01	-.21 P= .20	.99 P= .00	.52 P= .00	-.33 P= .04	.99 P= .00	.37 P= .02	1.00 P= .		
Standard Deviation	.57 P= .00	-.30 P= .06	.38 P= .01	.99 P= .00	-.39 P= .01	.36 P= .03	1.00 P= .00	.37 P= .02	1.00 P= .	
Variance	.37 P= .02	.23 P= .15	.07 P= .67	.20 P= .22	.24 P= .14	.08 P= .63	.21 P= .20	.07 P= .67	.21 P= .20	1.00 P= .

Table 6.8
Correlation Coefficients and P-Values for Variance of Image and Field Variables

M-39	Green	LAI	NDVI	NIR*	Percent Cover	RVI	Red*	SAVI	Standard Deviation*	Variance
Green	1.00 P= .									
LAI	.12 P= .47	1.00 P= .								
NDVI	.26 P= .11	.29 P= .07	1.00 P= .							
NIR*	.45 P= .01	-.20 P= .09	.01 P= .98	1.00 P= .						
Percent Cover	.09 P= .60	.86 P= .00	.37 P= .02	-.33 P= .04	1.00 P= .					
RVI	.36 P= .02	.24 P= .14	.97 P= .00	.12 P= .49	.28 P= .08	1.00 P= .				
Red*	.30 P= .06	-.35 P= .03	.07 P= .69	.94 P= .00	-.39 P= .02	.15 P= .36	1.00 P= .			
SAVI	.26 P= .11	.29 P= .07	1.00 P= .00	.01 P= .97	.37 P= .02	.98 P= .00	.07 P= .68	1.00 P= .		
Standard Deviation*	.32 P= .05	-.35 P= .02	.08 P= .62	.94 P= .00	-.39 P= .02	.16 P= .33	.99 P= .00	.08 P= .62	1.00 P= .	
Variance	.19 P= .26	-.07 P= .68	.54 P= .00	.47 P= .00	.03 P= .87	.57 P= .00	.56 P= .00	.54 P= .00	.53 P= .00	1.00 P= .

Correlation Analysis using Variance of Variables

Table 6.8 indicates the r values obtained for the variance dataset. Overall, the values obtained for LAI were weak, and not statistically significant. The highest correlation coefficient between LAI and the image variables was with the variance of red reflectance (-0.35). The relationship is weak, but significant ($p=0.03$). Since the variance is essentially a 1st order texture measure, the same logic applied to the Standard Deviation texture measure can be used here. As the variance in red decreases, there is a smoother grey level surface, an increase in the absorption of red energy, more vegetation present, and therefore, the LAI increases.

The variance of the Standard Deviation texture measure also obtained a significant ($p=0.02$) correlation with LAI (-0.35). While the correlation between the two was weak, the relationship is interpreted: as the variance of the Standard Deviation texture increases, the LAI decreases because there are more openings within the canopy. Similar relationships were obtained with percent cover and the variables discussed above. Again, the correlations between percent cover and the image variables were higher than those obtained for LAI.

An interesting result that appeared when using the variance as a summary statistic was that the 1st order texture, the variance of green, red, and NIR were significantly correlated with the Standard Deviation and Variance, 2nd order texture measures ($p=0.05$). Correlation coefficients themselves were 'strong' for the Standard Deviation texture measure and relatively 'weak' for the Variance texture measure. The higher

coefficients were obtained with the red variance, which is to be expected as the texture measures were determined using the red spectral information.

Summary of Correlation Analysis

Similar relationships were observed for correlations obtained from both the mean and variance datasets. The correlation coefficients for both LAI and percent cover with the Standard Deviation texture data are very similar to the coefficients obtained for the red band with LAI and percent cover. This is because they are highly correlated themselves, 1.00 for mean and 0.99 for variance. Both relationships were highly significant, both obtaining a p-value of 0.00. This is a result of the fact that the Standard Deviation texture information was determined using the red spectral information. Thus, the addition of either one into a regression analysis will provide the same information. However, the use of other texture measures which are not highly correlated with the spectral data may improve the strength of the regression coefficient even more than the ones identified in this research.

Results obtained for LAI and percent cover were generally more significant and the correlation coefficients were typically higher than the mean of the variables using the variance of the variables. The correlation coefficients obtained for percent cover were better than LAI for both of the datasets. The difference between the values obtained for LAI and those obtained for percent cover could be a reflection of the sampling methods used in the field. As well, locational errors in image sampling could favour one parameter over the other. The visual estimate of percent cover could allow for more

error in image sampling, whereas the field measurement of LAI is a more standard and less arbitrary measurement, maintaining consistency over different plots and for different surveyors. The values that were obtained for the correlation between all the image and field variables (LAI and percent cover) were weak overall, but in most instances statistically significant. Similar results were found by Bulter *et al.* (1995) and Franklin *et al.* (1997) where correlations with LAI were weak but statistically significant.

6.4.2 Regression Analysis

Results of stepwise regression analysis conducted on the mean and variance datasets are presented in Tables 6.9 and 6.10. The purpose of this analysis was to determine if vegetation indices or textural information increase the ability of the spectral data obtained from the imagery to predict field measured values of LAI and percent cover. The variables used in the regression were tested for linearity. Those that were not linear, were corrected. Results will be discussed in the same way as the correlation analysis; regression analysis using the mean dataset will be discussed first, followed by the results of the variance dataset.

Regression Analysis using Mean of Variables

Tables 6.9 and 6.10 identify the five regression analyses conducted using the mean of the variables for LAI and percent cover and are identified by the additional variable to the spectral data: the texture measures, Standard Deviation and Variance, and the vegetation indices: RVI, NDVI, and SAVI. Each will be discussed independently with a summary at the end of this section addressing similarities and differences.

Table 6.9
Stepwise Regression Results for Mean of Image Variables and LAI

Regression Variables	Step 1						Step 2					
	Variable Entered	r ² value	Standard Error	F statistic	Signif. of F	Slope	Variable Entered	r ² value	Standard Error	F statistic	Signif. of F	Slope
Spectral plus Standard deviation	NIR	0.07	1.24	3.96	0.05	0.05	Green	0.39	1.00	13.27	0.00	0.00
Spectral plus Variance	NIR	0.07	1.24	3.96	0.05	0.05	Green	0.39	1.00	13.27	0.00	0.00
Spectral plus RVI	NIR	0.07	1.24	3.96	0.05	0.05	Green	0.39	1.00	13.27	0.00	0.00
Spectral plus NDVI	NIR	0.07	1.24	3.96	0.05	0.05	Green	0.39	1.00	13.27	0.00	0.00
Spectral plus SAVI	NIR	0.07	1.24	3.96	0.05	0.05	Green	0.39	1.00	13.27	0.00	0.00
Regression Variables	Step 3						Step 4					
	Variable Entered	r ² value	Standard Error	F statistic	Signif. of F	Slope	Variable Entered	r ² value	Standard Error	F statistic	Signif. of F	Slope
Spectral plus Standard deviation	Std Dev	0.41	0.99	9.9	0.01	0.17	Red	**				
Spectral plus Variance	Red	0.41	0.99	9.9	0.01	0.17	Variance	0.41	0.99	7.48	0.00	0.45
Spectral plus RVI	Red	0.41	0.99	9.9	0.01	0.17	RVI*	0.40	1.00	7.31	0.00	0.62
Spectral plus NDVI	Red	0.41	0.99	9.9	0.01	0.17	NDVI*	0.40	1.00	7.29	0.00	0.65
Spectral plus SAVI	Red	0.41	0.99	9.9	0.01	0.17	SAVI*	0.40	1.00	7.35	0.00	0.57

** This variable was not entered into the regression equation
italics indicate variables that significantly contributed to the regression equation

Table 6.10
Stepwise Regression Results for Mean of Image Variables and Percent Cover

Regression Variables	Step 1							Step 2						
	Variable Entered	r ² value	Standard Error	F statistic	Signif. of F	Slope	Variable Entered	r ² value	Standard Error	F statistic	Signif. of F	Slope		
Spectral plus Standard deviation	NIR	0.14	25.69	7.41	0.01	0.01	Green	0.53	19.10	22.20	0.00	0.00		
Spectral plus Variance	NIR	0.14	25.69	7.41	0.01	0.01	Green	0.53	19.10	22.20	0.00	0.00		
Spectral plus RVI	NIR	0.14	25.69	7.41	0.01	0.01	Green	0.53	19.10	22.20	0.00	0.00		
Spectral plus NDVI	NIR	0.14	25.69	7.41	0.01	0.01	Green	0.53	19.10	22.20	0.00	0.00		
Spectral plus SAVI	NIR	0.14	25.69	7.41	0.01	0.01	Green	0.53	19.10	22.20	0.00	0.00		
Regression Variables	Step 3							Step 4						
	Variable Entered	r ² value	Standard Error	F statistic	Signif. of F	Slope	Variable Entered	r ² value	Standard Error	F statistic	Signif. of F	Slope		
Spectral plus Standard deviation	Std Dev	0.59	17.88	18.90	0.00	0.02	Red	**						
Spectral plus Variance	Red	0.59	17.91	18.79	0.00	0.02	Variance	0.58	17.94	14.27	0.00	0.35		
Spectral plus RVI	RVI*	0.59	17.83	19.08	0.00	0.02	Red	0.58	18.09	13.91	0.00	0.91		
Spectral plus NDVI	NDVI*	0.59	17.82	19.12	0.00	0.02	Red	0.58	18.09	13.95	0.00	0.86		
Spectral plus SAVI	SAVI*	0.59	17.84	19.05	0.00	0.02	Red	**						

** This variable was not entered into the regression equation
Italics indicate variables that significantly contributed to the regression equation

The first regression analysis was conducted using the mean values of green, red, NIR, and Standard Deviation texture against LAI and then percent cover. In the LAI regression equation, the NIR variable was the first to be added into the equation, followed by the green, and finally the Standard Deviation texture. The variable 'red' was not added into the equation. As mentioned, this could have occurred because the red and Standard Deviation are highly correlated. The Standard Deviation was added in to the equation because it was more significant to the equation than the red data. The addition of the Standard Deviation texture data to the equation produced a better r^2 (0.41) than with the NIR and green data alone (0.39). The addition of the Standard Deviation texture increased the regression coefficient but the increase was not statistically significant because the slope of the Standard Deviation, when it was entered into the equation, was not significant (0.15). The addition of the Standard Deviation does improve the equation because the standard error of the equation decreased from 1.00 to 0.99, although, the equation with NIR, green, and Standard Deviation is not as statistically significant as the one based on NIR and green spectral data alone. The standard errors obtained were high, therefore, at this point, equations for the prediction of field variables were not developed.

Regression analysis for percent cover exhibited similar results; exclusion of the red data and an increase in the r^2 from 0.53 to 0.59 with the addition of the Standard Deviation texture information to the NIR and green data. The difference between the LAI equation and the percent cover equation using these variables is that the equation

for percent cover with Standard Deviation is statistically significant because the slope of the Standard Deviation variable (0.02), when it was entered into the equation in step 3, is significant at the 95% confidence interval.

The second regression equation that was conducted used the mean of the Variance texture data with the spectral data. The addition of the Variance texture data did not improve the LAI equation. It actually resulted in a lower regression coefficient than with the spectral data alone. The value decreased from 0.42 for NIR, green, and red data to 0.41 with the addition of the Variance texture. Similar results were again obtained for the regression of percent cover, although the values were higher (0.58) for both the spectral data and the addition of the Variance texture. However, the addition of the Variance texture was not significant because the standard error increased from 17.91 to 17.94. Furthermore, the slope of the Variance texture information, when it was added into the equation, was not significant (0.35).

The third regression analysis was conducted using the spectral data and the ratio vegetation index. The ratio variable was added in at the fourth step of the regression equation. The ratio vegetation index did not add anything to the LAI regression equation. The regression coefficient decreased from 0.42 with the spectral data only to 0.40 with the addition of the ratio data. The regression equation for percent cover was actually improved with the addition of the ratio data, increasing from 0.53 with the NIR and green data to 0.59 with the addition of the ratio data. The increase was also statistically significant because the standard error decreased and the slope of the ratio

variable was 0.02 which is significant at the 95% confidence interval. However, when the red variable was added into the equation after the ratio variable, the regression coefficient decreased to 0.58 and the standard error increased.

The final two regression analyses conducted used the spectral data with the addition of NDVI and SAVI. The results obtained for both LAI and percent cover for both NDVI and SAVI were similar to those obtained by the ratio vegetation index. For the LAI regression, the vegetation indices are added in at the last step, lowering the regression coefficient value and increasing the standard error. For the percent cover equation, they were added in the third step, increasing the regression coefficient and lowering the standard error. The addition of both NDVI and SAVI to the percent cover equation is statistically significant because the slopes for both variables was 0.02, which are significant at the 95% confidence level when they are entered into the equation. In the case of SAVI, the red variable was not entered into the percent cover equation because the minimum tolerance of 1.00×10^{-4} was exceeded by the red variable (6.9×10^{-4}). Furthermore, adding the red variable into the equation would reduce the r^2 value as indicated by the 'Beta In' value of 0.40. This 'Beta In' value is the standardized regression coefficient that would result if the variable was entered into the equation at the next step (Norusis, 1993). The similarity between all three vegetation indices occurs because they are highly correlated with each other.

Overall, the regression analyses produced better results for percent cover than for LAI. This is similar to the correlation analysis, where correlations between percent

cover and the image variables were better than with LAI. With respect to the spectral data alone, the NIR variable was always entered into the equation at the first step, and this was followed by the green variable at the second step. The addition of the green variable always resulted in a significant ($p < 0.05$) increase in the regression coefficient.

The addition of Standard Deviation texture improved the equations for both LAI and percent cover, but the improvement was only statistically significant for percent cover. However, the standard error for the LAI equation was reduced even though the slope of the Standard Deviation variable for the LAI equation was not significant. Therefore, the addition of the Standard Deviation texture data could be considered valuable for the prediction of both LAI and percent cover. The addition of the Variance texture improved only the percent cover regression coefficient, although, the improvement was not statistically significant because the standard error increased and the variable's slope was greater than the 0.05 significance level.

The three vegetation indices all produced similar results, improving the percent cover equation and decreasing the regression coefficient for LAI. The regression coefficients obtained for both LAI and percent cover with the addition of each vegetation index were all relatively similar. However, NDVI produced the highest value for the percent cover equation while SAVI produced the highest for the LAI equation, despite the value decreasing when SAVI was added into the equation. This indicates that any of the three vegetation indices investigated in this research could be used to improve the estimation of percent cover from imagery measured variables.

In addition, the incorporation of Standard Deviation texture data to the spectral data in a regression analysis could also be used to determine LAI. This is the only variable that was able to improve on the strength of the regression coefficient obtained by the spectral data alone. Standard Deviation texture could also be used with spectral data to determine percent cover and obtained a regression coefficient similar to those produced by the vegetation indices. It can also be used to obtain a stronger regression for LAI. However, it is recommended that if the means of the various image variables are used, then the addition of Standard Deviation texture data to the spectral information would be better than using a vegetation index as LAI can be estimated in addition to percent cover using the texture data, whereas the vegetation indices only achieved a better regression coefficient for percent cover.

Regression Analysis using Variance of Variables

The same five regression analyses conducted using the variance of the regression variables are identified in Tables 6.11 and 6.12. The r^2 values are much lower than those of the mean dataset but the same pattern of variable additions at each step was evident. The addition of the Standard Deviation texture information to the equation resulted in a lower regression coefficient for both LAI and percent cover. For LAI, the regression coefficient decreased from 0.14 for the green and red spectral information to 0.12 with the addition of the variance of the Standard Deviation texture. A similar decrease was obtained for percent cover, decreasing from 0.15 to 0.13. The addition of the Variance texture resulted in the same regression coefficient for both LAI (0.14). This similarity in

the regression coefficients with the addition of the Variance texture could be because the texture measure is derived from the red spectral information which had already been added into the equation in the previous step. The addition of Variance increased the regression coefficient from 0.13 to 0.20 for percent cover. The difference between the two equations is that the increase for the LAI was not statistically significant and the increase for percent cover was. The three vegetation indices all produced similar results. The regression coefficients for both LAI and percent cover were both significantly improved when the variance of the vegetation indices were added into their equations.

Comparison of Regression Results for the Mean and Variance Datasets

One of the major differences between the two datasets is that the variance dataset resulted in weaker regression relationships. However, for both datasets, the regression analyses for percent cover produced stronger regressions than did LAI. Furthermore, the mean of the Standard Deviation could be used to predict both LAI and percent cover, yet the variance of Standard Deviation could not. The situation was reversed for the Variance texture measure; the variance could be used over the mean to predict LAI and percent cover. However, it is recommended that the mean of the Standard Deviation be used because of the stronger regression relationships derived. The mean of the vegetation indices only improved the percent cover model, whereas their variance improved the regression coefficients of both LAI and percent cover.

Table 6.11
Stepwise Regression Results for Variance of Image Variables and LAI

Regression Variables	Step 1							Step 2						
	Variable Entered	r ² value	Standard Error	F statistic	Signif. of F	Slope	Variable Entered	r ² value	Standard Error	F statistic	Signif. of F	Slope		
Spectral plus Standard deviation	Red*	0.10	1.22	5.28	0.03	0.03	Green	0.14	1.20	3.98	0.03	0.12		
Spectral plus Variance	Red*	0.10	1.22	5.28	0.03	0.03	Green	0.14	1.20	3.98	0.03	0.12		
Spectral plus RVI	Red*	0.10	1.22	5.28	0.03	0.03	RVI	0.17	1.17	4.86	0.01	0.05		
Spectral plus NDVI	Red*	0.10	1.22	5.28	0.03	0.03	NDVI	0.18	1.16	5.27	0.01	0.04		
Spectral plus SAVI	Red*	0.10	1.22	5.28	0.03	0.03	SAVI	0.18	1.16	5.27	0.018	0.04		

Regression Variables	Step 3							Step 4						
	Variable Entered	r ² value	Standard Error	F statistic	Signif. of F	Slope	Variable Entered	r ² value	Standard Error	F statistic	Signif. of F	Slope		
Spectral plus Standard deviation	Std Dev*	0.12	1.21	2.64	0.06	0.69	NIR*	0.09	1.23	1.95	0.12	0.80		
Spectral plus Variance	Variance	0.14	1.20	2.99	0.04	0.32	NIR*	0.12	1.21	2.26	0.08	0.61		
Spectral plus RVI	NIR*	0.18	1.17	3.74	0.02	0.25	Green	0.16	1.18	2.78	0.04	0.68		
Spectral plus NDVI	NIR*	0.21	1.15	4.28	0.01	0.02	Green	0.19	1.16	3.17	0.03	0.69		
Spectral plus SAVI	NIR*	0.21	1.15	4.29	0.01	0.16	Green	0.19	1.16	3.18	0.03	0.69		

Italics indicate variables that significantly contributed to the regression equation

Table 6.12
Stepwise Regression Results for Variance of Image Variables and Percent Cover

Regression Variables	Step 1						Step 2					
	Variable Entered	r ² value	Standard Error	F statistic	Signif. of F	Slope	Variable Entered	r ² value	Standard Error	F statistic	Signif. of F	Slope
Spectral plus Standard deviation	<i>Red*</i>	0.13	25.94	6.57	0.02	0.02	<i>Green</i>	0.15	25.58	4.41	0.02	0.16
Spectral plus Variance	<i>Red*</i>	0.13	25.94	6.57	0.02	0.02	<i>Variance</i>	0.20	24.89	5.66	0.01	0.05
Spectral plus RVI	<i>Red*</i>	0.13	25.94	6.57	0.02	0.02	<i>RVI</i>	0.23	24.40	6.63	0.01	0.03
Spectral plus NDVI	<i>Red*</i>	0.13	25.94	6.57	0.02	0.02	<i>NDVI</i>	0.27	23.78	7.94	0.00	0.01
Spectral plus SAVI	<i>Red*</i>	0.13	25.94	6.57	0.02	0.02	<i>SAVI</i>	0.27	23.78	7.93	0.00	0.01

Regression Variables	Step 3						Step 4					
	Variable Entered	r ² value	Standard Error	F statistic	Signif. of F	Slope	Variable Entered	r ² value	Standard Error	F statistic	Signif. of F	Slope
Spectral plus Standard deviation	<i>Std Dev*</i>	0.13	25.91	2.90	0.04	0.76	<i>NIR*</i>	0.11	26.28	2.12	0.10	0.89
Spectral plus Variance	<i>Green</i>	0.22	24.51	4.60	0.01	0.15	<i>NIR*</i>	0.20	24.83	3.39	0.02	0.72
Spectral plus RVI	<i>NIR*</i>	0.22	24.53	4.58	0.01	0.44	<i>Green</i>	0.20	24.84	3.38	0.02	0.72
Spectral plus NDVI	<i>NIR*</i>	0.27	23.70	5.73	0.00	0.28	<i>Green</i>	0.25	24.02	4.21	0.02	0.77
Spectral plus SAVI	<i>NIR*</i>	0.27	23.70	5.73	0.00	0.28	<i>Green</i>	0.25	24.02	4.21	0.02	0.77

italics indicate variables that significantly contributed to the regression equation

6.5 Summary of Results

The following section summarizes the results of both phases of the research and highlights those of importance. The conclusions of this work and their impact on forest regeneration assessment are presented in Chapter 7.

6.5.1 Phase 1

Per pixel separabilities that were obtained for the eleven land cover classes were generally 'poor', particularly for the vegetation classes. The addition of two co-occurrence texture measures improved the separabilities of the land cover classes, but they were still 'poor'. This lack of good separability between land cover classes led to a large percentage of individual pixel errors when identifying conifer seedlings. However, since the seedling cores were generally well classified, an assessment of accuracy of seedling counts was conducted. The five classifications, of the twelve, which obtained the lower percentage of errors in the counting the conifer seedlings were selected. Errors of omission and errors of commission were identified for those five classifications for each of the three plots on the experimental units where no competition was present. This condition was used to simulate leaf-off imagery which would normally be used in conifer seedling identification and counting. The User's and Producer's accuracies for each of the classifiers were determined. The classification that produced the highest accuracies for all plots was the neural network using the spectral data plus the Standard Deviation co-occurrence texture measure. It was well over 90% accurate for all counts except for the User's accuracy in the fireweed plot. Of the five classifications, four

contained co-occurrence texture information. The accuracies of conifer seedling counts obtained in this research are as good as those achieved by Hall and Aldred (1992) through manual interpretation of stereo images, although the site used in this research was a more controlled situation than the study areas used by Hall and Aldred. However, the results obtained in this research suggest that automated methods can be used to classify and count conifer seedlings. However, it must be conducted in leaf-off conditions because as the density of competition increases counting accuracy decreases. A combination of manual and automated methods, such as the use of stereo images in locating training samples could mitigate the effect of density.

Testing of the neural network with spectral and Standard Deviation texture information was conducted on the imagery of the operational cutover site at Searchmont. Of the two plots evaluated, the plot with the lesser amount of competition achieved a higher user's accuracy (77.6%) than the other plot (21.8%).

6.5.2 Phase 2

The correlation coefficients for the image variables and field variables for both datasets (mean and variance) generally indicated that there is a good potential to predict plant parameters such as LAI and percent cover from image variables. However, correlation coefficients were generally lower for the variance of the regression variables than for the mean, representing a 'weaker' relationship when the variance of the variables was used. Percent cover obtained better correlation coefficients against the image variables for both of the datasets than LAI.

Spectral data alone can be used to predict the field measurements (LAI and percent cover), although the use of the mean of the Standard Deviation co-occurrence texture information and the mean of the three vegetation indices (RVI, NDVI, SAVI) could be used to strengthen the relationship. Although regression relationships were 'weak', they were statistically significant and were better than those obtained using the variance of the variables. Furthermore, it is recommended that a stepwise multiple regression be used to conduct the analysis because, in some cases, the addition of spectral variables did not significantly contribute to the equation. These variables can be identified in a stepwise method and excluded from the model. For example, when adding vegetation indices to the spectral data, the vegetation index was added before the green spectral data, and when the green spectral data was added, the strength of the regression relationship was reduced. The use of a stepwise method can allow the user to determine which variables should be included in the equation. This method was also recommended by Gong *et al.* (1995) as they obtain the lower prediction errors than with other methods of regression analysis.

Chapter 7

Conclusions

7.1 Introduction

This chapter outlines the major conclusions that were reached as part of this research, discusses the limitations that were encountered over the course of this research, and provides recommendations to improve on this work.

The research conducted for this thesis focused specifically on the evaluation of information derived from digital camera imagery which can be used in decision making for planning silvicultural activities during the regeneration of coniferous forest sites prior to these sites being assessed for free-to-grow status. The evaluation was conducted in two phases. The first phase assessed the capability for conifer identification and counting using statistical analysis and automated classification procedures. The second phase determined the capability for statistical modelling of biophysical parameters (leaf area index and percent cover) of regenerating vegetation using spectral and textural information extracted from digital camera imagery.

7.2 Potential of Airborne Digital Camera Imagery in Vegetation Classification and Biophysical Modelling

Under simple structural conditions, there appears to be a strong potential for airborne digital camera imaging in provision of thematic maps of conifer seedlings and in

biophysical modelling of vegetation structure. Specific conclusions reached for each phase of this research are:

Phase 1

1. In absence of competition and non-overlapping crowns, very high accuracies were obtained for conifer counts. Accuracy was highest for the neural network classification with user's and producer's accuracies over 90%, with the exception of the user's accuracy for the fireweed plot which was 66%. This level of accuracy is indicative of what should be achievable using imagery acquired in leaf-off conditions.
2. Use of automated classifications to produce thematic maps obtained better results for very low densities of competition than for higher levels of competition. This was best demonstrated by the counting error curves for the various densities at the Arboretum site
3. The addition of co-occurrence texture measures improved the separabilities and the accuracy of the thematic maps.
4. A per-pixel accuracy assessment is not suitable for classifications obtained from high resolution imagery such as that used in this research. An object-based accuracy assessment was developed, where the percentages of over- and under-estimates of conifer counts were obtained for a range of pixel groupings that constituted an object. Although a suitable number of pixels to use in representation of a seedling could not be determined, results indicate that conifer counts can be highly accurate if the number of pixels is equal to the number of pixels classified correctly in conifer crowns (i.e. core crown area).

Phase 2

1. Multiple regression of combined spectral and textural image data showed very good potential for use in prediction of LAI and percent cover as r^2 values ranged from 0.4 to 0.58. However, standard errors were high, being approximately 1.0 for LAI and 17% for percent cover.
2. The addition of vegetation indices to the spectral information resulted in a statistically significant increases in the strength of models predicting field measured variables. The model for percent cover did not include the red spectral data, yet the r^2 value was higher for this model than the LAI model although the standard error was greater for percent cover.

3. The use of the mean statistics for correlation and regression variables produced better results than the variance statistics.
4. The use of the Standard Deviation co-occurrence texture measure in addition to the spectral information results in an increase in the strength of the model for the prediction of LAI and percent cover.
5. A stepwise regression equation should be used to conduct the regression analysis to enable the selection of variables that are statistically significant to the model and avoid those that could produce a 'weaker' model.

Overall

1. The imagery obtained using the digital camera may be suitable for use in forest vegetation management, although the spectral quality of the imagery could certainly be improved. Poor spectral quality is demonstrated by the inverse correlation between NIR and LAI. The relationship should be positive, as NIR increases, the amount of vegetation increases, therefore, the LAI will increase.
2. The pixel size of the imagery obtained also may be suitable for forest vegetation management applications, specifically forest regeneration assessment. Small pixel sizes are necessary for the identification of conifer seedlings, which would not be visible at larger pixel sizes.

7.3 Discussion

7.3.1 Benefits of this Research

This research demonstrated that airborne digital camera imagery has potential for use in determination of the status and structure of conifer regeneration areas. The methodology and technology examined over the course of this work may provide an effective operational support tool for forest vegetation management. The cost of digital camera image acquisition is lower than other high resolution imagery. Furthermore, the learning principles for digital cameras are less complex than those for hyperspectral sensors and the computer processing, software and operator training requirements are

also less. Interpretation of digital frame camera imagery can be based on similar methods used for aerial photography, which is currently the most common remote sensing medium used in regeneration assessment. Digital camera systems can offer numerous advantages over conventional aerial photography: elimination of the need for film development, in-flight viewing of images, computer control of exposure levels, and a linear response to radiance (King, 1995). The spatial resolution used in this research (2.5 cm) reflects the operational requirements, in that the resolution was chosen based on the need to 'see' individual conifer seedlings. Most other sensors (e.g. CASI and other line scanners) do not have the capability to acquire data at such high resolution and are thus limited to analysis of the canopy and not of individual seedlings. The need to image individual conifer seedlings is a requirement if it is the growth of individual trees that is to be monitored from a young age. Given the above benefits of high resolution airborne digital camera imaging, there is a much greater potential for cost-effective integration of the methods evaluated in this research into operational regeneration assessment than exists for other current sensors.

7.3.2 Limitations and Recommendations

To adapt the methods presented in this research to an operational situation, improvements in the technology and methods are needed to provide consistent results, under a wide range of conditions. The following recommendations should be implemented in further research. 1. Sample plots on the ground are needed for either training classifiers or for biophysical modelling. However, in order to obtain proper

coverage of these plots, larger format digital frame cameras (e.g. 3k x 2k pixels) than the one used in this research should be used. The identification of sample plots is also important. The use of stereo images should improve tree identification when there is competition present over the monoscopic viewing used in this thesis and also reduce the locational error present during the selection of training samples. 2. Use of a digital camera with narrow spectral bandwidths ($< 100\text{nm}$). This may reduce the amount of error in classification and identification of conifer seedlings by improving separability between vegetation classes. 3. If training samples are going to be selected over a number of images in a mosaic, radiometric correction of the imagery could increase separability and improve accuracy of conifer seedling counts, although at added cost. 4. The addition of other information from the imagery itself, such as other co-occurrence texture measures, which are less correlated with the spectral data than the two measures used in this research, may reduce the amount of error in conifer seedling counts. The importance of obtaining an acceptable amount of error is critical when the information is being used to support forest vegetation management decisions as both long-term and short-term costs can be affected. Furthermore, the modelling of biophysical parameters, such as LAI and percent cover, can also be improved upon by the above recommendations.

The timing of acquisition is another operational consideration that was a limitation of this research for conifer classification and counting. Classification and counting of conifers can be improved if the images are acquired in early spring or late

fall, when there are no leaves present on the competition. However, images cannot be acquired at this time if the competition species and density, or overall vegetation structure are to be assessed. By acquiring images at different phenological stages, the separability between vegetation classes can improve because some of the competition plants may be flowering. This is, however, a costly proposition as growth sequences of various species are different. Therefore, datasets from various dates would need to be combined, a process which would be difficult and not operationally efficient. Consequently, the potential for single date imagery in classification of competing vegetation is very limited while multi-date imaging is probably not a cost-effective approach. Pitt *et al.* (1997) suggested an imaging schedule for use in several forest management activities which should be followed when planning the timing of image acquisition.

7.4 Concluding Remarks

As discussed at the beginning of this thesis, forests play an integral role not only for the country as a whole, but for communities and individual Canadians as well. Ensuring the successful regeneration of Canada's forest is therefore essential. The evaluation of remote sensing technologies in forest management is not new, although, few such technologies have proven to be cost-effective and are therefore rarely used on an operational basis. As the requirements of forest vegetation management change, the technologies and methods used must also adapt. This paper evaluated one such

technology using various methods to provide information on conifer status and vegetation structure in support of the decision-making processes required for monitoring and ensuring the successful regeneration of forests. Real potential has been demonstrated for the given applications. The next stage should be an evaluation of cost-effectiveness of the methods in an operational pilot project setting.

REFERENCES

- Aird, P.L., (1994). Conservation for the sustainable development of forests worldwide: A compendium of concepts and terms. *The Forestry Chronicle*, 70(6): 666-674.
- Arnup, R.W. and P.A. Rusnak, (1997). *Free-growing regeneration assessment manual for Ontario - draft*. Ontario Ministry of Natural Resources, in preparation. 47 pages plus appendices.
- Augusteijn, M.F., L.E. Clemens, and K.A. Shaw, (1995). Performance evaluation of texture measures for ground cover identification in satellite images by means of a neural network classifier. *I.E.E.E Transactions on Geoscience and Remote Sensing*, 33(3): 616-625.
- Bulter, H., R.A. Peart, and S.E. Franklin, (1995). Estimating canopy leaf area using aerial optical imagery in Kananaskis Country, Alberta. In proceedings of the 17th Canadian Symposium on Remote Sensing. Canadian Remote Sensing Society, Saskatoon, Saskatchewan, pp. 650-653.
- Campbell, J.B., (1987). *Introduction to Remote Sensing*. The Guilford Press, New York. 551 pages.
- Carlson, G.E. and W.J. Ebel, (1995). Co-occurrence matrices for small region texture measurement and comparison. *International Journal of Remote Sensing*, 16(18): 1417-1423.
- Carlson, T.N. and D.A. Ripley, (1997). On the relation between NDVI, fractional vegetation cover, and leaf area index. *Remote Sensing of the Environment*, 62: 241-252.
- Carr, J.R., (1996). Spectral and textural classification of single and multiple band digital images. *Computers and Geoscience*, 22(8): 849-865.
- Chaudhry, M.A., (1981). *Regeneration survey manual for Ontario*. Ontario Ministry of Natural Resources, Toronto, Ontario. 29 pages plus appendices.
- Diekhoff, G., (1992). *Statistics for the social and behavioural sciences: univariate, bivariate, multivariate*. Wm. C. Brown Publishers, United States of America. 418 pages.

- Elvidge, C.D. and Z. Chen, (1995). Comparison of broad-band and narrow-band red and near-infrared vegetation indices. *Remote Sensing of the Environment*, **54**: 38-48.
- Franklin, S.E., M.B. Lavigne, M.J. Deuling, M.A. Wulder, and E.R. Hunt Jr., (1997). Estimation of forest Leaf Area Index using remote sensing and GIS data for modelling net primary production. *International Journal of Remote Sensing*, **18**(16): 3459-3471.
- Gobron, N., B. Pinty, and M.M. Verstraete, (1997). Theoretical limits to the estimation of the leaf area index on the basis of visible and near-infrared remote sensing data. *IEEE Transactions on Geoscience and Remote Sensing*, **35**(6):1438-1445.
- Gong, P., R. Pu, and J.R. Miller, (1995). Coniferous forest leaf area index estimation along the Oregon transect using compact airborne spectrographic imager data. *Photogrammetric Engineering and Remote Sensing*, **61**(9): 1107-1117.
- Gopal, S., and C. Woodcock, (1996). Remote sensing of forest change using artificial neural networks. *IEEE Transactions on Geoscience and Remote Sensing*, **34**(2): 398-403.
- Gougeon, F.A. (1995). Comparison of possible multispectral classification schemes for tree crowns individually delineated on high spatial resolution MEIS Images. *Canadian Journal of Remote Sensing*, **21**(1): 1-9.
- Greenfield, Paul and Paul A. Maus, (1997). The use of color infrared digital imagery for burned area emergency rehabilitation. In proceedings of the 16th Biennial Workshop on Color Photography and Videography in Resource Assessment. American Society for Photogrammetry and Remote Sensing, Weslaco, Texas, April 29 - May 1, pp. 7-16.
- Haddow, K.A., D.J. King, and D.G. Pitt, (1997). Spectral separability of regenerating conifer and competitor species in large scale airborne CIR digital camera imagery. In proceedings of the 16th Biennial Workshop on Color Photography and Videography in Resource Assessment. American Society for Photogrammetry and Remote Sensing, Weslaco, Texas, April 29 - May 1, pp. 20-29.
- Hall, R.J., (1984). Use of large-scale serial photographs in regeneration assessments. Information Report NOR-x-264, Northern Forest Research Centre, Canadian Forest Service, 31 pages.

- Hall, F.G., D.R. Peddle, and E.F. Ledrew, (1996). Remote sensing of biophysical variables in boreal forest stands of *Picea mariana*. *International Journal of Remote Sensing*, 17(15): 3077-3081.
- Hall, R.J. and A.H. Aldred, (1992). Forest regeneration appraisal with large-scale aerial photographs. *The Forestry Chronicle*, 68(1): 142-150.
- Kartikeyan, B., B. Gopalakrishna, M.H. Kalubarme, and K.L. Majumder, (1994). Contextual techniques for classification of high low resolution remote sensing data. *International Journal of Remote Sensing*, 15(5): 1037-1051.
- Kneeshaw, D.D. and Y. Bergeron, (1996). Ecological factors affecting the abundance of advance regeneration in Quebec's southwestern boreal forest. *Canadian Journal of Forest Research*, 26: 888-898.
- King, D. J., (1995). Airborne multispectral digital camera and video sensors: A critical review of system designs and applications. *Canadian Journal of Remote Sensing*, 21(3): 245-273.
- Jensen, J.R. (1996). *Introductory Digital Image Processing: A Remote Sensing Perspective*, Prentice-Hall, New Jersey. 316 pages.
- Law, B.V., (1995). Estimation of leaf area index and light intercepted by shrubs from digital videography. *Remote Sensing of the Environment*, 51: 276-280.
- Lillesand, T.M. and R.W. Kiefer, (1994). *Remote Sensing and Image Interpretation*. John Wiley & Sons, Inc. New York, New York. 750 pages.
- Miller, D.M., E.J. Kaminsky, and S. Rana, (1995). Neural network classification of remote-sensing data. *Computers and Geosciences*, 21(3): 377-386.
- Natural Resources Canada, (1996). *The State of Canada's Forests: 1995-1996*, Canadian Forest Service, Ottawa, Ontario, K1A 0E4. 112 pages.
- Norusis, Marija (1993). *SPSS for Windows Base System User's Guide Release 6.0* SPSS Inc., Chicago, 828 pages.

- Olthof, I. and D.J. King, (1997). Evaluation of textural information in airborne CIR digital camera imagery for estimation of forest stand leaf area index. In proceedings of the 1st North American Symposium on Small Format Aerial Photography. American Society for Photogrammetry and Remote Sensing, Cloquet, Minnesota, October 29, pp. 154-164.
- Omer, John R., (1997). Digital infrared camera used for damage detection of eastern forests. In proceedings of the 16th Biennial Workshop on Color Photography and Videography in Resource Assessment. American Society for Photogrammetry and Remote Sensing, Weslaco, Texas, April 29 - May 1, pp. 17-19.
- Ontario Ministry of Natural Resources, (1995). *Forest Operations and Silviculture Manual*. Ministry of Natural Resources, Ontario, Canada. 64 pages.
- Palubinskas, G., R.M. Lucan, G.M. Foody, and P.J. Curran, (1995). An evaluation of fuzzy and texture-based classification approaches for mapping regenerating tropical forest classes from Landsat-TM data. *International Journal of Remote Sensing*, 16(4): 747-759.
- Paola, Justin D. and Robert A. Schowengerdt, (1995) A detailed comparison of backpropagation neural network and maximum-likelihood classifiers for urban land use classification. *IEEE Transactions on Geoscience and Remote Sensing*, 33(4): 981-996.
- PCI Enterprises Inc., (1996) *Using PCI Software*. Richmond Hill, Ontario, Canada.
- Peddle, D.R., G.M. Foody, A. Zhang, S.E. Franklin, and E.F. Ledrew, (1994). Multisource image classification II: an empirical comparison of evidential reasoning and neural network approaches. *Canadian Journal of Remote Sensing*, 20(4): 396-407.
- Peddle, D.R., (1993) An empirical comparison of evidential reasoning, linear discrimination analysis, and maximum likelihood algorithms for alpine land cover classification. *Canadian Journal of Remote Sensing*, 19(1): 31-44.
- Peddle, D.R., and S.E. Franklin, (1991). Image texture processing and data integration for surface pattern discrimination. *Photogrammetric Engineering and Remote Sensing*, 57(4): 413-420.
- Pitt, D.G., R.G. Wagner, R.J. Hall, D.J. King, D.G. Leckie, and U. Runesson, (1997). Use of remote sensing for forest vegetation management: A problem analysis. *The Forestry Chronicle*, 73(4): 459-478.

- Pitt, D.G. and G.R. Glover, (1996). Measurement of woody plant attributes from large-scale aerial photographs. In press *New Zealand Journal of Forest Science*.
- Pitt, D.G., G.R. Glover, and R.H. Jones, (1996). Two-phase sampling of woody and herbaceous plant communities using large-scale aerial photographs. *Canadian Journal of Forest Research*, **26**(4): 509-524.
- Pitt, D.G. and G.R. Glover, (1993). Large-scale 35-mm aerial photographs for assessment of vegetation-management research plots in eastern Canada. *Canadian Journal of Forest Research*, **23**(10): 2159-2169.
- Price, J.C. and W.C. Bausch, (1995). Leaf area index estimation from visible and near-infrared reflectance data. *Remote Sensing of the Environment*, **52**: 55-65.
- Rondeaux, G., (1995). Vegetation monitoring by remote sensing: a review of biophysical indices. *Photo Interpretation*, **33**(3): 197-212.
- Ross, M.M. (1995). *Forest Management in Canada*. Canadian Institute of Resources Law, Calgary, pp. 108-204.
- Smith, J.L., S.M. Zedaker, and R.C. Heer, (1989). Estimating pine density and competition condition in young pine plantations using 35mm aerial photography. *Southern Journal of Applied Forestry*, **13**: 107- 112.
- Statutes of Ontario, Chapter 25, (1994). Crown Forest Sustainability Act. Queen's Printer, Ontario. 40 pages.
- Stehman, S.V., (1997). Selecting and interpreting measures of thematic classification accuracy. *Remote Sensing of the Environment*, **64**: 77-89.
- Thompson, W.A. and G.F. Weetman, (1995). Decision support systems for silviculture planning in Canada. *The Forestry Chronicle*, **71**(3): 291-298).
- Wagner, R.G., (1993). Research directions to advance forest vegetation management in North America. *Canadian Journal of Forest Research*, **23**: 2317-2327.
- Wulder, M.A., S.E. Franklin, and M.B. Lavigne, (1996). High spatial resolution optical image texture for improved estimation of forest stand leaf area index. *Canadian Journal of Remote Sensing*, **22**(4): 441-449.

Appendix A**Statistics and Transformed Divergence Separability
Results of Training Samples using Spectral Data
for the Arboretum Site**

Table A-1
Training Sample Statistics for Arboretum Site
from Spectral Data

Class	Number of Pixels Sampled	Green		Red		Near IR	
		Mean	Std Dev	Mean	Std Dev	Mean	Std Dev
Jack Pine	453	90.35	7.56	66.04	6.83	54.17	6.25
Black Spruce	433	87.82	7.57	72.19	6.09	63.43	5.70
Fireweed	474	85.16	9.68	77.54	13.60	59.46	9.99
Upland Willow	522	106.20	6.13	83.54	6.78	73.07	7.97
Red Raspberry	477	110.21	10.08	83.73	8.45	71.31	9.28
Blue-Joint Grass	389	87.89	7.97	75.71	7.36	63.86	7.15
Large-Leaved Aster	384	96.53	10.42	109.07	10.82	91.00	7.89
Soil	548	67.10	4.83	92.10	5.81	79.03	4.33
Grass	543	75.62	6.68	64.69	6.95	57.10	6.08
Shadows	413	30.01	5.23	32.11	5.31	29.90	4.21
Null	568	0	0	0	0	0	0

Table A-2
Transformed Divergence Separabilities for the Arboretum Site
Training Samples Using Spectral Data

	Jack Pine	Black Spruce	Fireweed	Upland Willow	Red Raspberry	Blue-Joint Grass	Large- Leaved Aster	Soil	Grass	Shadows
Black Spruce	1.1254									
Fireweed	1.6631	1.4996								
Upland Willow	1.4185	1.3355	1.7443							
Red Raspberry	1.2508	1.3665	1.7004	0.2872						
Blue-Joint Grass	1.3400	0.5355	0.6581	1.3699	1.4568					
Aster	1.9996	1.9980	1.8083	1.9746	1.9911	1.9122				
Soil	2.0000	1.9999	1.9942	1.9999	1.9999	1.9983	1.4217			
Grass	1.4232	0.6899	1.3076	1.9057	1.8755	0.9707	1.9789	1.9984		
Shadows	1.9999	1.9999	1.9999	2.0000	2.0000	1.9999	2.0000	2.0000	2.0000	1.9996

Table A-3
K-Means Unsupervised Cluster Statistics for Arboretum Site
Spectral Data

Cluster	Pixels	Mean Position	Std Dev
(1)	2116184	0.00958 0.00695 0.00574	0.47655 0.34592 0.28975
(2)	1210636	44.78409 38.71128 33.49008	9.98268 8.05914 7.38750
(3)	3279321	69.96330 58.24697 50.07249	8.02363 5.97416 5.75519
(4)	2235045	88.91564 73.33978 62.65425	9.13446 7.06622 6.46398
(5)	1128914	66.82279 82.97275 70.13397	6.58805 6.71605 5.72978
(6)	1439787	76.95976 98.99581 82.96462	6.97598 5.49615 4.97176
(7)	609467	91.68109 110.80635 93.56657	11.99981 7.89890 7.04288
(8)	98744	101.66858 131.12549 113.17224	10.58897 8.57333 10.50304
(9)	20695	128.18014 174.94245 169.88997	13.58401 15.48578 15.76933
(10)	12416	147.47769 219.77118 211.86042	15.16935 19.81150 18.12022
(11)	13437	184.81603 232.43611 243.27707	16.78556 12.96389 10.13004
Total	----- 12169430		

Appendix B**Deviation Statistics and Transformed Divergence Separability
Results of Training Samples using Spectral and Co-occurrence Texture Data
for the Arboretum and Searchmont Sites**

Table B-1
Training Sample Statistics for Arboretum Site
from Standard Deviation and Variance Texture Data

Class	Number of Pixels Sampled	Standard Deviation		Variance	
		Mean	Std Dev	Mean	Std Dev
Jack Pine	453	65.96	6.37	17.83	6.33
Black Spruce	433	72.47	5.72	17.53	8.79
Fireweed	474	76.76	12.53	28.84	11.64
Upland Willow	522	82.85	5.55	21.15	8.65
Red Raspberry	477	82.66	7.15	23.72	12.16
Blue-Joint Grass	389	75.64	6.57	16.04	7.78
Large-Leaved Aster	384	107.87	9.77	19.64	8.39
Soil	548	103.05	12.39	13.76	7.60
Grass	543	64.71	6.51	16.02	6.73
Shadows	413	31.80	4.88	11.73	8.29
Null	568	0	0	0	0

Table B-2
Transformed Divergence Separabilities for the Arboretum Site
Training Samples Using Spectral and Standard Deviation Texture Data

	Jack Pine	Black Spruce	Fireweed	Upland Willow	Red Raspberry	Blue-Joint Grass	Large- Leaved Aster	Soil	Grass	Shadows
Black Spruce	1.2451									
Fireweed	1.8347	1.6706								
Upland Willow	1.5098	1.3857	1.8238							
Red Raspberry	1.3755	1.4518	1.8328	0.3456						
Blue-Joint Grass	1.5501	0.7195	0.7830	1.4266	1.5503					
Aster	1.9999	1.9998	1.8552	1.9987	1.9998	1.9593				
Soil	2.0000	2.0000	1.9970	2.0000	2.0000	1.9995	1.5120			
Grass	1.4954	0.7151	1.4087	1.9173	1.9004	1.0619	1.9918	1.9998		
Shadows	1.9999	1.9999	1.9999	2.0000	2.0000	1.9999	2.0000	2.0000	1.9996	

Table B-3
Transformed Divergence Separabilities for the Arboretum Site
Training Samples Using Spectral and Variance Texture Data

	Jack Pine	Black Spruce	Fireweed	Upland Willow	Red Raspberry	Blue-Joint Grass	Large- Leaved Aster	Soil	Grass	Shadows
Black Spruce	1.1734									
Fireweed	1.7747	1.6248								
Upland Willow	1.5670	1.4980	1.7618							
Red Raspberry	1.4337	1.5591	1.7015	0.4008						
Blue-Joint Grass	1.3697	0.5506	1.0667	1.5257	1.6226					
Aster	1.9996	1.9985	1.8214	1.9766	1.9920	1.9224				
Soil	2.0000	1.9999	1.9954	1.9999	1.9999	1.9985	1.5117			
Grass	1.4580	0.8345	1.5235	1.9376	1.9075	1.0366	1.9822	1.9986		
Shadows	1.9999	1.9999	1.9999	2.0000	2.0000	2.0000	2.0000	2.0000	2.0000	1.9998

Table B-4
Training Sample Statistics for Searchmont Site
from Spectral and Standard Deviation Texture Data

Class	Number of Pixels Sampled	Green		Red		Near IR		Standard Deviation	
		Mean	Std Dev	Mean	Std Dev	Mean	Std Dev	Mean	Std Dev
Conifers	464	98.88	13.28	77.41	11.49	67.99	12.95	106.18	27.90
Competition	518	94.36	13.28	77.89	8.94	65.16	7.94	106.79	20.79
Soil	472	85.15	10.48	112.89	15.95	95.38	13.45	188.05	31.66
Shadow	487	33.63	11.16	32.34	13.96	27.87	11.32	20.69	22.89
Null	451	0	0	0	0	0	0	0	0

Table B-5
Transformed Divergence Separabilities for the Searchmont Site
Training Samples Using Spectral and Standard Deviation Data

	Conifers	Competition	Soil
Competition	0.6476		
Soil	1.9999	1.9943	
Shadow	1.9955	1.9854	1.9654

Appendix C

Examples of Thematic Maps obtained from Unsupervised Clustering, Maximum Likelihood, Neural Network, and Context Classification

Thematic Map Legend












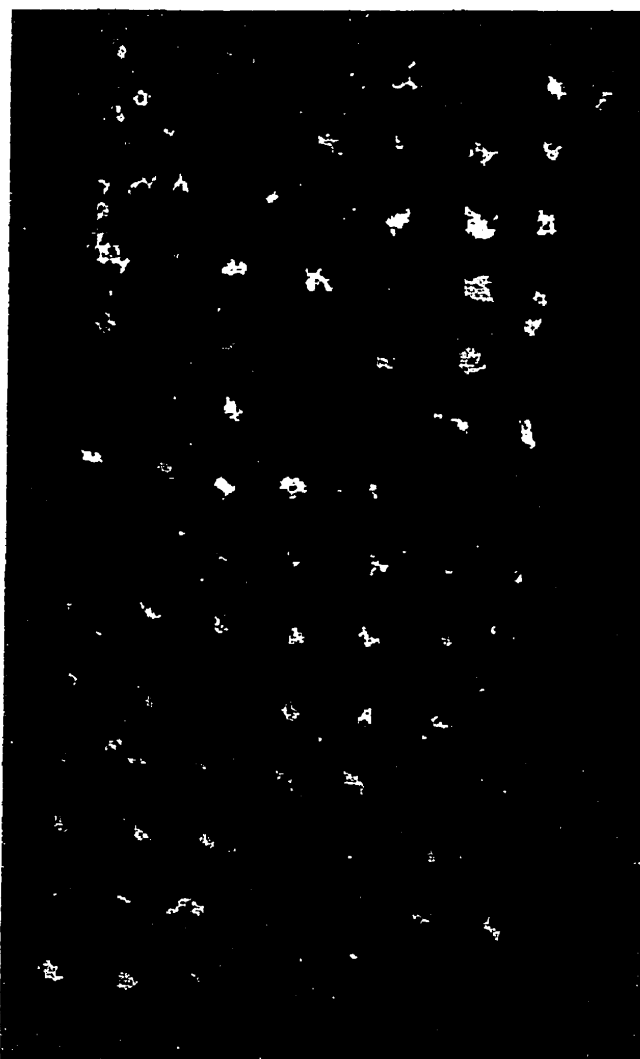
	Jack Pine
	Black Spruce
	Fireweed
	Upland Willow
	Red Raspberry
	Blue-Joint Grass
	Large-Leaved Aster
	Soil
	Grass
	Shadows
	Null

Figure C-1
Example of Plot Classification used in determination
of User's and Producer's Accuracies



Each coloured polygon indicates a conifer identified by the classification. The colour of the polygons represents the unique polygon identification that was assigned and aided in the accuracy assessment.

Figure C-2
Example Spectral Cluster Map of Arboretum Site
Using Unsupervised Clustering on Spectral
Information Only

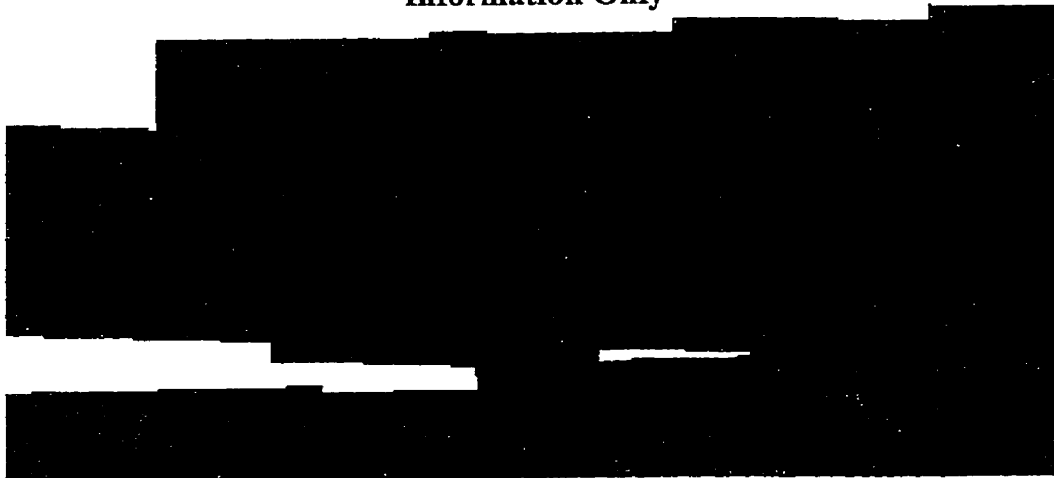
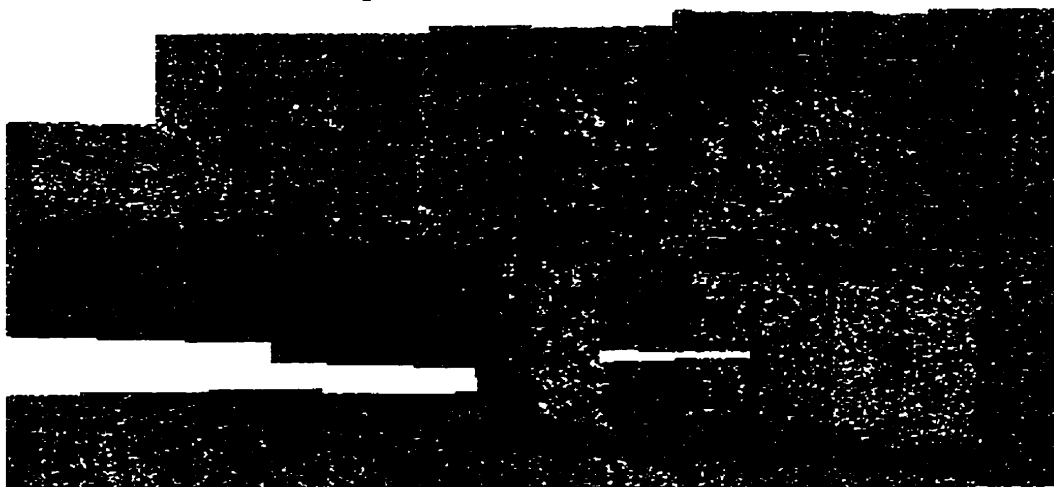


Figure C-3
Example Thematic Map of Arboretum Site
Using a Maximum Likelihood Classification on
Spectral Information Only



For Legend please see preceding page

Figure C-4
Example Thematic Map of Arboretum Site
Using a Neural Network Classification on
Spectral Information Only

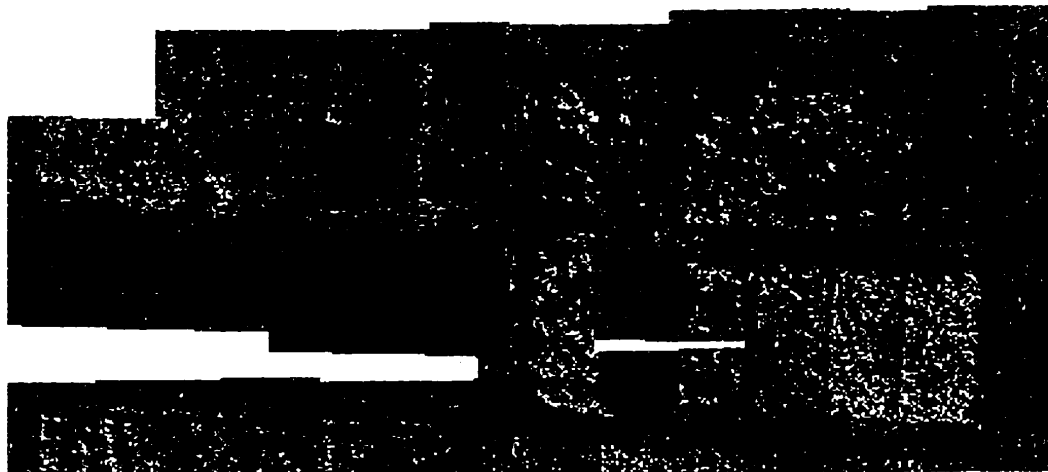


Figure C-5
Example Thematic Map of Arboretum Site
Using a Context Classification on
Spectral Information Only








For Legend please see preceding page

Figure C-6
Neural Network Classification with Spectral and Standard Deviation
Texture Data on the Searchmont Site



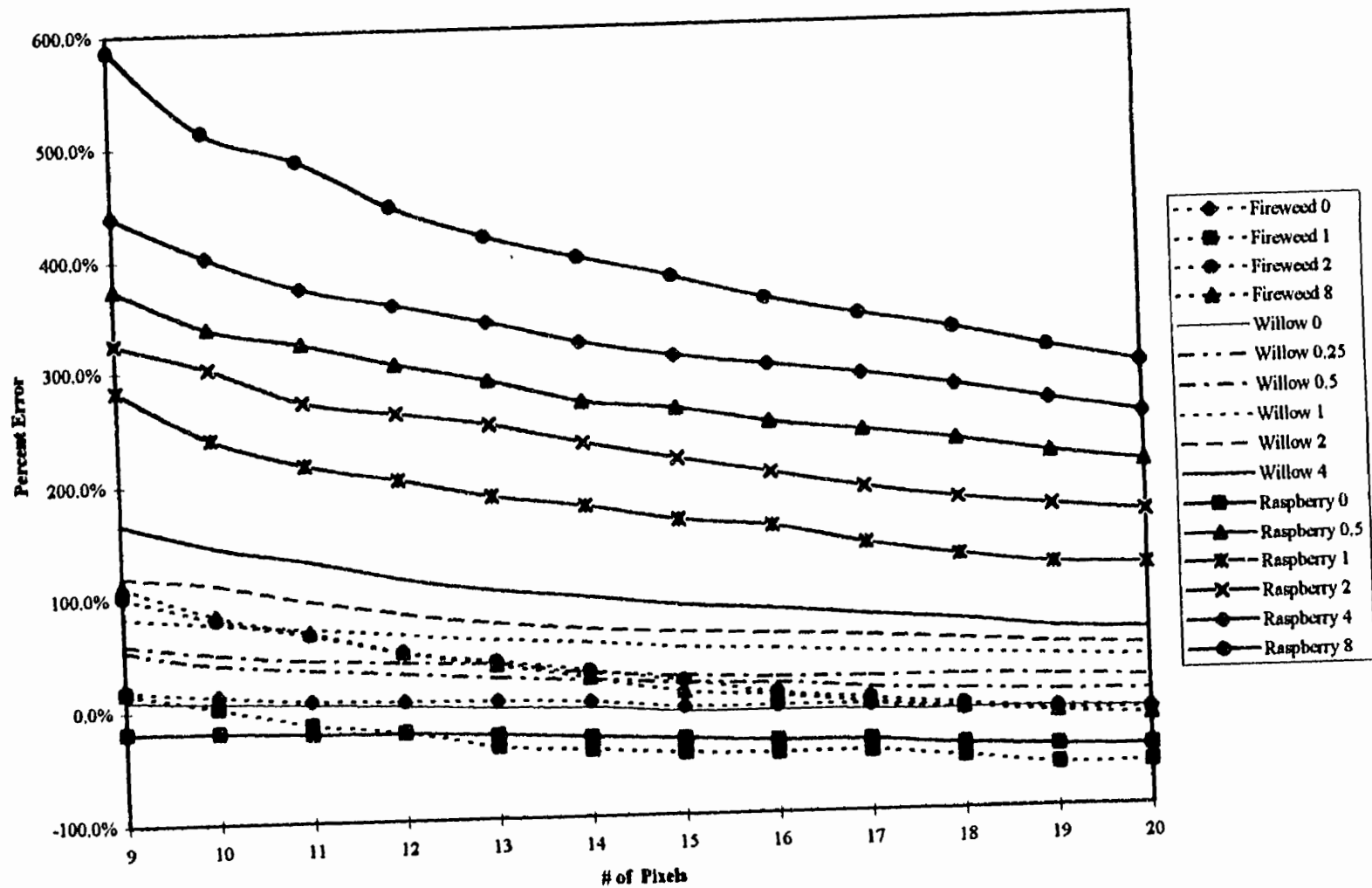
Thematic Map Legend

- | | |
|---|-------------|
|  | Conifers |
|  | Competition |
|  | Soil |
|  | Shadows |
|  | Null |

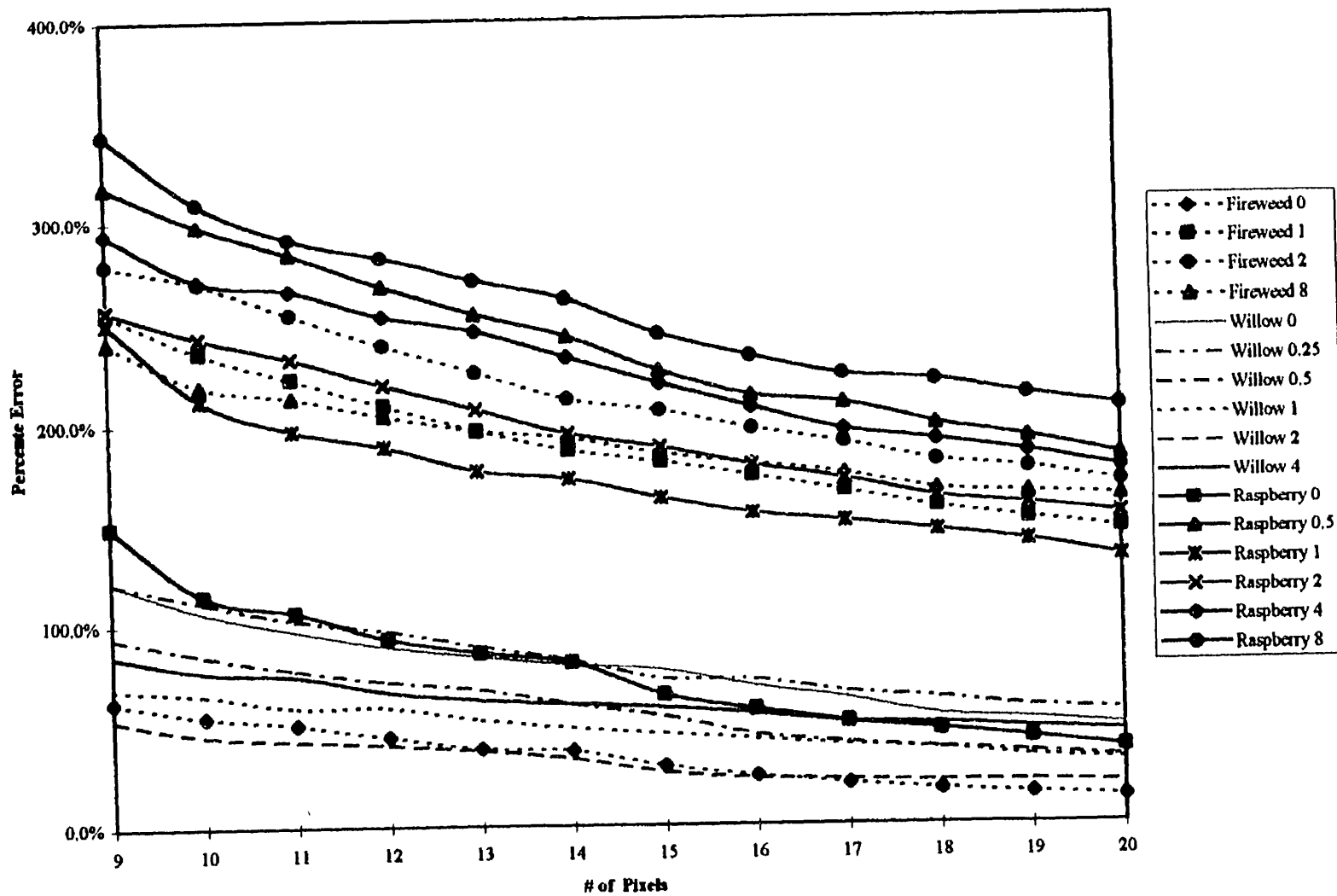
Appendix D

Conifer Counting Error Graphs for all Classifications expressed in Percent as a Function of Competition Species and Density, and the Number of Pixels Defining a Seedling Core

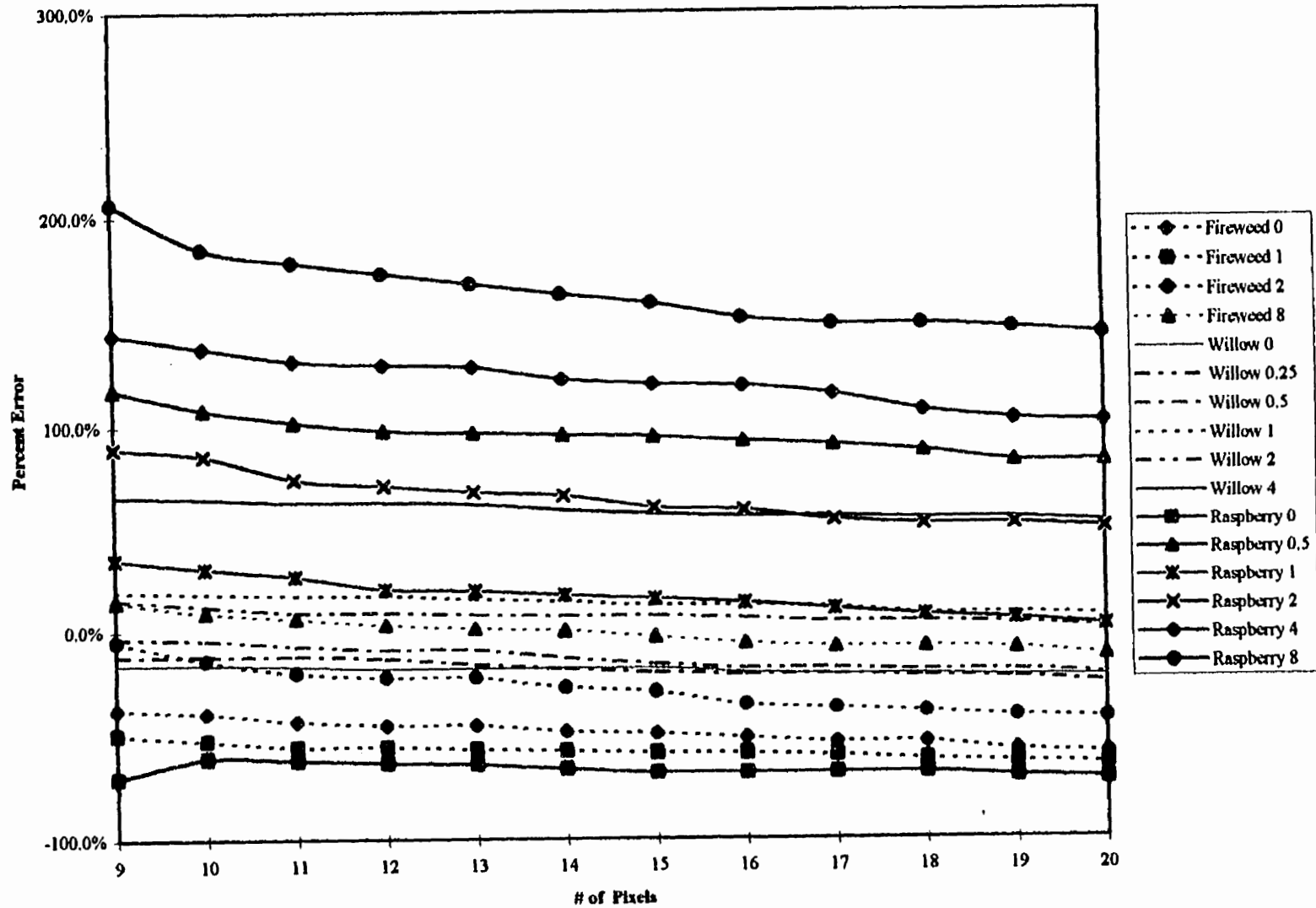
Conifer Counting Error (%) for Maximum Likelihood Classifier with Spectral and Standard Deviation Texture Data as a Function of Competition Species and Density, and the # of Pixels Defining a Seedling



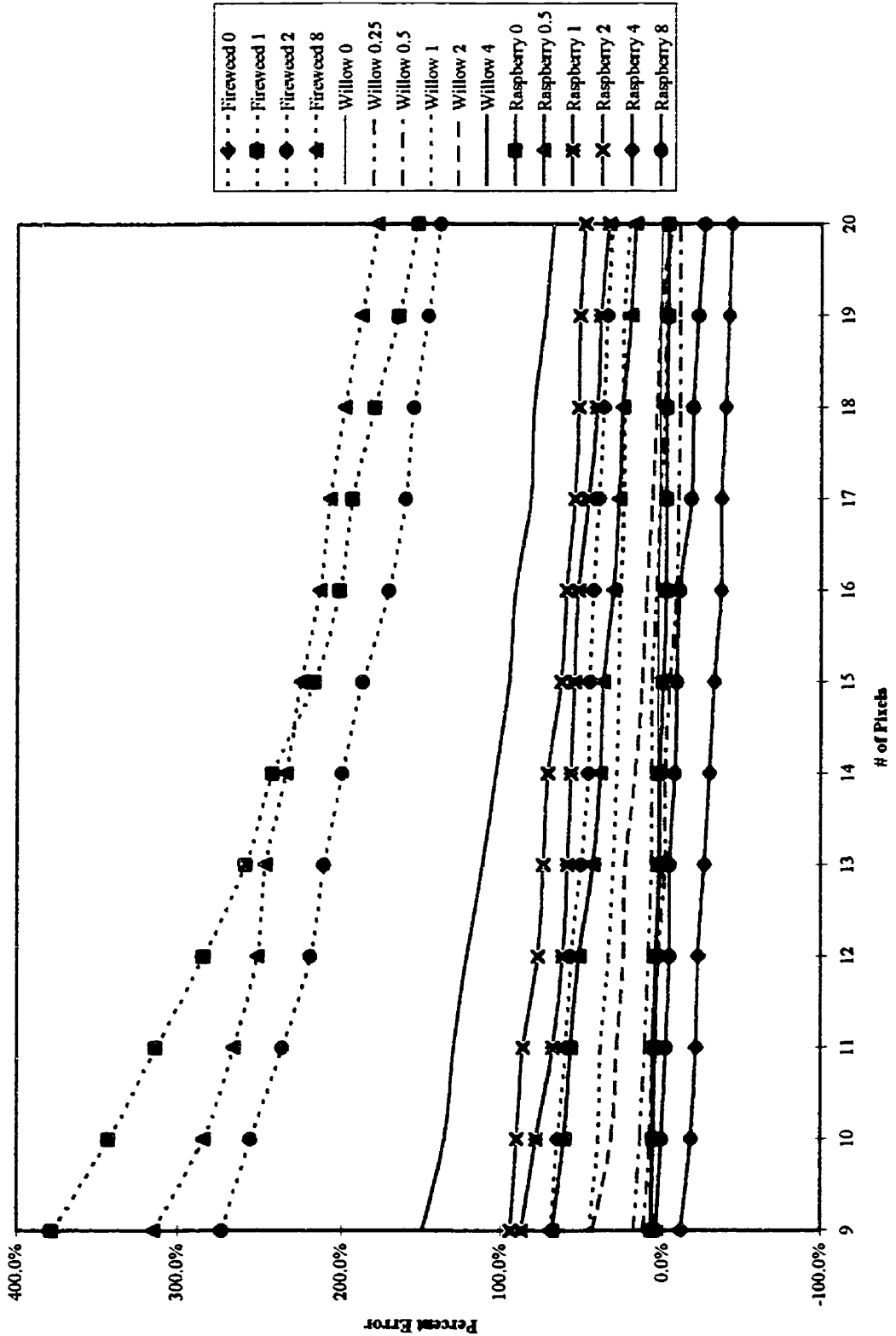
Conifer Counting Error (%) for Context Classifier with Spectral and Standard Deviation Texture Data as a Function of Competition Species and Density, and the # of Pixels Defining a Seedling



Conifer Counting Error (%) for Context Classifier with Spectral and Variance Texture Data as a Function of Competition and Density, and the # of Pixels Defining a Seedling



Coalifer Counting Error (%) for Unsupervised Clustering with Spectral Data as a Function of Competition Species and Density, and the # of Pixels Defining a Seedling



Appendix E

**Statistical Database used in modelling LAI and Percent
Cover from Image Derived Information**

Table E-1
Means of Image and Field Variables for use in
Correlation and Regression Analysis

Sample #	Green	Red	NIR	Sid Dev	Variance	NDVI	SAVI	RVI	% Cover	LAI	NDVI*	SAVI*	RVI*
1	64.18	59.85	48.55	563.94	0.84	-0.10	-0.15	0.82	65	2.4	.53	.38	36.40
2	70.87	66.72	54.80	629.11	0.87	-0.10	-0.14	0.83	70	2.3	.54	.39	37.17
3	58.40	55.12	43.56	520.05	0.75	-0.12	-0.17	0.80	30	1.4	.48	.32	33.62
4	49.75	41.19	32.18	387.62	0.51	-0.12	-0.18	0.79	80	2.1	.47	.31	33.25
5	74.22	64.30	52.60	606.35	0.92	-0.10	-0.14	0.83	80	3.5	.54	.39	37.54
6	67.50	62.66	49.74	590.66	0.90	-0.11	-0.17	0.80	75	3.8	.49	.34	34.41
7	63.70	55.93	41.52	527.21	0.75	-0.15	-0.22	0.75	70	3.1	.39	.23	28.64
8	57.34	55.45	44.15	523.19	0.71	-0.11	-0.17	0.80	35	1.4	.49	.34	34.48
9	58.87	54.05	42.71	509.32	0.64	-0.12	-0.17	0.80	65	2.2	.48	.32	33.51
10	64.64	69.33	58.15	652.80	0.70	-0.08	-0.13	0.85	5	.3	.59	.45	39.83
11	68.30	83.63	70.38	786.41	0.74	-0.08	-0.12	0.85	30	1.1	.61	.46	40.57
12	67.98	82.09	69.17	772.18	0.74	-0.08	-0.12	0.85	10	1.3	.61	.47	40.64
13	62.14	63.42	53.50	597.03	0.64	-0.08	-0.12	0.85	5	.2	.60	.46	40.57
14	80.27	77.37	65.19	728.72	0.65	-0.08	-0.13	0.85	0	.0	.59	.45	39.58
15	43.05	42.90	36.36	403.16	0.52	-0.08	-0.12	0.86	0	.0	.61	.48	41.31
16	75.98	77.87	66.25	734.11	0.67	-0.08	-0.12	0.86	20	.7	.61	.47	41.04
17	78.54	75.25	62.10	709.15	0.67	-0.09	-0.14	0.83	40	.9	.55	.40	37.40
18	59.49	59.49	49.18	560.67	0.72	-0.09	-0.13	0.84	30	.4	.57	.42	38.83
19	75.52	79.20	65.83	745.54	0.60	-0.09	-0.13	0.84	10	.8	.57	.42	38.57

Table E-1 - Continued
Means of Image and Field Variables for use in
Correlation and Regression Analysis

Sample #	Green	Red	NIR	Std Dev	Variance	NDVI	SAVI	RVI	% Cover	LAI	NDVI*	SAVI*	RVI*
20	77.49	61.92	53.66	584.22	0.59	-0.07	-0.10	0.87	60	4.4	.65	.51	42.96
21	87.13	68.55	58.05	646.64	0.67	-0.08	-0.13	0.85	75	3.9	.59	.44	39.60
22	72.47	54.35	43.74	512.81	0.73	-0.11	-0.16	0.81	70	4.2	.50	.34	34.59
23	68.90	53.40	45.54	503.85	0.61	-0.08	-0.12	0.86	45	2.8	.61	.47	40.79
24	80.55	58.36	47.13	551.30	0.62	-0.11	-0.16	0.81	75	1.5	.51	.35	35.07
25	90.80	79.73	68.94	750.50	0.75	-0.07	-0.11	0.87	10	.3	.64	.50	42.51
26	66.09	68.37	56.57	644.54	0.74	-0.09	-0.14	0.83	10	.2	.56	.41	38.13
27	72.53	74.07	62.93	698.17	0.70	-0.08	-0.12	0.86	10	.1	.61	.47	40.99
28	64.05	61.79	51.66	580.78	0.74	-0.08	-0.13	0.85	20	1.7	.59	.45	40.05
29	77.36	87.33	71.79	821.20	0.67	-0.10	-0.14	0.83	5	.4	.55	.39	37.10
30	74.17	64.46	53.86	608.25	0.79	-0.09	-0.13	0.84	30	1.1	.57	.42	38.59
31	73.14	61.92	52.00	583.69	0.82	-0.09	-0.13	0.85	20	1.0	.59	.44	39.79
32	77.26	69.41	57.20	653.63	0.82	-0.09	-0.14	0.84	15	.8	.56	.41	38.39
33	66.06	66.24	54.24	623.40	0.82	-0.09	-0.14	0.83	15	.9	.55	.40	37.69
34	90.26	67.02	58.34	631.48	0.82	-0.07	-0.10	0.87	50	2.2	.65	.52	43.29
35	84.91	64.00	54.18	603.53	0.77	-0.08	-0.12	0.85	75	3.1	.60	.46	40.41
36	104.37	74.36	62.24	700.75	0.80	-0.09	-0.13	0.84	85	3.7	.57	.43	38.75
37	88.92	67.88	60.14	640.98	0.90	-0.06	-0.09	0.89	55	2.3	.68	.56	45.07
38	83.47	64.66	56.62	610.00	0.84	-0.07	-0.10	0.88	55	1.2	.66	.53	43.94
39	72.93	56.34	48.46	531.76	0.74	-0.07	-0.11	0.87	45	2.1	.64	.50	42.52

Table E-2
Variances of Image and Field Variables for use in
Correlation and Regression Analysis

Sample #	Green	Red	NIR	Std Dev	Variance	NDVI	SAVI	RVI	% Cover	LAI	Red*	NIR*	Std Dev*
1	315.77	419.04	251.09	33569.07	0.18	0.002	0.005	0.007	65	2.4	6.04	5.53	10.42
2	170.00	238.34	143.98	17934.77	0.12	0.002	0.004	0.006	70	2.3	5.47	4.97	9.79
3	216.30	264.34	150.99	21214.24	0.14	0.003	0.006	0.007	30	1.4	5.58	5.02	9.96
4	378.83	332.08	189.44	28163.12	0.21	0.004	0.009	0.011	80	2.1	5.81	5.24	10.25
5	345.08	395.30	221.45	30660.86	0.19	0.004	0.008	0.010	80	3.5	5.98	5.40	10.33
6	238.70	314.37	167.79	24121.09	0.18	0.003	0.006	0.008	75	3.8	5.75	5.12	10.09
7	262.56	258.90	130.32	20528.67	0.11	0.003	0.006	0.007	70	3.1	5.56	4.87	9.93
8	304.04	279.10	161.30	22914.90	0.10	0.003	0.006	0.007	35	1.4	5.63	5.08	10.04
9	347.43	314.17	194.70	26323.99	0.12	0.003	0.006	0.007	65	2.2	5.75	5.27	10.18
10	377.76	693.10	447.50	58266.09	0.13	0.002	0.004	0.005	5	.3	6.54	6.10	10.97
11	301.64	564.03	325.29	46240.24	0.18	0.001	0.003	0.004	30	1.1	6.34	5.78	10.74
12	280.77	514.68	295.33	41813.61	0.14	0.001	0.003	0.004	10	1.3	6.24	5.69	10.64
13	452.42	678.47	439.69	57828.14	0.15	0.002	0.004	0.006	5	.2	6.52	6.09	10.97
14	180.94	275.75	176.82	21793.97	0.11	0.001	0.002	0.003	0	.0	5.62	5.18	9.99
15	265.94	260.56	164.63	21712.45	0.12	0.003	0.006	0.008	0	.0	5.56	5.10	9.99
16	329.40	397.21	249.05	32557.90	0.11	0.001	0.003	0.004	20	.7	5.98	5.52	10.39
17	313.85	264.96	165.88	21233.18	0.08	0.001	0.003	0.003	40	.9	5.58	5.11	9.96
18	319.74	437.33	243.45	36148.34	0.14	0.002	0.005	0.007	30	.4	6.08	5.49	10.50
19	310.06	402.06	238.60	33379.40	0.08	0.001	0.002	0.003	10	.8	6.00	5.47	10.42

Table E-2 - Continued
Variates of Image and Field Variables for use in
Correlation and Regression Analysis

Sample #	Green	Red	NIR	Std Dev	Variance	NDVI	SAVI	RVI	% Cover	LAI	Red*	NIR*	Std Dev*
20	461.23	246.03	178.83	20717.75	0.06	0.002	0.003	0.005	60	4.4	5.51	5.19	9.94
21	353.39	268.20	211.10	22014.29	0.08	0.002	0.004	0.005	75	3.9	5.59	5.35	10.00
22	260.28	181.95	137.09	14142.01	0.11	0.003	0.006	0.008	70	4.2	5.20	4.92	9.56
23	315.61	177.26	135.89	14695.88	0.07	0.002	0.005	0.007	45	2.8	5.18	4.91	9.60
24	317.24	169.77	118.17	14062.31	0.06	0.002	0.004	0.005	75	1.5	5.13	4.77	9.55
25	296.01	189.64	134.02	13954.24	0.11	0.001	0.003	0.005	10	.3	5.25	4.90	9.54
26	224.98	417.24	258.74	34107.03	0.13	0.002	0.005	0.006	10	.2	6.03	5.56	10.44
27	174.43	332.13	200.16	26849.11	0.10	0.002	0.004	0.005	10	.1	5.81	5.30	10.20
28	502.16	575.81	353.90	47765.16	0.19	0.003	0.006	0.009	20	1.7	6.36	5.87	10.77
29	257.35	182.46	96.79	13401.40	0.11	0.001	0.002	0.003	5	.4	5.21	4.57	9.50
30	414.04	323.86	229.18	25923.52	0.14	0.002	0.005	0.006	30	1.1	5.78	5.43	10.16
31	497.28	331.60	224.05	26807.87	0.15	0.003	0.007	0.010	20	1.0	5.80	5.41	10.20
32	477.45	385.63	215.84	30840.69	0.15	0.003	0.007	0.009	15	.8	5.95	5.37	10.34
33	337.44	455.48	252.61	36945.88	0.14	0.003	0.006	0.008	15	.9	6.12	5.53	10.52
34	439.52	304.91	232.32	23990.19	0.12	0.002	0.005	0.007	50	2.2	5.72	5.45	10.09
35	560.84	356.26	242.16	28865.56	0.12	0.002	0.005	0.007	75	3.1	5.88	5.49	10.27
36	249.54	183.30	130.21	13291.13	0.09	0.002	0.004	0.005	85	3.7	5.21	4.87	9.49
37	357.05	253.91	222.66	18978.85	0.15	0.002	0.005	0.007	55	2.3	5.54	5.41	9.85
38	505.55	319.62	243.31	25150.49	0.16	0.002	0.004	0.006	55	1.2	5.77	5.49	10.13
39	625.82	318.61	220.37	25877.55	0.12	0.002	0.005	0.008	45	2.1	5.76	5.40	10.16

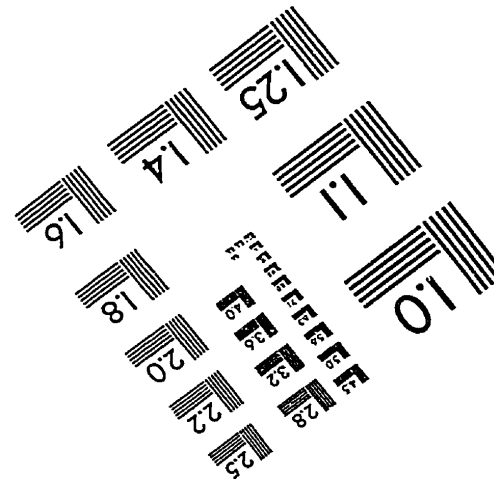
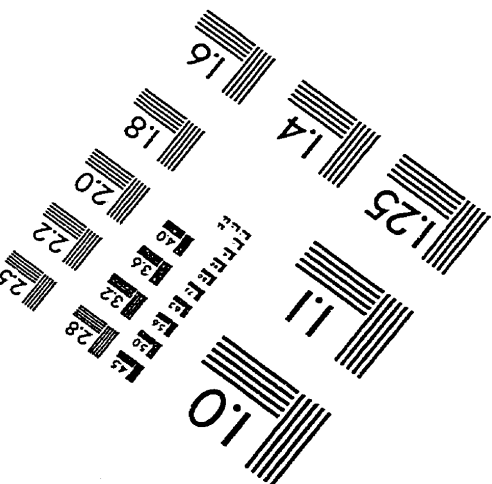
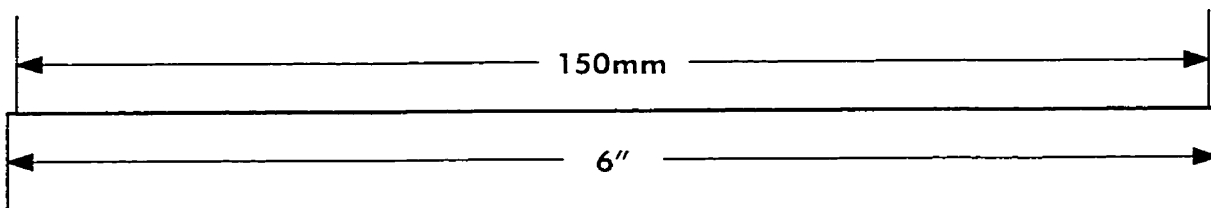
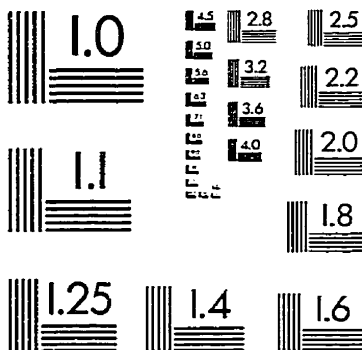
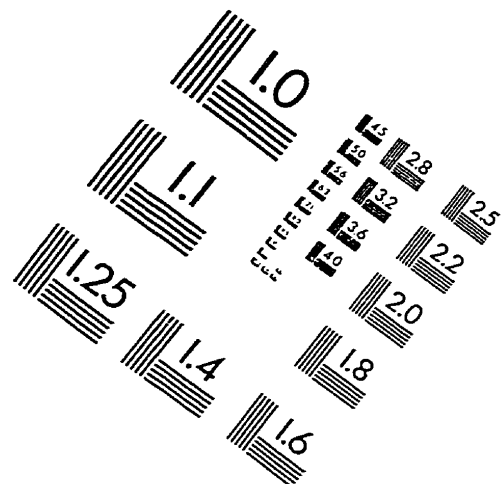
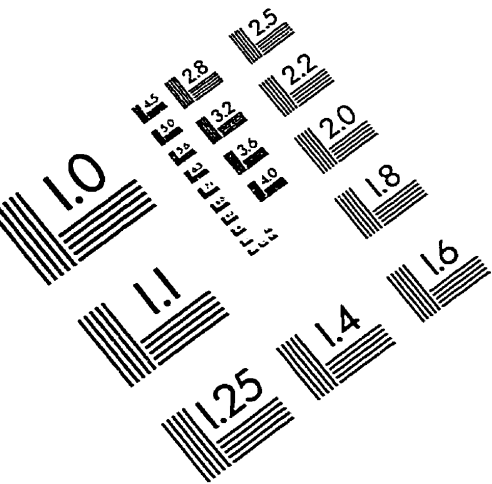
Table E-3
Skewness and Kurtosis Values for the
Means of the Image and Field Variables

Variable	Kurtosis	S.E. Kurt	Skewness	S.E. Skew
SAVI	1.60	.74	-1.01	.38
NDVI	1.60	.74	-1.01	.38
SAVI*	.36	.74	-.52	.38
NDVI*	.71	.74	-.70	.38
Variance	-.28	.74	-.16	.38
RVI	1.34	.74	-.90	.38
LAI	-.74	.74	.58	.38
RVI*	.68	.74	-.64	.38
% Cover	-1.50	.74	.13	.38
NIR	-.30	.74	-.14	.38
Red	.02	.74	-.04	.38
Green	.79	.74	.17	.38
Std Dev	.04	.74	-.06	.38

Table E-4
Skewness and Kurtosis Values for the
Variance of the Image and Field Variables

Variable	Kurtosis	S.E. Kurt	Skewness	S.E. Skew
NDVI	.15	.74	.33	.38
SAVI	.11	.74	.32	.38
RVI	-.24	.74	.17	.38
Variance	-.31	.74	.14	.38
LAI	-.74	.74	.58	.38
NIR*	.15	.74	.21	.38
Red*	-.30	.74	.20	.38
Std Dev*	-.25	.74	.17	.38
% Cover	-1.50	.74	.13	.38
NIR	2.22	.74	1.28	.38
Red	1.03	.74	1.08	.38
Green	.14	.74	.68	.38
Std Dev	1.29	.74	1.15	.38

IMAGE EVALUATION TEST TARGET (QA-3)




APPLIED IMAGE, Inc
 1653 East Main Street
 Rochester, NY 14609 USA
 Phone: 716/482-0300
 Fax: 716/288-5989

© 1993, Applied Image, Inc.. All Rights Reserved